

Alma Mater Studiorum – Università di Bologna

DOTTORATO DI RICERCA IN

**SCIENZE BIOMEDICHE: PROG. N. 2 “EMATOLOGIA CLINICA
E SPERIMENTALE ED EMATOPATOLOGIA”**

Settore/i scientifico-disciplinare/i di afferenza: Med 15

**"Depicting the role of *CDKN2A/ARF* alterations in
adult *BCR-ABL1*-positive acute lymphoblastic
leukemia patients: from genomic deletions to
prognostic impact"**

Presentata da: **Dott.ssa Anna Ferrari**

Coordinatore Dottorato

Stefano Pileri

Relatore

Giovanni Martinelli

Correlatore

Ilaria Iacobucci

Esame finale anno 2011

TABLE OF CONTENTS

- RIASSUNTO	pag. 5
- ABSTRACT	pag. 6
1. INTRODUCTION	pag. 7
1.1 Acute Lymphoblastic Leukemia (ALL) Philadelphia Chromosome Positive (Ph+)	pag. 8
1.2 Molecular basis of the Philadelphia chromosome translocation	pag. 8
1.2.1 Structure and functions of the Bcr and Abl proteins	pag. 8
1.2.2 <i>BCR-ABL</i> fusion gene	pag. 10
1.2.2.1 Breakpoints in <i>ABL</i>	pag. 10
1.2.2.2 Breakpoints in <i>BCR</i>	pag. 10
1.2.3 Mechanisms of BCR-ABL-mediated leukaemogenesis	pag. 12
1.2.3.1 Altered cellular adhesion	pag. 12
1.2.3.2 Activation of mitogenic signaling pathways	pag. 12
- Ras and the mitogen-activated protein kinase pathways	pag. 12
- Janus kinase–signal transducer and activator of transcription pathway	pag. 13
- Phosphatidylinositol 3 kinase pathway	pag. 13
- Myc pathway	pag. 14
1.2.3.3 Inhibition of apoptosis	pag. 14
1.2.3.4 Proteasomal degradation	pag. 14
1.3 Discovery of novel alterations in ALL Ph+	pag. 16
1.4 9p21 locus (<i>INK4a/INK4b/ARF/ANRIL</i>)	pag. 19
1.4.1 <i>ARF/p14^{ARF}</i>	pag. 23
1.4.1.1 Gene structure	pag. 23
1.4.1.2 ARF is a peculiar protein with unusual primary structure	pag. 25
1.4.1.3 Expression and turnover	pag. 25

-	Expression	pag. 25
-	Degradation	pag. 25
	1.4.1.4 Biological function	pag. 26
-	The <i>ARF</i> tumour suppressor is a critical activator of the p53 pathway	pag. 26
-	Nucleolar functions of the <i>ARF</i> tumour suppressor	pag. 27
-	<i>ARF</i> regulates the protein turnover and function of most of its interacting partners	pag. 27
-	<i>ARF</i> promotes the sumoylation of its binding partners	pag. 31
	1.4.2 <i>CDKN2A/INK4A/p16^{INK4A}</i>	pag. 31
	1.4.3 <i>CDKN2B/INK4B/p15^{INK4A}</i>	pag. 34
	1.4.4 <i>ANRIL/CDKN2BAS</i>	pag. 35
	1.5 <i>CDKN2A locus</i> alterations	pag. 38
	1.6 Single Nucleotide Polymorphisms (SNPs) in 9p21 <i>locus</i>	pag. 41
	1.7 Prognostic significance of 9p21 inactivation	pag. 43
	1.8 Treatment of Ph+ Acute Lymphoblastic Leukemia	pag. 47
	1.8.1 Standard chemotherapy and allogeneic stem cell transplantation (alloSCT)	pag. 47
	1.8.2 Tyrosine kinase inhibitors	pag. 48
	1.8.2.1 Imatinib mesylate. (Gleevec, Glivec; STI571)	pag. 48
	1.8.2.2 Second-generation tyrosine kinase inhibitors	pag. 49
	2 AIMS	pag. 51
	3 PATIENTS AND METHODS	pag. 53
	4 RESULTS	pag. 64
	5 DISCUSSION	pag. 77
	6 REFERENCES	pag. 81
-	APPENDIX A	pag. 88

RIASSUNTO

La tesi è basata sull'analisi dei meccanismi responsabili della patogenesi e resistenza al trattamento con inibitori tirosino-chinasici (TKI) nei pazienti con leucemia acuta linfoblastica (LAL) Philadelphia positiva (Ph+). Tale forma di leucemia rappresenta il più frequente e prognosticamente sfavorevole sottotipo di LAL dell'adulto. In particolare i suoi obiettivi sono stati quelli di analizzare, con una metodica ad alta risoluzione (SNP array), la frequenza e l'estensione delle delezioni nel locus 9p21 in 112 pazienti adulti con LAL Ph+ e di determinare i principali meccanismi di inattivazione, al fine di definire nuovi marcatori diagnostici e prognostici ed identificare nuovi meccanismi coinvolti nella progressione leucemica. La regione cromosomica 9p21 è un sito frequentemente alterato in differenti tumori umani, sia solidi che ematologici. Questo locus codifica per importanti proteine coinvolte nella regolazione del ciclo cellulare e nell'apoptosi (*ARF*, *CDKN2A* e di *CDKN2B*), inoltre viene trascritto un RNA non codificante, *ANRIL*. L'analisi dei dati di SNP ha dimostrato alterazioni genomiche alla diagnosi in *CDKN2A/ARF* e in *CDKN2B* rispettivamente nel 29 e nel 25% dei pazienti alla diagnosi. Mentre *ANRIL* era deleta nel 29% dei casi. Nel 72% dei casi le delezioni erano monoalleliche. In particolare, nel 43% dei casi la delezione era limitata ai geni *CDKN2A* e *CDKN2B*, mentre nel 57% si estendeva anche ai geni vicini o all'intero cromosoma 9. Nel 28%, invece, la delezione era biallelica e nella maggior parte di questi casi era limitata ai soli geni *CDKN2A* e *CDKN2B*. Al fine di valutare se le delezioni di *CDKN2A/B* potessero essere coinvolte nella progressione leucemica, abbiamo analizzato le alterazioni genetiche nel locus 9p21 (30 pazienti) al momento della ricaduta. Solo in *CDKN2A/ARF* abbiamo riscontrato un incremento quasi significativo ($p = 0.06$) nella percentuale di delezione (47%) rispetto a quella della diagnosi. Sia alla diagnosi che al *relapse* le delezioni erano in eterozigosi nella maggior parte dei casi. Per verificare se nella nostra casistica anche le mutazioni puntiformi potessero inattivare il locus 9p21 abbiamo analizzato la sequenza di tutti gli esoni di *ARF*, *CDKN2A* e di *CDKN2B*. Mutazioni sono state raramente riscontrate, e solo una, ha comportato una sostituzione amminoacidica. In conclusione si può affermare che l'inattivazione degli oncosoppressori *CDKN2A* e *ARF* è un evento frequente nelle LAL Ph+, che il principale meccanismo di inattivazione è dato dalle delezioni genomiche, mentre le mutazioni che comportano la sostituzione amminoacidica sono rare, e che le delezioni sono frequentemente acquisite al momento della progressione leucemica e risultano essere un sfavorevole marcatore prognostico.

ABSTRACT

This 9p21 *locus*, encode for important proteins involved in cell cycle regulation and apoptosis containing the p16/CDKN2A (cyclin-dependent kinase inhibitor 2a) tumor suppressor gene and two other related genes, p14/ARF and p15/CDKN2B. This *locus*, is a major target of inactivation in the pathogenesis of a number of human tumors, both solid and haematologic, and is a frequent site of loss or deletion also in acute lymphoblastic leukemia (ALL) ranging from 18% to 45% ¹.

In order to explore, at high resolution, the frequency and size of alterations affecting this locus in adult *BCR-ABL1*-positive ALL and to investigate their prognostic value, 112 patients (101 *de novo* and 11 relapse cases) were analyzed by genome-wide single nucleotide polymorphisms arrays and gene candidate deep exon sequencing. Paired diagnosis-relapse samples were further available and analyzed for 19 (19%) cases.

CDKN2A/ARF and *CDKN2B* genomic alterations were identified in 29% and 25% of newly diagnosed patients, respectively. Deletions were monoallelic in 72% of cases and in 43% the minimal overlapping region of the lost area spanned only the *CDKN2A/2B* gene locus. The analysis at the time of relapse showed an almost significant increase in the detection rate of *CDKN2A/ARF* loss (47%) compared to diagnosis ($p = 0.06$). Point mutations within the 9p21 locus were found at very low level with only a non-synonymous substitution in the exon 2 of *CDKN2A*. Finally, correlation with clinical outcome showed that deletions of *CDKN2A/B* are significantly associated with poor outcome in terms of overall survival ($p = 0.0206$), disease free-survival ($p = 0.0010$) and cumulative incidence of relapse ($p = 0.0014$).

The inactivation of 9p21 locus by genomic deletions is a frequent event in *BCR-ABL1*-positive ALL. Deletions are frequently acquired at the leukemia progression and work as a poor prognostic marker.

1. INTRODUCTION

1.1 ACUTE LYMPHOBLASTIC LEUKEMIA (ALL) PHILADELPHIA CHROMOSOME POSITIVE (Ph+)

The Philadelphia chromosome (Ph) is the most common cytogenetic abnormality associated with adult acute lymphoblastic leukemia (ALL). Age is an important determinant of prognosis and outcome for patients with acute lymphoblastic leukemia. Long-term survival rates approach 80% in children aged <5 years but decrease to approximately 50% to 60% in adolescents and young adults, to approximately 30% in adults ages 45 to 54 years, and rarely exceed 15% in older adults. Prognostic changes that occur with increasing age may be attributable in part to age-dependent increases in unfavorable cytogenetic abnormalities. Although Ph+ ALL occurs in only approximately 5% of patients with ALL aged <20 years, the incidence escalates to 33% in patients aged 40 years and is 49% in patients aged >40 years; the incidence decreases to 35% in patients aged >60 years ².

1.2 MOLECULAR BASIS OF THE PHILADELPHIA CHROMOSOME TRANSLOCATION

The Philadelphia chromosome is observed in 95% of adult chronic myeloid leukaemia (CML), 15–20% of adult ALL, 3–5% of childhood ALL and very rarely in acute myeloid leukaemia (AML)^{3,4}. It was the first specific genetic lesion identified in a human cancer and it results from a reciprocal translocation (t) between chromosomes 9 and 22 [t(9;22)]. This translocation creates a fusion of human homologue of the Abelson Murine Leukaemia virus *ABL* on 9q34 with breakpoint cluster region *BCR* on 22q11. Bcr-Abl fusion proteins are constitutively active tyrosine kinases that can alter multiple signaling pathways, contributing to tumor growth and proliferation. The breakpoint may occur within 1 of 4 sites on the *BCR* gene to produce 3 proteins of different sizes: p190, p210, and p230 ². Immunophenotyping is pre-B (CD19+, CD10+), often associated to the expression of myeloid markers (CD13+, CD33+).

1.2.1 Structure and functions of the Bcr and Abl proteins

The *BCR* and *ABL* genes are expressed ubiquitously.

Bcr is a 160-kd cytoplasmic protein with several functional domains. The N-terminal 426 amino acids of Bcr, encoded by the first exon, are retained in all Bcr-Abl fusion protein isoforms. This region contains a serine-threonine kinase domain, whose only known substrates are Bcr and Bap-1 (a member of the 14-3-3 family of proteins), and two serine/threonine-rich regions that bind

Src homology (SH)2 domains. The proximal SH2-binding domain is essential for transformation of rat fibroblasts by Bcr-Abl⁵. The two key motifs of the first *BCR* exon are tyrosine 177 and the coiled-coil domain contained in amino acids 1 to 63. Phosphorylated tyrosine 177 forms a binding site for Grb-2 (an adapter molecule that links BCR to the Ras pathway) and is required for the induction of myeloid leukemia⁶. The coiled-coil is crucial for dimerization of Bcr-Abl⁷, which in turn is required for activation of Abl kinase activity and oncogenicity of Bcr-Abl. *BCR* regions of exon 1 are not essential to oncogenicity but influence the specific phenotype of the leukaemia (Fig. 1.1).

The *ABL* gene, the human homolog of v-abl (the oncogene of the Abelson murine leukemia virus), codes for a 145-kd nonreceptor tyrosine kinase. Two isoforms exist that differ in the first exon (1a and 1b). Only Abl type 1b protein contains a myristoylation site and, therefore, can be anchored to the plasma membrane. Three domains located toward the N-terminus of Abl are named after their homology to the respective domains in Src, the prototype non-receptor tyrosine kinase. The SH1 domain carries the tyrosine kinase function, the SH2 domain binds phosphotyrosine-containing consensus sites, and the SH3 domain binds to proline-rich consensus sequences in proteins like Crk⁸ and Crkl⁹. Abl differs from Src in having a long (~90-kd) C-terminal region that contains actin- and DNA-binding domains⁷, three nuclear localization signals, and one nuclear export signal. Another unique feature of Abl is the N-terminal ‘‘Cap’’ region that is critical to the regulation of kinase activity. Abl is expressed predominantly in the nucleus¹⁰ but shuttles between nucleus and cytoplasm. The functions of the Abl protein are complex and include cell cycle inhibition, cellular responses to genotoxic stress¹¹, and signal transduction from growth factor receptors and from integrins¹² (Fig. 1.1).

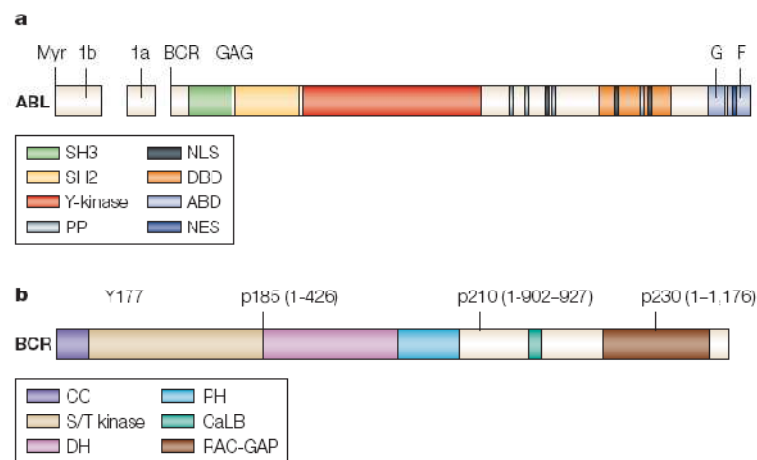


Fig. 1.1 Schematic representation of the Abl (a) and Bcr (b) proteins. There are several important domains that make up ABL and BCR proteins¹³.

1.2.2 *BCR-ABL fusion gene*

1.2.2.1 *Breakpoints in ABL*

Breakpoints within the *ABL* gene can occur anywhere within a 50 segment that extends for over 300 kilobases (kb)¹⁴. Typically, breakpoints are within intronic sequences, most frequently between the two alternative first exons of *ABL*. Thus, *BCR-ABL* fusion genes may contain both exons 1b and 1a, exon 1a alone, or neither of the alternative first exons. *BCR-ABL* mRNA lacks exon 1, regardless of the structure of the fusion gene, with the transcript consisting of *BCR* exons fused directly to *ABL* exon a2.

1.2.2.2 *Breakpoints in BCR*

The breakpoints within the *BCR* gene on chromosome 22 are found within three defined regions. In 95% of patients with CML and approximately one third of patients with ALL, the *BCR* gene is truncated within a 5.8-kb region known as the major breakpoint cluster region. This region contains five exons, originally named b1 to b5, but now referred to as e12 to e16, according to their true positions in the gene. Most breakpoints are within introns immediately downstream of exon 13 (b2) or exon 14 (b3). Because processing of *BCR-ABL* mRNA results in the joining of *BCR* exons to *ABL* exon a2, hybrid transcripts are produced that have an e13a2 (b2a2) or an e14a2 (b3a2) junction. In both cases, the mRNA consists of an 8.5-kb sequence that encodes a 210-kd fusion protein, p210 Bcr-Abl (Fig. 2). In two-thirds of patients with Ph⁺ ALL and in rare cases of CML and AML, the breakpoint in *BCR* occurs in a region upstream of the major breakpoint cluster region known as the minor breakpoint cluster region. This region consists of the 54.4-kb intron between the two alternative second exons of the *BCR* gene, e20 and e2. *BCR-ABL* fusion genes that have breakpoints within the minor breakpoint cluster region contain both BCR alternative first exons (e1 and e10) together with the alternative second exon (e20). The hybrid mRNA consists of sequences that are approximately 7 kb in length in which exon e1 from *BCR* is joined to exon a2 of *ABL*. The translated product is a 190-kd fusion protein, p190 Bcr-Abl (also referred to as p185 Bcr-Abl). Interestingly, transcripts with an e1a2 junction are detectable at very low levels in patients with a major breakpoint cluster region rearrangement. The third defined breakpoint cluster region within the *BCR* gene was named “micro” breakpoint cluster region¹⁵. In this case, the breaks occur within a 30 segment of the *BCR* gene between exons e19 and e20 (known as c3 and c4 in the original nomenclature) (Fig. 1.2). Transcription of the hybrid gene yields an e19a2 *BCR-ABL* fusion transcript that encodes a 230-k protein, p230 *BCR-ABL*.

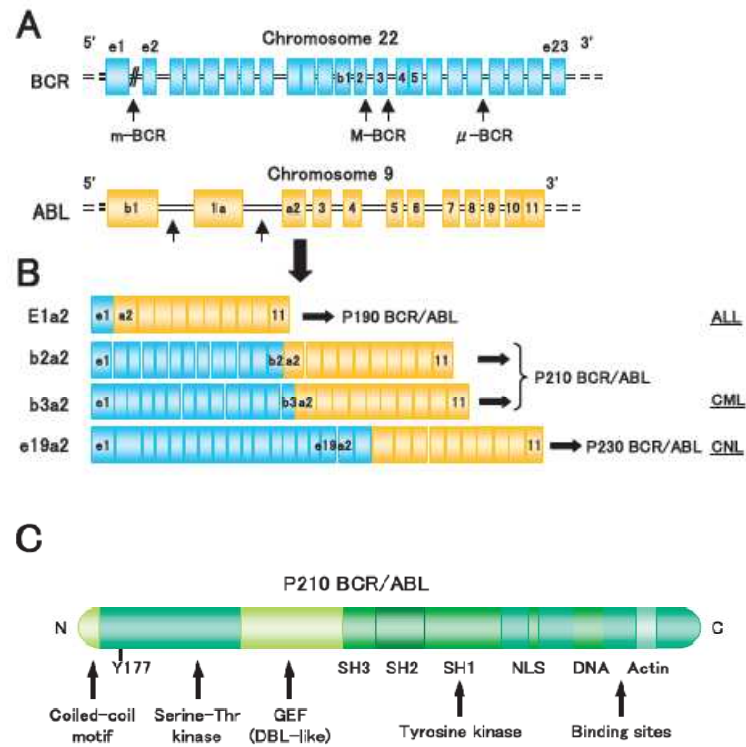


Fig. 1.2 Three *BCR-ABL* variants and association of leukemia types. (A) Locations of the breakpoints in the *ABL* and *BCR* genes and (B) structure of the chimeric *BCR-ABL* mRNA transcripts derived from the various breaks. (C) Functional domains of p210 *BCR-ABL*.

The p190 *BCR-ABL* fusion gene occurs in about 90% of children with Ph+ ALL and between 50% and 80% of adults with Ph+ ALL. The p210 *BCR-ABL* gene constitutes the rest of the Ph+ ALL population. The p230 *BCR-ABL* mutation is associated with Ph+ chronic neutrophilic leukemia².

1.2.3 Mechanisms of BCR-ABL-mediated leukaemogenesis

Tyrosine kinase enzymatic activity is central to cellular signaling and growth, and constitutively elevated kinase activity has been associated with transformation in several systems. The Abl protein is a non-receptor tyrosine kinase whose enzymatic activity is under close physiologic control¹⁶. In contrast, Bcr-Abl proteins are constitutively active tyrosine kinases. The degree of transforming activity of Bcr-Abl correlates with the degree of tyrosine kinase activity. p190 Bcr-Abl, which has higher tyrosine kinase activity, is therefore associated with the development of the more aggressive acute leukemia phenotype, while p210 Bcr-Abl plays a role in the more indolent chronic leukemia phenotype.

1.2.3.1 Altered cellular adhesion

In normal hematopoiesis, progenitor cells adhere to the stromal cells of the bone marrow and their associated extracellular matrix. The latter contains proteins such as fibronectin that function as adhesive ligands for receptors expressed on the surface of hematopoietic progenitor cells. Current thinking holds that the process of adhesion is essential for the regulation of hematopoiesis, providing a means of anchoring progenitors within the vicinity of cytokine-secreting cells¹⁷, exposing them to specific signals that determine their fate. Ph⁺ progenitors exhibit reduced adhesion to stromal cells and the extracellular matrix¹⁸, which “liberates” them from the regulatory signals that are supplied to normal, adherent hematopoietic progenitors. It also may explain why their homing to the bone marrow is disturbed, leading to the appearance of immature cells in the peripheral blood. There is evidence that the function of β integrins on the surface of CML progenitor cells is perturbed, the net effect being reduced adhesion and increased proliferation¹⁷. In addition, migration, in response to certain chemokines such as MIP-1a, is abnormally high¹⁹.

1.2.3.2 Activation of mitogenic signaling pathways

Bcr-Abl is known to activate several signaling pathways with mitogenic potential²⁰. It is important to remember that in many cases, the available data comes from experiments in Bcr-Abl-positive cell lines, and activation of some of these pathways in primary CML cells has yet to be verified.

Ras and the mitogen-activated protein kinase pathways

Bcr-Abl binds directly to proteins that activate Ras²¹. Autophosphorylation of tyrosine 177 generates a binding site for the adapter molecule Grb-2⁵. Grb-2 associates with the Sos protein,

which stimulates the conversion of the inactive GDP-bound form of Ras to the active GTP-bound state²¹. Ras also may be activated by two other adapter molecules, Shc and CrkL, which are substrates of Bcr-Abl²². Although CrkL appears to be necessary for the transformation of fibroblasts by Bcr-Abl, direct binding of CrkL to Bcr-Abl is not required for the transformation of myeloid cells. Activated Ras binds to the serine/threonine kinase Raf-1, recruiting it to the plasma membrane where it is activated by tyrosine phosphorylation and initiates a signaling cascade by way of the mitogen-activated protein kinase (MAPK) pathway. Grb-2 also recruits the scaffolding adapter Gab2, which then is phosphorylated by Bcr-Abl, resulting in activation of phosphatidylinositol 3 (PI-3) kinase/Akt and Ras/Erk²³. Bcr-Abl activates different types of mitogen-activated protein kinases, including extracellular signal-related kinases (ERK)-1/2 and JNK or stress-activated protein kinase. Ultimately, these pathways regulate gene transcription.

Janus kinase–signal transducer and activator of transcription pathway.

Phosphorylation of members of the signal transducer and activator of transcription (STAT) family of transcription factors has been reported in Bcr-Abl–positive cell lines²⁴ and in primary CML cells. Physiologically, STATs are phosphorylated by Janus kinases (Jak) that are downstream of growth factor receptors. In contrast, phosphorylation of STAT5 in Bcr-Abl–expressing myeloid cells appears to be mediated by the Src family kinase, Hck, which binds the SH2 and SH3 domains of Bcr-Abl²⁵. There is evidence that activation of STAT5 by p210 Bcr-Abl contributes to malignant transformation of K562 cells²⁶ and inhibits apoptosis by up-regulating the transcription of Bcl-xL²⁷. STAT5, however, is not required for leukemia induction by Bcr-Abl in mice, casting doubt on its relevance in a more physiologic context. Interestingly, p190 Bcr-Abl differs from p210 Bcr-Abl in that it also is able to activate STAT6. It remains to be seen whether the predominantly lymphoblastic phenotype associated with p190 Bcr-Abl is related to this property of the shorter form of the oncoprotein.

Phosphatidylinositol 3 kinase pathway.

Proliferation of *BCR-ABL*–positive cell lines and primary cells is dependent on PI-3 kinase. Bcr-Abl apparently activates this pathway by forming a multimeric complex with PI-3 kinase, p120Cbl, and the adaptor molecules Crk and CrkL. In *BCR-ABL*–expressing cells, activated PI-3 kinase stimulates the serine-threonine kinase Akt²⁸, which in turn phosphorylates the forkhead transcription factor, *FKHRL1*. The net result of activating this pathway appears to be the proteasome-mediated degradation of the key cell cycle inhibitor p27Kip1, although the precise intermediates are unknown. Activated Akt may function in an antiapoptotic capacity. A key substrate of Akt is the proapoptotic protein or “death agonist” Bad. Bad promotes cell death by

binding to and thereby inactivating the antiapoptotic Bcl-2 and Bcl-xL. Thus, phosphorylation of Bad by Akt may prevent it from binding to these proteins, resulting in reduced apoptosis. Indeed, increased Bad phosphorylation was seen in *BCR-ABL*-positive cells; however, even with Bad completely dephosphorylated, a fraction of cells survived, indicating the existence of Bad-independent survival pathways.

Myc pathway.

Myc is classed as a proto-oncogene because it is overexpressed in many human malignancies. As a transcription factor and immediate early response gene, Myc converts mitogenic signals to alterations of gene expression. Not surprisingly, Myc targets include genes related to cell cycle and apoptosis. Within Bcr-Abl, the SH2 domain²⁹ and the C-terminus are required for full activation of Myc. It recently has been shown that Jak2 is involved in Myc induction by Bcr-Abl, apparently by way of induction of Myc mRNA and by stabilization of the protein.

1.2.3.3 Inhibition of apoptosis

Apoptosis caused by growth factor withdrawal is eliminated when factor dependent cell lines are transfected with exogenous *BCR-ABL*. The mechanisms by which Bcr-Abl inhibits apoptosis in cell lines are not well understood. The release of cytochrome C from mitochondria, a prerequisite for caspase-3 activation, apparently is blocked in *BCR-ABL*-expressing cell lines. Members of the Bcl-2 family of proteins may be involved in mediating the antiapoptotic effect of Bcr-Abl. Up-regulation of Bcl-2 by Bcr-Abl has been demonstrated in two different cellular contexts: one dependent on the Ras pathway and the other on the PI-3 kinase pathway. Bcl-2 targets Raf-1 to mitochondria where it inactivates the proapoptotic protein Bad by phosphorylating it on serine residues³⁰. Down-regulation of interferon consensus sequence binding protein (ICSBP) by Bcr-Abl also has been implicated as an important antiapoptotic event; conversely, ICSBP antagonizes Bcr-Abl by decreasing Bcl-2 expression. Another regulator of apoptosis targeted by Bcr-Abl is Bcl-xL, the expression of which is dependent of STAT5 activation. Surprisingly, a recent report has demonstrated that Bcr-Abl can actively induce apoptosis when trapped in the nucleus³¹. Treatment of human and murine Bcr-Abl-positive cell lines with imatinib stimulated entry of the oncoprotein into the nucleus.

1.2.3.4 Proteasomal degradation

It recently was reported that Bcr-Abl tyrosine kinase activity induced the proteasome-mediated degradation of the ABL-interactor proteins Abi-1 and Abi-2³⁰. Bcr-Abl was found to cause down-regulation of the DNA repair protein DNA-PKcs in cell lines. Loss of DNA-PKcs activity

was correlated with impaired DNA repair and may facilitate the acquisition of additional genetic lesions that lead to disease progression. Another important degradation target is the cell p27, a crucial inhibitor of progression from the G1 to the S phase of the cell cycle. Furthermore, Bcr-Abl can stabilize the expression of Mdm2, a protein that targets the tumor suppressor p53 for ubiquitination, which also would promote genomic instability³².

1.3 DISCOVERY OF NOVEL ALTERATIONS IN ALL PH+

The recent coming of new “genome-wide” techniques, like gene expression profiling (GEP) and analysis of single nucleotide polymorphism (SNP) arrays has enabled to identify multiple novel genetic alterations targeting key cellular pathways, including lymphoid differentiation, cell cycle, tumor suppression, apoptosis and drug responsiveness. By GEP analysis, several down/up-expressed genes have been identified. By genome-wide SNP array analysis of leukaemia blast cells of paediatric and adult CML blastic phases and Ph+ ALL patients³³, the presence of three frequent genetic deletions affecting *IKZF1* (IKAROS), *PAX5* deletions (Fig. 1.3) and the *CDKN2A/B* locus was identified.

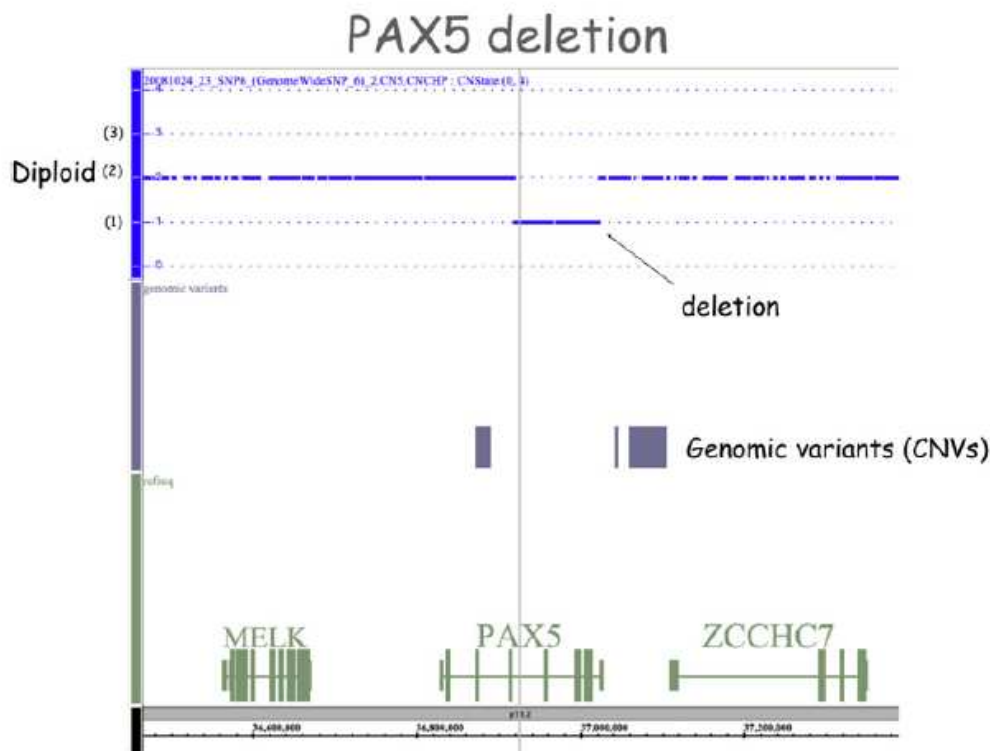


Fig. 1.3 Schematic representation of *PAX5* deletion in a patient with Ph+ ALL as detected by SNP array analysis. The interrupted blue line represents the diploid genome (2) in the region containing *MELK*, *PAX5* and *ZCCHC7* genes. Deletion is represented by a stretch of SNPs, below the level of the diploid line (1). Copy number variations (CNVs) are represented by grey boxes³⁴.

IKZF1 and *PAX5* encode transcription factors required for normal lymphoid development. *CDKN2A/B* locus encodes three tumour suppressor genes that are widely inactivated in many human cancers. At diagnosis, 84% of patients had already sustained *IKFZI* deletions and more than 50% of patients exhibited *PAX5* loss; mono- or biallelic losses, encompassing the entire *CDKN2A* (*CDKN2A* and *ARF*) and *CDKN2B* gene cluster were also recognized in half of the patients (Tab. 1.1). Several other recurring deletions were identified in *BCR-ABL1* ALL, albeit at a lower frequency, including *C20orf94*, *RBI*, *MEF2C* and *EBF1*.

Tab. 1.1 Frequency of deletions in Ph+ ALL (Modified from C. G. Mullighan, *Gene and Development* 2008)³⁵.

Subcategory	Number of cases	Gene deletion frequency (%)		
		IKAROS	PAX5	CDKN2A/B
Ph+ B-ALL ^a	43	84	51	54
Non Ph+ B-ALL	211	11	30	32
T-ALL	50	4	10	72

^a No significant differences in gene deletion frequencies were observed between 21 paediatric and 22 adult cases subjected to analysis. Study of the *CDKN2A/B* gene cluster in 41 of these cases by quantitative PCR using primers directed to each of the *INK4A*, *ARF* and *INK4B* exons indicated an overall deletion frequency of 64%.

IKFZI deletions, limited to the gene in the majority of the cases, were mostly monoallelic and were responsible for the expression of a dominant-negative isoform³⁶. In T-cell ALL, the frequencies of *IKFZI* and *PAX5* deletions were much lower (Tab. 1.1), consistent with findings that these two genes play key roles in regulating B-cell lineage commitment and differentiation³⁷. Although differentiation arrest is a distinctive feature of ALL, the manner by which *IKFZI* and *PAX5* inactivation collaborate with *BCR-ABL* to induce lymphoblastic leukemia is not yet understood. *CDKN2A/B* deletions occur in all lymphoid malignancies (Tab. 1.1), pointing to their general role in tumor suppression in both T- and B-cell ALL, as well as in many other tumor types. The fact that deletion of *PAX5* and *CDKN2A/B* generally occurred together with *IKFZI* loss implies that disruption of each of these genes contributes independently to Ph+ B-cell ALL³⁵. GEP is providing a new diagnostic marker and could identify some therapeutic targets, having a major impact on the way we diagnose and treat Ph+ leukaemia patients. Although considerable work remains to be done before these predictions are realized, our capacity to obtain these type of data continues to mature at a rapid speed. Thus, the fruits of GEP should soon help us to accurately identify specific leukaemia subtypes, abnormally expressed or

spliced genes and to select targeted therapies. For instance, recent GEP studies have identified a new ALL subtype with a gene-expression pattern resembling that of *BCR-ABL1*-positive ALL. This newly recognized group includes 15–20% of all precursor B-ALL cases and is associated with an unfavourable outcome.

1.4 9p21 LOCUS (*INK4A/ ARF/ INK4B/ ANRIL*)

The chromosome 9p21 segment is a 40-kb region encoding two members of the *INK4* family of Cyclin-Dependent Kinase inhibitors, *CDKN2B* ($p15^{INK4B}$, ENSG00000147883) and *CDKN2A* ($p16^{INK4A}$, ENSG00000147889), and one other related gene *ARF* ($p14^{ARF}$), transcribed in an Alternative Reading Frame compared to *CDKN2A*; all of them encode critical factors for the regulation of cell cycle and for the influence on key physiological processes such as replicative senescence, apoptosis, and stem-cell self-renewal. 9p21 also contains a newly annotated non-coding RNA, termed *ANRIL* (*CDKN2BAS*, ENSG00000240498), which spans 126.3 kb and overlaps at its 5' end with *CDKN2B*, and it is transcribed from the opposite strand to *CDKN2A/B* (Fig. 1.4).

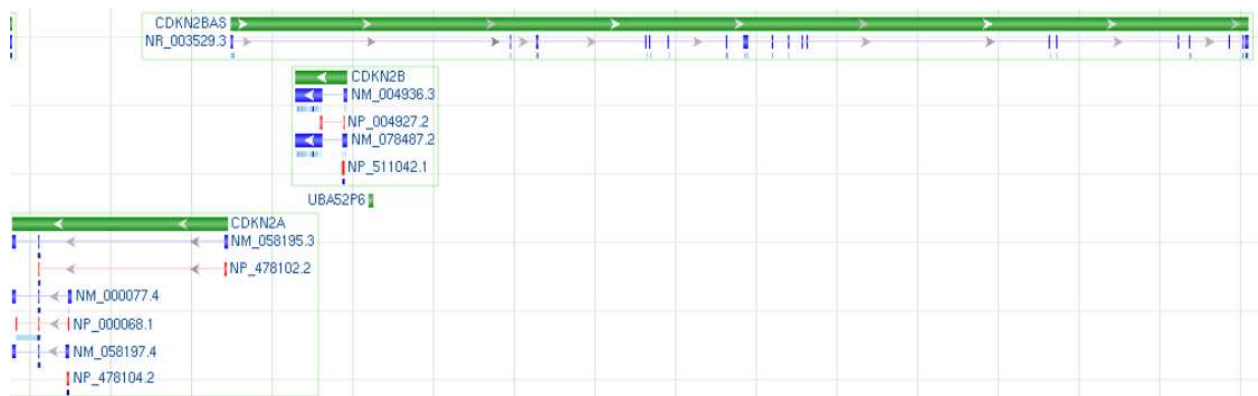


Fig. 1.4 9p21 Locus NC_000009.11 *Homo sapiens* chromosome 9, GRCh37.p2 primary reference assembly MapViewer representation. Green bars show the length and the gene transcription verse. Blu bars show exons and red bars represent gene translation. Modified from NCBI MapViewer <http://www.ncbi.nlm.nih.gov/nucore/224589821>

CDKN2B and *CDKN2A* arose from a gene duplication event and are consequently very similar (77% amino acid sequence identity in humans). *CDKN2A* and *ARF* have different promoter and different first exons (1α and 1β , respectively) (Fig. 1.5), giving rise to products in alternate reading frames with no homology at the protein level and with distinct functions in the cells.

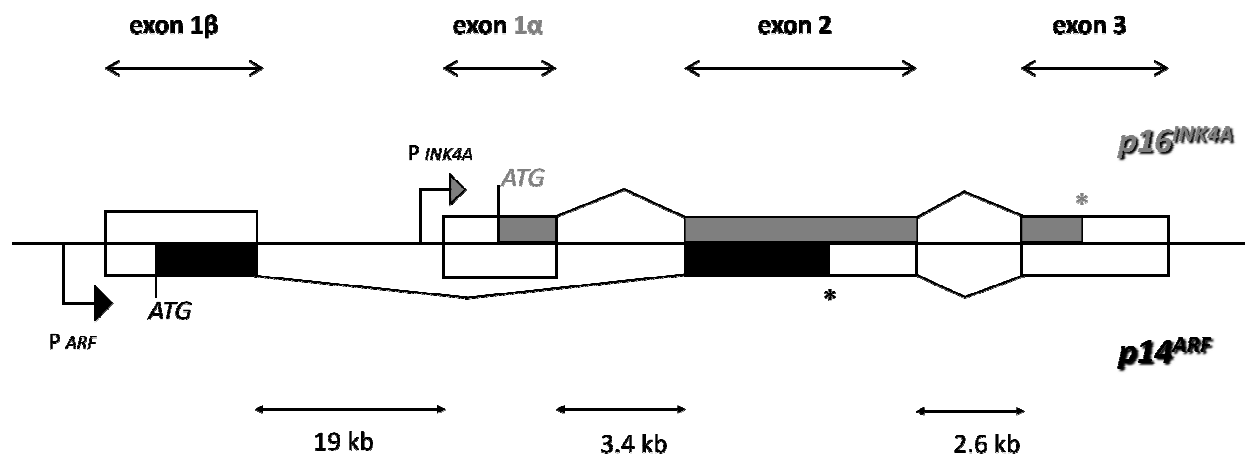


Fig. 1.5 Organization of the *CDKN2A/ARF* locus. The coding regions of *p16^{INK4A}* are shown in gray, and those of *p14^{ARF}* are in black. The alternative first exons are transcribed from different promoters (arrows). *Denotes the *p16^{INK4A}* and *p14^{ARF}* termination codons. Exon 1 β of the *p14^{ARF}* gene is 19 kb upstream of exons 1 α of the *CDKN2A* (*p16*) gene. Intronic sizes derived from <http://snpper.chip.org> are indicated. Modified from Stuart J.Gallagher, *Int J Biochem Cell Biol*, 2006 ³⁸.

Exons 1 α , 2, and 3 encode *p16^{INK4A}*, which induces G1 cell cycle arrest via the Rb pathway. Exons 1 β , 2, and 3 encode *p14^{ARF}*, which inhibits p53 degradation via binding to Mdm2 ³⁹. Therefore, the 9p21 *locus* has a unique gene structure that generates two distinct open reading frames (ORFs) that initiate in different first exons and continue in alternative reading frames in a common second exon. This unusual utilization of overlapping exonic sequences in mammalian cells enables a single gene to encode two completely unrelated protein products ⁴⁰. Adjacent to the gene *CDKN2A*, in a more centromeric position, two exons encode for another tumor suppressor gene: *CDKN2B* (*p15^{INK4B}*).

Therefore on chromosome 9p21.3 there are two main transcripts of *CDKN2A locus*, isoforms '1' and '4' (Appendix A), each contains three exons and spans: 7,382 (according with NCBI, http://www.ncbi.nlm.nih.gov/nuccore/NM_000077.4) and 26740 bp (<http://www.ncbi.nlm.nih.gov/gene/1029>), respectively. They encode proteins of 156 and 173 amino acids; isoform '1' encodes *p16* (*INK4A*), while isoform '4' encodes *p14* (*ARF*), a protein that is structurally unrelated to *p16* but acts in cell cycle G1 control by stabilizing the tumor suppressor protein p53.

The chromosome band 9p21 shows a significant evolutionary conservation only in the exon 2, where a multispecies sequence alignment shows 76% sequence identity and 94% sequence

similarity across six mammalian species. While exon 2 of both alternative reading frames overlaps, the drop in conservation beyond the coding region of isoform 4 suggests that this isoform is more responsible for the observed conservation⁴¹.

The *CDKN2A/ARF* locus encodes proteins that function upstream of both RB and p53. p53 and RB are at the heart of the two main tumour-suppressor pathways that control cellular responses to potentially oncogenic stimuli. Each pathway consists of several upstream regulators and downstream effectors. The pathways interact at several points, and cross-regulate each other (Fig. 1.6). p53 is a transcription factor that regulates apoptosis and cellular senescence by inducing the transcription of specific genes; the RB pathway directly regulates the cell cycle and hence cellular senescence, but is also important in apoptosis, probably by interacting with the p53 pathway.

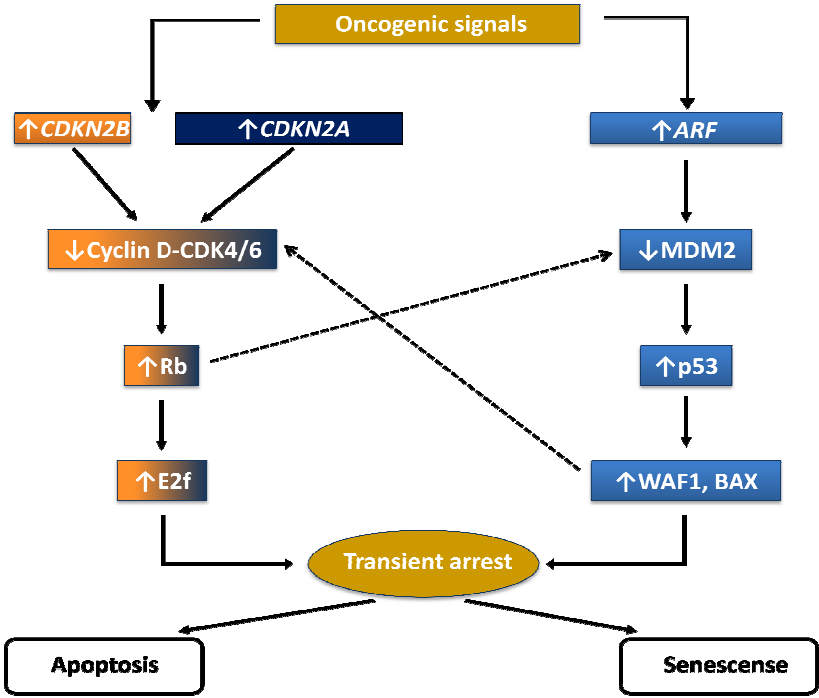


Fig. 1.6 The *CDKN2A/ARF/CDKN2B* locus and the p53 and RB tumour-suppressor pathways. Members of the INK4 family of cyclin-dependent kinase inhibitors bind to and inactivate CDK4/6. ARF inhibits MDM2, resulting in p53 stabilization. Modified from Judith Campisi, Nature Reviews Cancer, 2003⁴².

In the p53 pathway, signals such as DNA damage induce *ARF*. The tumor suppressor activity of *ARF* is largely ascribed to its ability to regulate p53 in response to aberrant growth or oncogenic stresses such as c-MYC activation. *ARF* increases p53 levels by sequestering Mdm2, which facilitates the degradation and inactivation of p53. One mechanism that has been proposed to explain how Mdm2 regulates p53 is that it acts as an E3 ubiquitin ligase to target p53 for proteasomal degradation. Although strong biochemical and genetic evidence link *ARF* and p53 in tumor suppression, several p53-independent functions of *ARF* have also been reported. Moreover, *ARF* has been reported to interact with multiple proteins other than Mdm2, including E2F-1, MDMX, HIF-1 α , topoisomerase I, MYC, and nucleophosmin (NPM). p53 has both transactivation and transrepression activity, and so controls the transcription of numerous genes. Among the p53 target genes are *WAF1*, an inhibitor of cyclin-dependent protein kinases (CDKs) that, among other activities, causes cell-cycle arrest, and *BAX*, which promotes apoptotic cell death.

CDKN2A/B inhibit the complex between cyclin-dependent kinases 4/6 (CDK4/6) and cyclin D (the binding of the INK4 proteins INK4A/INK4B to CDK4/6 induces an allosteric change that abrogates the binding of these kinases to D-type cyclins) that phosphorylate, and therefore inactivate, RB during the mid-late G1 phase of the cell cycle (RB phosphorylation interrupts its interactions with both histone deacetylase HDAC and E2F, enabling E2F to promote S phase entry). RB also controls the expression of numerous genes, although it does so primarily by recruiting transcription factors and chromatin remodelling proteins. One downstream consequence of RB activity is the inhibition of E2F activity, which is important for the transcription of several genes that are required for progression through the G1 and S phases of the cell cycle. RB also regulates p53 activity through a trimeric p53–Mdm2–RB complex^{42,43}.

The *ARF/CDKN2A/B* proteins are established tumour suppressors altered in a range of human cancers including familial cutaneous malignant melanoma, glioma (60%), head and neck cancers (50%) and bladder cancers (45%). High frequencies of 9p21.3 deletions have been documented in acute lymphoblastic leukemia ranging from 18% to 45%¹. Moreover, the chromosome 9p21.3 region adjacent to the *loci* encoding *CDKN2A* and *CDKN2B* is an important susceptibility locus for several diseases with a complex genetic background. Recent genome-wide association (GWA) studies have shown that single nucleotide polymorphisms (SNPs) in this region are associated with coronary artery disease (CAD), ischaemic stroke, aortic aneurysm, type II diabetes, glioma, and malignant melanoma. Candidate gene approaches have also reported SNPs in this region to be associated with breast, ovarian, and pancreatic carcinoma, melanoma, and

acute lymphoblastic leukaemia⁴⁴. Most of the risk variants in the chromosome 9p21 region identified by GWA studies are in non-coding regions, suggesting that their effects are likely to be mediated by influences on gene expression. Sequence variation can influence expression by *cis* or *trans* mechanisms⁴⁵.

Finally, the human *CDKN2A/ARF* locus encodes one additional transcript, isoform '3' (p12), and perhaps others as well. The *p12* transcript represents a p16^{INK4A}-isoform that shares the p16^{INK4A} promoter, 5' UTR, ATG and exon 1 α , but then uses an alternative splice donor within the first intron of p16^{INK4A} to splice to exon 2. The extra sequence contains a stop codon, and therefore the transcript produces a 12 kDa protein that shares the only first ankyrin repeat of p16^{INK4A}. In non-diseased tissue, this transcript is only expressed in pancreas but not other human tissues. The significance and function of this transcript is unknown, but based on crystal structure studies of INK4 proteins, p12 would not be predicted to bind cdk4 or cdk6. Even if the *p12* transcript does not encode a direct tumor suppressor protein, however, its intimate relationship with the *INK4A/ARF* locus makes it likely that its transcription influences the expression of p16^{INK4A} and/or p14^{ARF}⁴⁶.

1.4.1 *ARF/p14*^{ARF}

1.4.1.1 *Gene structure*

The *ARF* tumor suppressor transcript was first identified in humans in 1995 (p14^{ARF})^{47,48}, and its protein product confirmed in mice (p19^{ARF}) that same year⁴⁹. Its gene *locus* is on the short arm of chromosome 9 in humans, and on a corresponding location on chromosome 4 in mice. *ARF* is an alternate reading frame (ARF) product of the *CDKN2A* locus. It spans approximately 26 kb of genomic DNA and comprise three exons 1 β , 2, and 3 (Fig. 1.7). The p14^{ARF} open reading frame is derived from a distinct first exon (exon 1 β), originating approximately 19 kb centromeric to the first exon of p16^{INK4A} (exon 1 α) and 23 kb centromeric to exon 2. Exon 1 β , under the control of its own promoter, is spliced to the second and third exons that are separated by 3 kb of intronic sequence and are shared with p16^{INK4A}. The open reading frame of the 1.1 kb *ARF* transcript is terminated within exon 2, with exon 3 comprising an untranslated 3' exon.



Fig. 1.7 ARF NM_058195.3 MapViewer representation. Green bar shows the length and the gene transcription verse. Blu bars show exons and red bars represent gene translation. Modified from NCBI MapViewer <http://www.ncbi.nlm.nih.gov/gene/1029#>.

1.4.1.2 ARF is a peculiar protein with unusual primary structure

The human protein comprises 173 amino acids with a molecular weight of 13,902 Da, whereas the mouse homologue of 169 amino acids has a molecular weight of 19,238 Da. Both proteins share only limited sequence homology (50%) that could explain some of their functional differences but both are capable of inducing cell cycle arrest at the G2/M as well as at G1/S cell cycle boundaries. The ARF proteins show significant sequence similarity within their amino-terminal 14 amino acids (11/14 identity), and this region retains many of the known ARF functions, including nucleolar localization, Mdm2 binding and ability to induce cell cycle arrest. The carboxy-terminus of ARF also encodes functional domains. In particular, the C-terminal region (amino acids 130–169) of p19^{ARF}, that is missing in p14^{ARF} is involved in p53-independent apoptosis. The ability of p14^{ARF} to promote the sumoylation of its binding partners also involves the C-terminal nucleolar localization sequence of p14^{ARF}³⁸. p14^{ARF} and p19^{ARF} are both composed of more than 20% arginine residues conferring them highly basic and hydrophobic properties. Interestingly, there are no recognizable structural motifs in ARF proteins and the protein probably needs to form complexes with other molecules, both to be folded and for its charge to be neutralized at physiological pH. This probably explains the increasing number of yet identified ARF partners. Mouse p19^{ARF} contains only one lysine and human p14^{ARF} has none. Mouse p19^{ARF} and human p14^{ARF} contain only single internal methionine residues (Met45 and Met48 respectively). Translational initiation from these methionine residues produces both in mouse and human a short form of the protein that, when overexpressed, localizes to mitochondria (smARF). Nevertheless, full-length ARF preferentially localizes in the nucleoli thanks to nucleolar localization signals (NoLS). p19^{ARF} contains a unique NoLS in its

exon1 β (aa 26-37) which deletion induces the nuclear translocation of the protein. The situation is more complex for p14^{ARF} as two NoLS have been identified in the protein. The first one localized in exon 1 β plays a key role in the antiproliferative function of p14^{ARF} as its deletion inhibits the ability of p14^{ARF} to stop the cell cycle and to bind Mdm2. The second one stands in exon 2 (aa 83-101) and is involved in the ability of p14^{ARF} to promote the sumoylation of its binding partners⁵⁰.

1.4.1.3 Expression and turnover

Expression

Normal cells contain low levels of ARF but the expression of a variety of proliferation-promoting proteins, including Myc, E2F, E1A, oncogenic Ras and v-Abl, upregulate ARF as part of a checkpoint response conveying on the well known p53-Mdm2 pathway. The discovery of multiple ARF interactors and the observation that, aside oncogenic stimuli, also viral, genotoxic, hypoxic and oxidative stresses activate an ARF-dependent response, suggest that ARF could exert a wider role to protect the cell. It is becoming clear that the ARF response is quite complex and is likely accomplished by the interaction with a multitude of different cellular partners that in part explain the p53-independent activities of ARF⁵¹. ARF is ubiquitously expressed and is elevated in cells lacking p53. In human cells p14^{ARF} expression levels remain low as cells near senescence and p14^{ARF} depleted cells still undergo a senescence-like arrest when challenged with Ras⁴⁶. Not much is known about the regulation of p14^{ARF} expression. p14^{ARF} transcription is induced by E2F1, but not by oncogenic Ras and while p14^{ARF} transcription is inhibited by Tbx-2, Tbx-3 and Cbx-7, it is not down-regulated by Bmi-1^{38,46,52}.

Degradation

ARF is a relatively stable protein, with half-life estimations ranging from approximately 1–6 h. p19^{ARF} and p14^{ARF} undergo amino-terminal ubiquitination and their degradation depends on the ubiquitin-proteasome pathway, and may be enhanced by Mdm2 expression. Stress induced nucleoplasmic redistribution of ARF destabilises the protein and targeting of a p14^{ARF} fragment encompassing amino acids 2–29 to the nucleolus increased its half-life⁵³. Consistent with these data, ARF-B23 complex formation, which restricts ARF to the nucleolus, stabilises ARF by blocking its ubiquitination⁵⁴. In contrast, Mdm2-ARF complex formation occurs preferentially in the nucleoplasm and this may allow for enhanced ARF ubiquitination and proteasomal degradation³⁸.

1.4.1.4 Biological functions

The ARF tumour suppressor is a critical activator of the p53 pathway

The ARF tumour-suppressor protein suppresses aberrant cell growth in response to oncogene activation by inducing the p53-pathway. The ARF induction of p53 is mediated through two ubiquitin ligases, Mdm2, a RING finger oncoprotein and ARF-BP1/Mule (*ARF-binding protein 1/Mcl-1 ubiquitin ligase E3*), a HECT (*homology to E6-AP C-terminus*) containing protein. Both Mdm2 and ARF-BP1 act as specific E3 ubiquitin ligases for p53, are highly expressed in various types of tumours, and have the potential to abrogate the tumour-suppressor functions of p53. ARF associates with Mdm2 to inhibit the ubiquitination, nuclear export and subsequent degradation of p53. It has been proposed that ARF physically sequesters Mdm2 in nucleoli, thus relieving nucleoplasmic p53 from Mdm2-mediated degradation⁵³. Recent data, however, suggest that nucleolar relocation of Mdm2 is not required for p53 activation and that the redistribution of ARF into the nucleoplasm enhances its interaction with Mdm2 and its p53-dependent growth-suppressive activity⁵⁴. This current model of ARF function supports the concept that nucleolar disruption contributes to p53 signalling since many stress signals perturb the nucleolus, causing the release of nucleolar proteins (including ARF, L5, L11, L23 and B23) that activate the p53 pathway. In addition to Mdm2, ARF-BP1 is a key regulator of the p53 cell cycle regulatory pathway; ARF-BP1 directly binds and ubiquitinates p53 in an Mdm2-independent manner. Silencing of ARF-BP1 extended the half-life of p53, resulted in the transcriptional activation of the p53 targets, p21^{Waf1} and BAX, and activated a p53-dependent apoptotic response. Unexpectedly, ARF-BP1 also ubiquitinates and promotes the degradation of the anti-apoptotic bcl-2 family member, Mcl-1, and down-regulation of ARF-BP1 expression can also render cells more resistant to killing by genotoxic agents. Thus, ARF-BP1 has been assigned both anti-apoptotic (via p53 degradation) and pro-apoptotic (via Mcl-1 degradation) functions. Whilst the effect of ARF on ARF-BP1-mediated Mcl-1 degradation is presently unexplored, the divergent roles of ARF-BP1 may be regulated by ARF. Following aberrant oncogene activation, ARF expression is induced and inhibits ARF-BP1 activity toward p53 in the nucleus, thereby leading to p53-dependent cell cycle arrest or apoptosis. In the cytoplasm, where ARF is not abundant, oncogene activation may lead to ARF-BP1 mediated Mcl-1 degradation further promoting apoptosis. ARF also enhances p53 function by promoting the phosphorylation and inhibiting the transcriptional activity of the RelA NF- κ B subunit. The NF- κ B family of transcription factors display anti-apoptotic activity and antagonise the p53 pathway through induction of Mdm2 and repression of p53. Thus, by counteracting the functions of Rel A, ARF increases the effectiveness of the p53 pathway³⁸.

Nucleolar functions of the ARF tumour suppressor

ARF is predominantly a nucleolar protein and rather than residing in inactive “storage” within the nucleolus, ARF may regulate ribosome biogenesis by retarding the processing of early 47S/45S and 32S rRNA precursors⁴⁶. These effects do not depend on Mdm2 or p53 but may involve the interaction of ARF with B23. B23 is an abundant nucleolar endoribonuclease that is required for the maturation of 28S rRNA and interacts with many cellular proteins, including p53, Mdm2, ARF, NPM3 and the BARD-BRCA1 ubiquitin ligase. The interaction of ARF and B23 retains both proteins in the nucleolus, bound to the pre-60S ribosome, where they appear to influence ribosome biogenesis and/or function. The actual role of the nucleolar ARF–B23 complex remains unclear; p19^{ARF} can promote the ubiquitination and degradation of B23, whereas p14^{ARF} had no effect on B23 protein expression. In response to cytotoxic drugs, such as actinomycin D and DNA damaging agents, including UV light, B23 and ARF undergoes nucleoplasmic redistribution, where Mdm2 and B23 compete for ARF binding. The nucleoplasmic translocation of ARF and B23 promotes the formation of the B23-Mdm2 and the ARF-Mdm2 binary complexes and induces potent activation of the p53 pathway. Thus, ARF may directly access ribosome function to inhibit cell growth through its nucleolar association with B23, and it may regulate the p53 cell cycle pathway via its nucleoplasmic interaction with Mdm2 and ARF-BP1³⁸.

ARF regulates the protein turnover and function of most of its interacting partners

ARF can also suppress the proliferation of mouse cells lacking both Mdm2 and p53, implying interactions with other regulators. Consistent with these findings, the spectrum of tumours seen in mice lacking ARF and p53, with or without Mdm2, was significantly greater than that associated with animals lacking either gene³⁸.

During the last years many efforts have been attempted in search of ARF partners that could partly explain the p53-Mdm2 ARF independent functions. In addition to its first “spouse” Mdm2, the ARF interactors “harem” consists of something like 30 different proteins involved in various cellular activities (Fig. 1.8, Tab. 1.2): proteins involved in transcriptional control, such as E2Fs, DP1, c-Myc, p63, Hif1a, Foxm1b, nucleolar proteins such as nucleolin/ C23 and nucleophosmin (NPM/B23), viral proteins such as HIV-1Tat, proteins involved in copper metabolism like COMMD1, proteins involved in chromosomal stability and/or chromatin structure such as Topoisomerase I, Tip60, and WRN helicase, ubiquitin ligases like Ubc9 (the E2 ligase required for sumoylation), Mdm2 and ARF-BP1/Mule, (E3-ubiquitin ligases)⁵¹.

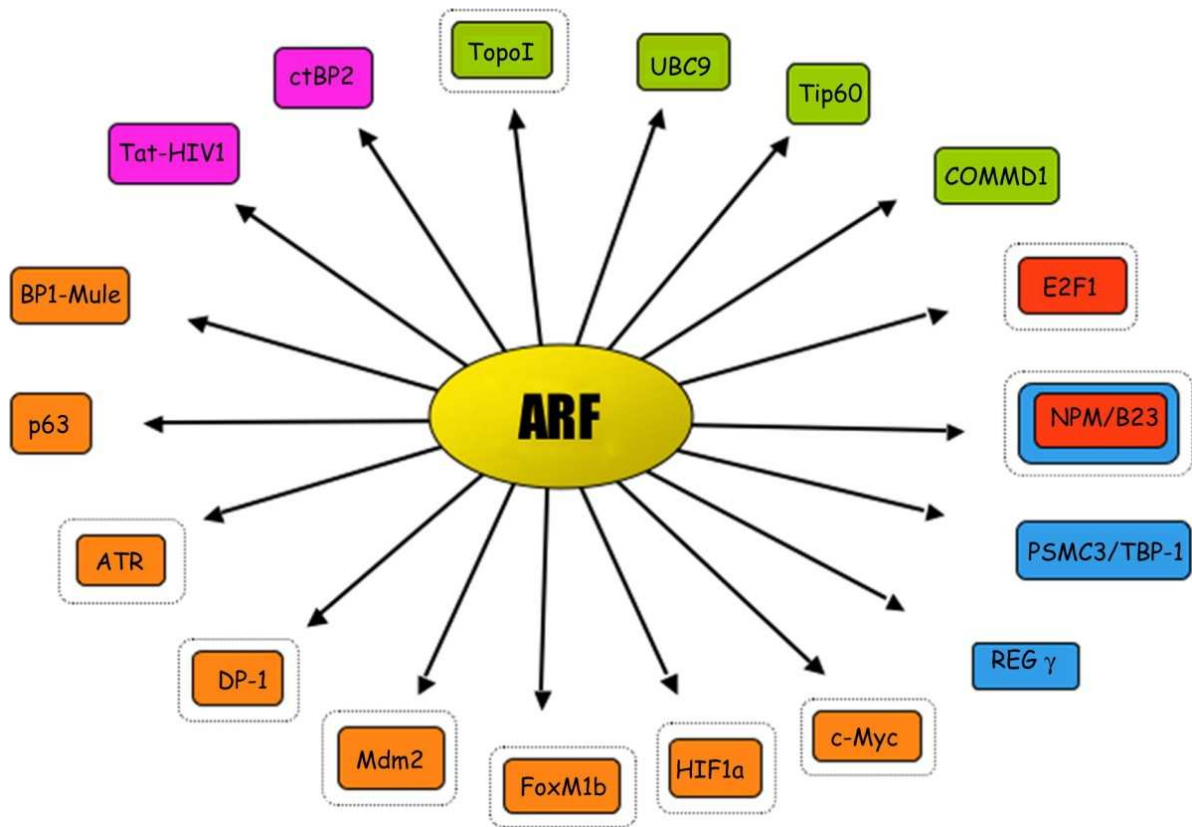


Fig. 1.8 A schematic view of the “ARF harem”. ■ Orange is for partners whose activity is blocked by ARF. ■ Red is for partners that are induced to proteasome and ubiquitin-dependent degradation by ARF. ■ Pink is for partners that are induced to proteasome and ubiquitin-independent degradation by ARF. ■ Green is for partners whose activity or stability are positively regulated by ARF. ■ Blue is for partners that regulate ARF protein turnover. A second black circle indicate nucleolar sequestration ⁵¹.

Tab. 1.2 Cellular protein partners of the ARF tumour-suppressor protein, and its biological effect. Modified from Stuart J.Gallagher, *Int J Biochem Cell Biol*, 2006 ³⁸.

ARF binding partner	Biological effect of ARF binding
APA-1	No apparent effects
ARF-BP1/Mule1	Inhibition of ARF-BP1 ubiquitin ligase activity
B23	Degradation of B23, inhibition of B23 shuttling
BCL6	Inhibition of BCL6 transcriptional activity
CARF	Enhanced ARF-mediated cell cycle arrest
c-MYC	Inhibition of c-MYC transactivation
COMMD1	Poly-ubiquitination of COMMD1
CtBP2	Degradation of CtBP2;
DP-1	Inhibition of ARF-induced E2F proteolysis
E2F-1, -2, -3	Degradation of E2F
Foxm1b	Inhibition of Foxm1b transactivation
HIF-1 α	Inhibition of HIF-1 α transactivation
HIV1-Tat protein	Ubiquitin-independent degradation of the HIV1-Tat protein
Mdm2	Inhibition of mdm2 ubiquitin ligase activity
MdmX	Enhanced p53 transactivation
Neurabin	Enhanced ARF-mediated cell cycle arrest
p120 ^{E4F}	Enhanced ARF-mediated cell cycle arrest
Pex19p	Inhibition of p19ARF, pex19p does not bind human ARF
SUMO	Conjugation of SUMO to p53 and MDM2
Tat-binding protein-1	Induces ARF stabilization
Topoisomerase I	Enhanced topoisomerase I activity
Ubc9	Probable involvement in p14ARF-mediated sumoylation
Werners helicase	Nucleolar exclusion of Werners helicase

Although the actual mechanism by which ARF affects the activity of its partners is still unclear, the functional consequence is, quite invariably, inactivation.

For some targets, ARF interaction causes alteration of stability. For example, B23/NPM and E2F become degraded by the proteasome in an ubiquitin-dependent manner, while the CtBP2 antiapoptotic transcriptional co-repressor and HIV-1 Tat become degraded by the proteasome in

a ubiquitin-independent manner. Other targets changes their localization like E2Fs, c-Myc, Foxm1B, Mdm2, ATR, DP-1, Hif1a upon ARF expression. Only few others, like Tip60, Topo I and COMMD1 become activated or stabilized. Finally, most of the partners become sumoylated although a precise function to this modification has not yet been assigned.

Particularly interesting is the inhibitory effect that ARF exerts on oncogenes such as members of the E2F family, required both for cell-cycle progression and to mediate ARF oncogenic activation, suggesting a potential role of these interactions as being part of a negative feedback loop. In a series of reports ARF was shown to interact with E2F1, and this interaction prevented the formation of active E2F1 transcriptional complexes, inhibited E2F1 transactivation potential, and promoted the proteasome-dependent degradation of E2F1, 2 and 3. In line with a role of ARF in promoting ubiquitin-dependent degradation of its partners is the observation that NPM/B23, an abundant nucleolar multifunctional protein involved in ribosome biogenesis, is a molecular target of ARF. The vast majority of ARF appears localized in nucleoli, tightly associated with NPM/B23. There is a regulative loop between ARF and B23, in which degradation and inhibition of both proteins is finely and tightly modulated by external stimuli. In such a situation, ARF serves a dual function to restrain both growth and proliferation.

Interestingly, ARF appears to mediate also ubiquitin-independent degradation like that of the antiapoptotic transcriptional co-repressor C-terminal binding protein 2 (CtBP2) and of the HIV1-Tat protein. Interestingly, Mdm2 has been shown to ubiquitinate HIV1-Tat, although, in this case, ubiquitination determines an increase of the Tat-mediated transactivation properties. This lead to the speculation that ARF could act on HIV-1Tat in two ways: directly mediating its degradation and inhibiting the Mdm2 activity versus Tat, thus blocking viral transcription. This hypothesis would intriguingly fit with the ARF role in viral defense.

As mentioned above, in some cases, ARF is able to stabilize its partners from proteasomal degradation. In a quite recent study, it has been described the ARF's ability to induce a non-classical poly-ubiquitination of a new interacting partner, the COMMD1 factor, a multifunctional protein involved in copper metabolism and apoptosis. While in normal conditions COMMD1 is degraded by the proteasome, ARF coexpression leads to a stabilization of the protein through its poly-ubiquitination on K63 lysine of the ubiquitin peptide.

Altogether, although these observations reinforce the idea that the ARF antioncogenic activity could be partly exerted through the cellular degradation machinery. In this sense, ARF interaction with the proteasome could serve dual roles: on one side it is necessary to regulate ARF protein turnover, while, on the other side, it could play a role in bringing ARF interacting partners in contact with the ubiquitin/proteasome machinery⁵¹.

ARF promotes the sumoylation of its binding partners

ARF can promote the conjugation of the small ubiquitin-like protein SUMO-1 to its binding partners, including Mdm2 and B23. Sumoylation is analogous to ubiquitination, and is the process by which the SUMO protein is conjugated to a target protein. The effects of this modification are target specific and include control of protein stability, formation of subnuclear structures and regulation of transcription factor activities. The diverse functional consequences of sumoylation provide a possible explanation for the versatility of ARF downstream effects. Although, ARF can promote sumoylation *in vivo*, the biological impact of target sumoylation has not been demonstrated for ARF binding partners and sumoylation sites on these proteins remain unidentified. However, the fact that a subset of melanoma-associated p14^{ARF} mutations failed to sumoylate Mdm2 *in vivo*, suggests that sumoylation may provide a mechanism for the diverse actions of the ARF tumour-suppressor protein³⁸.

1.4.2 CDKN2A/INK4A/p16^{INK4A}

CDKN2A (cyclin dependent kinase inhibitor 2A) is a member of the Inhibitor of cyclin-dependent Kinase 4 (INK4) family of proteins which also includes p15^{INK4B}, p18^{INK4C} and p19^{INK4D}. The INK4 proteins are roughly 40% homologous to one another, but individual members are highly conserved across species. Family members have in common a basic structural motif: a series of ankyrin repeats responsible for interaction with cyclin-dependent kinases 4/6 (CDK4/6). *CDKN2A* gene encompasses 6.6 kb and is encoded, how previously said, by three exons: 1 α , 2 and 3 (Fig. 1. 9).

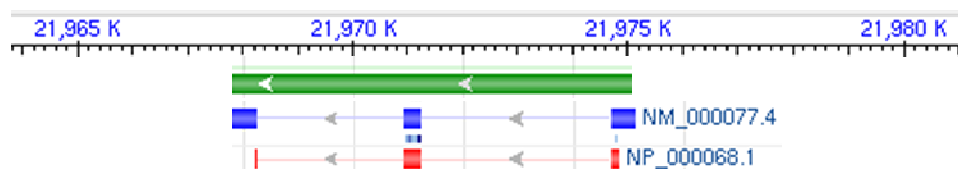


Fig. 1.9 CDKN2A NM_000077.4 MapViewer representation. Green bar shows the length and the gene transcription verse. Blu bars show exons and red bars represent gene translation. Modified from NCBI MapViewer <http://www.ncbi.nlm.nih.gov/gene/1029>.

The human protein comprises 156 amino acids with a molecular weight of ~15.8kD. Its structure consists of repeated ‘ankyrin’ subunits containing two antiparallel helices and a loop, creating a cleft that binds *CDK4* or *CDK6*. The first helix of each pair and the last several aminoacids of each β -hairpin loop are exposed to the cdk binding site; helix 2 and some loop residues provide structural support (Fig. 1.10)⁵⁵.

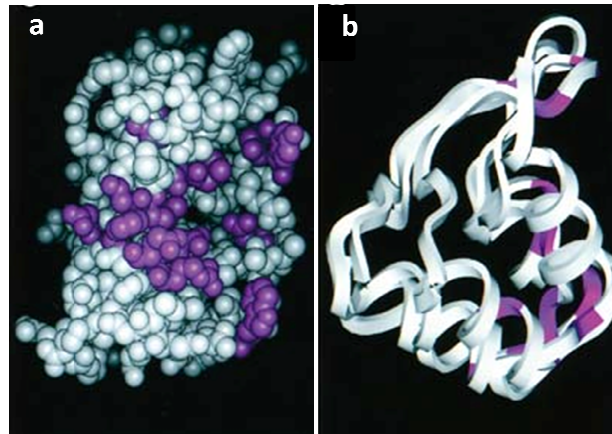


Fig. 1.10 Structural models of p16. Images **a**, on the left shows the front (binding cleft, helices to the left, loops to the right) of the p16 structure, while **b**, on the right, shows the back (helices to the right) of the p16 structure. **a** and **b** show in purple the aminoacids in the binding cleft that contact CDK6. In **b**, the p16 backbone is rendered as a ribbon, and the molecule is viewed down the axis of the cleft. Modified from M S Greenblatt, *Oncogene*, 2003⁵⁵.

CDKN2A expression levels are low in normal tissue. Following controversy concerning the cellular localization of p16 it has recently been shown that p16 can be expressed in both the nuclear and cytoplasmic compartments and that both nuclear and cytoplasmic p16 forms complexes with *CDK4* and *CDK6*. Cytoplasmic p16 occurs in two forms whilst nuclear p16 appears predominantly in just one. p16 is upregulated in cells during *in vitro* senescence consistent with a role in ageing. Expression of p16 is often lost during progression of a tumour. INK4 binding to CDK4/6 inhibits its kinase activity and thereby arrests progression through the cell cycle in mid-late G1 (Fig. 1.11). Induction of p16 leads to a competition with D-cyclins for association with CDK4/6, shifting the CDK4/6 kinases to inactive complexes containing p16 instead of active complexes with cyclin D. Inhibition of CDK4/6 kinase activity prevents pRB phosphorylation leading to restraint of E2F transactivation of the expression of genes important

for entry into S-phase (Fig. 1.11). The expression of pRB is essential for transducing p16's signal to cause a cell cycle arrest.

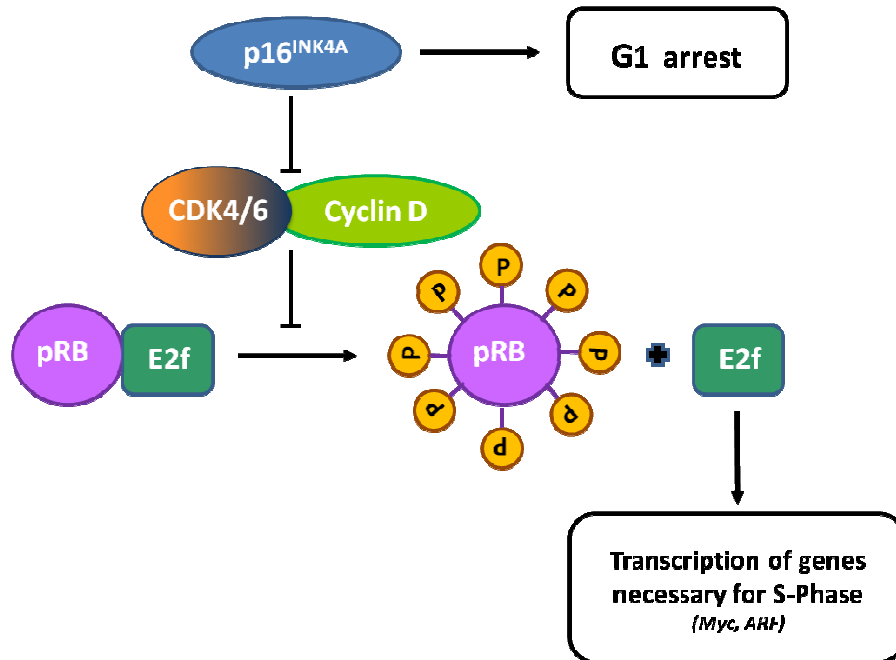


Fig. 1.11 p16^{INK4A}/pRB pathways. p16^{INK4A} inhibits the complex between cyclin-dependent kinase 4/6 and cyclin D that phosphorylate, and therefore inactivate, RB during the mid-late G1 phase of the cell cycle. Hyperphosphorylated pRB dissociates from E2F1 transcription factor enabling transcription of S-phase genes, such as *myc*, as well as *ARF*.

In the absence of pRB, forced induction of p16 does not cause cell cycle arrest. As a result, in many tumors that retain p16 expression, especially gliomas, other alterations occur in the p16-cyclinD-CDK4-pRB pathway: loss of pRB expression or overexpression of CDK4 or cyclin D1. A negative feedback loop exists between pRB and p16: transcription of p16 is repressed by pRB. Therefore, it is not surprising that cells with inactive pRB frequently have elevated levels of p16 expression, although in this setting p16 becomes ineffective in restraining cell proliferation⁵⁶. According to repository data into UVM BioDesktop-CDKN2a Database Project (<https://biodesktop.uvm.edu/perl/p16> and <http://atlasgeneticsoncology.org/Genes/CDKN2aID146.html>) the majority of mutations identified so far in *CDKN2A* are located in exons 1a and 2. These mutations affect either p16 alone or both p16 and p14^{ARF} and appear to be associated solely with

susceptibility to melanoma. A small number of mutations have been identified in exon 1b which appear to affect p14^{ARF} alone.

Germline mutations affecting the *CDKN2A* locus have been described for a number of melanoma-astrocytoma syndrome families. Concurrent loss of both p14 and p16 may therefore be responsible for the development of nervous system tumors in this syndrome. In one family a deletion affecting the p14^{ARF}-specific exon 1β was observed which was not predicted to affect p16 function suggesting abnormal p14^{ARF} function alone may be the key factor in this family.

According to COSMIC somatic mutations of *CDKN2A* are found in approximately 24% of sporadic melanoma and around 22% of tumours of the central nervous system dependent on tumour type.

(<http://atlasgeneticsoncology.org> / <http://atlasgeneticsoncology.org/Genes/CDKN2aID146.html>)

1.4.3 *CDKN2B/INK4B/p15^{INK4B}*

CDKN2B (cyclin-dependent kinase inhibitor 2B) lies adjacent to the tumor suppressor gene *CDKN2A* in a region that is frequently mutated and deleted in a wide variety of tumors. This gene encodes a cyclin-dependent kinase inhibitor, which forms a complex with CDK4 or CDK6, and prevents the activation of the CDK kinases, thus the encoded protein functions as a cell growth regulator that controls cell cycle G1 progression. The expression of this gene was found to be dramatically induced by TGF beta, which suggested its role in the TGF beta induced growth inhibition. Two alternatively spliced transcript variants of this gene, which encode distinct proteins, have been reported (Fig. 1.12). The shorter protein has a distinct C-terminus when compared to longer isoform.



Fig. 1.12 *CDKN2B* MapViewer representation. Green bar shows the length and the gene transcription verse. Blu bars show exons and red bars represent gene translation. Modified from NCBI MapViewer <http://www.ncbi.nlm.nih.gov/gene/1030>

The human protein (the longer one) comprises 138 amino acids with a molecular weight of 14,722 Da; like *CDKN2A* has a basic structural motif of a series of four ankyrin repeats responsible for protein–protein interactions.

Whereas the tumour suppressor functions for *CDKN2A* and *ARF* have been firmly established, the role of *CDKN2B* remains ambiguous. However, many 9p21 deletions also remove *CDKN2B*, so we hypothesized a synergistic effect of the combined deficiency for *CDKN2B*, *ARF* and *CDKN2A* ⁵⁷.

In leukemias, the *CDKN2B* gene is commonly inactivated in association with promoter region hypermethylation involving multiple sites in a 5'-CpG island, whereas point mutations are rare ⁵⁸. Hypermethylation of the *CDKN2B* gene was more frequent in cases with T-cell origin ALL (46.2%), but similar among children with B-cell origin ALL (13.0%) and AML (18.8%). Hypermethylation of *CDKN2B* may be involved in the pathogenesis of T-cell origin ALL, but not in that of AML or B-cell origin ALL ⁵⁹.

1.4.4 *ANRIL/CDKN2BAS (CDKN2B-AS1 CDKN2B antisense RNA 1)*

In the 9p21 *locus* overlaps a newly annotated non-coding RNA (ncRNA), termed *ANRIL*, for “antisense noncoding RNA in the *INK4 locus*”. *ANRIL* spans 126.3 kb, with a first exon located in the promoter of the *ARF* gene and overlapping at its 5' end the two exons of *CDKN2B*. It consists of 20 exons subjected to alternative splicing, that are transcribed in the anti-sense orientation (Fig. 1.13).

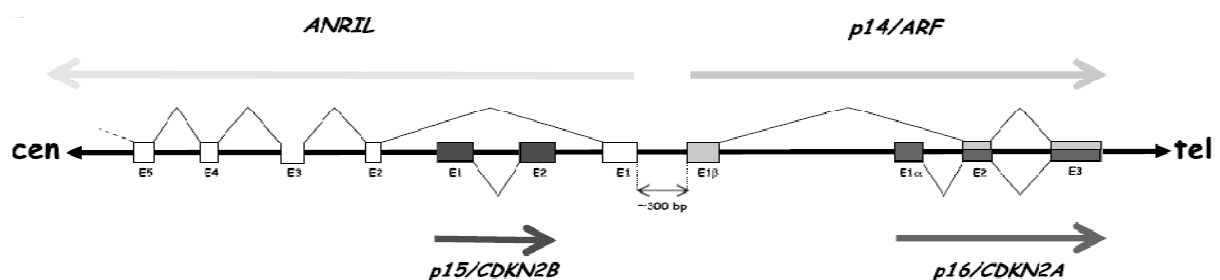


Fig. 1.13 A genomic organization of the 9p21 gene cluster. Boxes, location of exons (approximately to scale). Exons 1 α , 2, and 3 of *CDKN2A* encode p16 protein, whereas exon 1 β , spliced to exons 2 and 3 of *CDKN2A* in a different reading frame and transcribed using a different promoter, encodes p14^{ARF} protein. The *ANRIL* gene overlaps the two exons of *CDKN2B* and is transcribed in the orientation opposite to the *CDKN2B-CDKN2A-ARF* gene cluster. Exon 1 of *ANRIL* is present about 300 bp upstream of the transcription start site of *ARF* (exon 1 β) ⁶⁰.

Up to now three *ANRIL* variants were identified. Full-length *ANRIL* (3834 bp), deposited under GenBank accession number DQ485353, encompasses the first 12 exons plus exons 14 to 20. At least 2 shorter variants of *ANRIL* that end with an alternative exon 13 have been reported, DQ485454 and EU741058. DQ485454 (2659 bp) comprises the first 12 exons and an alternative exon 13, whereas EU741058 (688 bp) encompasses exons 1, 5 to 7, and 13 (Fig. 1.14).

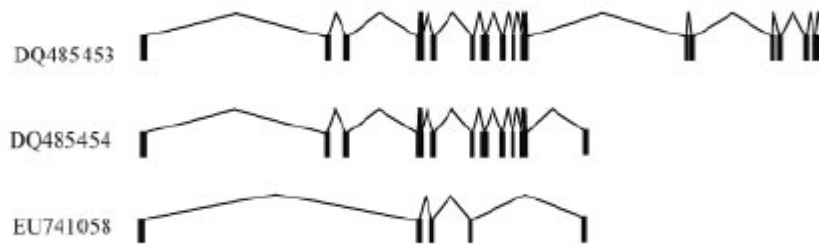


Fig. 1.14 Physical Map of the 9p21.3 region. *ANRIL* produces alternative transcripts DQ485453, DQ485454, and EU741058. Modified from Olga Jarinova, *Arterioscler Thromb Vasc Biol*, 2009⁶¹.

Exon sequences of *ANRIL* are highly conserved in primates, furthermore, several exons of *ANRIL* retain repetitive elements and encompasses multiple binding sites for transcription factors that regulate transcriptional repression. Thus, exons 7 and 12 of *ANRIL* consist entirely of Alu repeats; exons 8 and 16 of Long Terminal Repeats (LTRs); exon 14 of the LINE2 element (long interdispersed elements), and exons 4, 17, and 20 contain multiple MIR SINEs (short interdispersed elements). The presence of repetitive elements within the *ANRIL* gene is surprising because low complexity DNA sequences are not usually found within coding regions. A recent study suggests that the presence of repetitive elements is a common signature for novel genes originated from retroposition and exon shuffling, and degeneration of such elements is correlated with the increasing ages of the genes. Thus, *ANRIL* may have arisen relatively recently in mammalian evolution before the divergence of the primate lineage and may possess novel primate-specific functions. Alternatively, low sequence conservation of *ANRIL* may reflect high rates of primary sequence evolution suggested for long ncRNAs.

Tumour suppressor genes (TSGs) inhibiting normal cellular growth are frequently silenced epigenetically in cancer. DNA methylation is commonly associated with TSG silencing, yet mutations in the DNA methylation initiation and recognition machinery in carcinogenesis are

unknown. An intriguing possible mechanism for gene regulation involves widespread non-coding RNAs such as microRNA, Piwi-interacting RNA and antisense RNAs. Widespread sense-antisense transcripts have been systematically identified in mammalian cells, and global transcriptome analysis shows that up to 70% of transcripts have antisense partners and that perturbation of antisense RNA can alter the expression of the sense gene. Therefore, noncoding RNAs such as *ANRIL* can alter expression of associated protein coding genes through multiple mechanisms that include RNA interference, gene silencing, chromatin remodeling, gene co-suppression, imprinting, or DNA methylation. There is growing evidence of involvement of ncRNAs transcribed from the 9p21 locus in disease etiology. A natural *p15* antisense, *p15AS*, triggers transcriptional silencing in *cis* and in *trans* of *p15* through heterochromatin formation but not DNA methylation and shows increased levels of expression in acute myeloid leukemia cell lines; in addition the silencing persisted after *p15AS* was turned off, although methylation and heterochromatin inhibitors reversed this process ⁶². Broadbent and colleagues have demonstrated that *ANRIL* is expressed in many cell types known to be affected by atherosclerosis and suggested that this gene is a possible candidate gene at the 9p21 CAD risk locus ⁶³. Jarinova *et al.* examined the structure and function of 4 conserved noncoding sequences (CNS) present in the 9p21.3 locus and demonstrated that the CNS3 regulatory region acts as an enhancer and significantly increases reporter gene expression. This regulatory activity is attributable to the presence of a single nucleotide polymorphism, rs1333045, in strong LD with representative SNPs of the previously defined 9p21.3 risk region. They also found that *CDKN2B* may be directly affected by alterations in *ANRIL* expression related to the 9p21.3 risk haplotype ⁶¹. Despite the potential importance of *ANRIL*, limited information is available on its genetic architecture.

Moreover, it cannot rule out the possibility that *ANRIL* gene could be able to produce mature miRNAs or encode a small peptide. Additional studies are thus necessary to elucidate the putative role via a genetic (or epigenetic) mechanism of *ANRIL* gene on the regulation (deregulation in tumorigenesis) of the *p15/CDKN2B-p16/CDKN2Ap14/ARF locus* ⁶⁰.

1.5 *CDKN2A* LOCUS ALTERATIONS

Genetic alterations including chromosomal translocation, promoter hypermethylation, somatic mutation, and gene deletion are thought to play a key role in oncogenesis. Alterations of the 9p21 locus have been implicated in many types of cancer, indicating a role for the tumor suppressor genes *CDKN2A/ARF* and *CDKN2B*. Loss of cell proliferation control and regulation of the cell cycle are known to be critical to cancer development. It has been reported that *CDKN2A* and *CDKN2B* are frequently inactivated in various hematologic malignancies⁶⁴. The mechanism of *CDKN2A/ARF* inactivation in human cancers is somewhat tumor specific. Homozygous deletions at *CDKN2A/9p21* are common in bladder tumors and have been described in a variety of other sporadic tumors, including melanomas and gliomas. Pancreatic adenocarcinomas show inactivation of *CDKN2A* by either homozygous deletion or point mutation, whereas esophageal tumors commonly show inactivation by point mutation. A third mechanism of inactivation, transcriptional silencing by promoter hypermethylation, is commonly found in colorectal carcinoma. Point mutations have only rarely been identified in bladder tumors and promoter methylation, only infrequently³⁹.

An excellent 1998 review (Drexler, 1998) summarized the alterations of the INK4 family members in leukemias of primary samples and cell lines⁶⁵. Most alterations occur by inactivation of *CDKN2A* and *CDKN2B* due to hypermethylation of CpG islands in their promoters or by deletions in the 9p21 region, frequently involving all three genes. A high frequency of hypermethylation of the *CDKN2B* promoter occurs in AML (79%) including acute promyelocytic leukemia (APL) (73%) and MDS (42%). T-ALL and Pre-B-ALL cells often have hypermethylation of the *CDKN2B* promoter (44%) and deletions of the *CDKN2A* (33%) and the *CDKN2B* (32%) genes⁶⁶.

Inactivation of *CDKN2A* and *CDKN2B* is primarily a consequence of mono- or biallelic 9p21.3 deletion rather than promoter methylation or mutations⁶⁷.

In fact, the chromosomal region of 9p is a frequent site of loss or deletion in several human cancers, lung cancer, esophageal cancer, melanoma, in glioma (60%), head and neck cancers (50%) and bladder cancers (45%)⁶⁸. Homozygous deletion of *CDKN2A* has been suggested as the dominant mechanism of its inactivation in leukemogenesis⁶⁴. High frequencies of 9p21.3 deletions have been documented also in acute lymphoblastic leukemia ranging from 18% to 45%^{69-79,1}.

The majority of human tumors with homozygous deletion of this genomic region have large deletions of the whole *CDKN2A/ARF* locus often including the gene encoding p15 (*CDKN2B*)³⁹.

A majority of interstitial deletions in lymphoid leukemia have been indicated to be mediated by illegitimate V(D)J recombination between two ectopic heptamer-recombination signal sequences (RSS) sites in the 9p21 segment, where DNA double-strand breaks (DSBs) trigger 9p21 deletions at no specific DNA sequences, although they preferentially occur in or near the *CDKN2A locus*. At present, nucleotide sequences susceptible to DSBs in the *CDKN2A locus* remain unclear. Interestingly, recent studies have indicated that the packaging structure of chromatin affects the susceptibility to several DNA damaging agents. Thus, it is also possible that the open chromatin structure associated with the *CDKN2A* gene expression rather than nucleotide sequences might be responsible for susceptibility to DSBs⁸⁰.

CDKN2A and *CDKN2B* deletions might be also initiated by 'off-target' effects of the lymphoid mutagenic enzymes Recombination Activating proteins 1 and 2 (RAG1 and RAG2) or activation-induced cytidine deaminase (AID).

Therefore, another possibility is that the association between increased risk of ALL and inherited variation in *CDKN2A* and *CDKN2B* reflects its structural or sequence-based vulnerability as a substrate⁶⁷.

In ALL patient samples, the size and position of 9p21.3 deletions seem to vary substantially, but in most cases *CDKN2A* is co-deleted with *CDKN2B* and *MTAP* (methylthioadenosine phosphorylase)^{77,79,1}. The frequency of genomic deletions is of 21% in B-cell precursor ALL and 50% in T-ALL patients¹.

In childhood ALL, the reported frequencies of both heterozygous and homozygous deletions vary, 9% to 27% and 6% to 33% in B-cell precursor (BCP) ALL and 7% to 18% and 30% to 83% in T-ALL, respectively⁶⁴. Sulong et al. (2009) demonstrated that genomic deletion of *CDKN2A* is substantially more prevalent in childhood ALL (20% in BCP-ALL and 50% in T-ALL) than either mutation or methylation. They concluded that genomic deletion is the principal mode of *CDKN2A* inactivation in childhood ALL. In agreement with previous large studies^{1,77,81}, they found that the incidence of *CDKN2A* deletions was significantly higher among T-ALL patients compared with BCP-ALL patients, which included the proportion of biallelic deletions. Among BCP-ALL patients, they found a frequency of *CDKN2A* deletions of 21%, which was the same as Kawamata et al.⁸² (21%) but lower than Bertin et al.⁷⁷ (31%), Usvasalo et al.¹ (46%) and Mullighan et al.⁸¹ (34%). They also found that 50% T-ALL harbored a *CDKN2A* deletion, a frequency substantially lower than that reported by Bertin et al.⁷⁷ (78%), Mullighan et al.⁸¹ (72%), and Kawamata et al.⁸² (78%)⁶⁴.

Compared with childhood, adult ALL deletions characterization in the 9p21 chromosomal band were less studied. Paulsson K. et al (2008) found *CDKN2A* deletions in the 47% of the cases.

Their findings in adult ALL are strikingly similar to what has recently been reported in pediatric ALL. Mullighan *et al.*⁸¹ detected deletions of *CDKN2A* in a high proportion of childhood cases; a finding that was subsequently confirmed by Kuiper *et al.*⁸¹. Kawamata *et al.*⁸² also reported frequent *CDKN2A* deletions in pediatric cases, although they used a different sampling populations or differing analytical methods. The similarity between childhood and adult ALL as regards *CDKN2A* deletions was unexpected considering that the cytogenetic patterns of these disease entities are quite different; in particular, adult ALLs display a higher frequency of t(9;22)-positive cases but virtually lack the most common pediatric abnormalities, t(12;21) and high hyperdiploidy. It is thus possible that microdeletions in comparison may play a more general leukemia-promoting role and may be shared among different clinical, morphological and cytogenetic subgroups of ALL⁸³.

In addition to deletions, the *CDKN2A* locus can also be inactivated by epigenetic silencing through DNA methylation of the CpG islands associated with their respective or by point mutations, both resulting in gene silencing. Methylation of *CDKN2A* and *CDKN2B* (frequencies of 6% and 57%, respectively) seems to lack prognostic significance in ALL⁸⁴, and the rate of point mutations has been extremely low in ALL^{1,78,85-89}.

The frequency of hypermethylation of the *CDKN2A* promoter has been reported to vary from 0 to 40% in childhood ALL⁹⁰⁻⁹⁴. As reported data on *CDKN2A* alterations in childhood ALL are discrepant, it remains important to reveal the role of this gene in cancer development. *CDKN2A* hypermethylation is not a disease-specific event because it has been observed in the mononuclear cells from normal participants⁶⁴.

Mutation or methylation was rare, whereas genomic deletion occurred in 21% of B-cell precursor ALL and 50% of T-ALL patients¹.

1.6 SINGLE NUCLEOTIDE POLYMORPHISMS (SNPs) IN 9p21 LOCUS

Until recently, little was known about alterations of cyclin dependent kinase inhibitors *CDKN2B*, *CDKN2A* and *ARF* due to SNPs located within the *CDKN2A/B* genes and/or neighboring *loci*, but in the last few years studies aimed to investigate the potential involvement of such common DNA sequence variants in tumour susceptibility increased.

For example Brian G.K. et al. published (Jan-2011) a study on a 58 kb region on chromosome 9p21.3 which consistently showed a strong association with coronary artery disease in multiple genome-wide association analyses in populations of European and East Asian ancestry. In this study, they characterized the role of genetic variants in 9p21.3 in African American individuals. Apparently healthy African American siblings of patients with documented CAD <60 years of age were genotyped and followed for incident CAD for up to 17 years. The findings demonstrated a significant protective effect of single SNP within the *CDKN2B* gene, rs3217989, against incident CAD in African American siblings of persons with premature CAD⁹⁵.

Also the rs10811661 polymorphism near the *CDKN2B/CDKN2A* genes was associated with impaired insulin release and impaired glucose tolerance (IGT), suggesting that this variant may contribute to type 2 diabetes by affecting β -cell function⁹⁶.

The *locus* 9p21.3 variants associate with multiple disease phenotypes CAD, type 2 diabetes mellitus (T2DM), ischemic stroke, and abdominal aortic aneurysm^{97,48}, breast, ovarian, pancreatic carcinoma, melanoma, and acute lymphoblastic leukaemia⁴⁴. Variants associated with these diseases are represented in Figure 1.15^{97,45}.

Nature Genetics published, on June 2010, a study showing that a common variation at 9p21.3 influences acute lymphoblastic pediatric leukemia risk. This SNP is the rs3731217, located in the intron between 1 β and 1 α of *CDKN2A/ARF* (Chr9: 21,974,661 base pairs; within a 174-kb region of linkage disequilibrium at 9p21.3)⁶⁷.

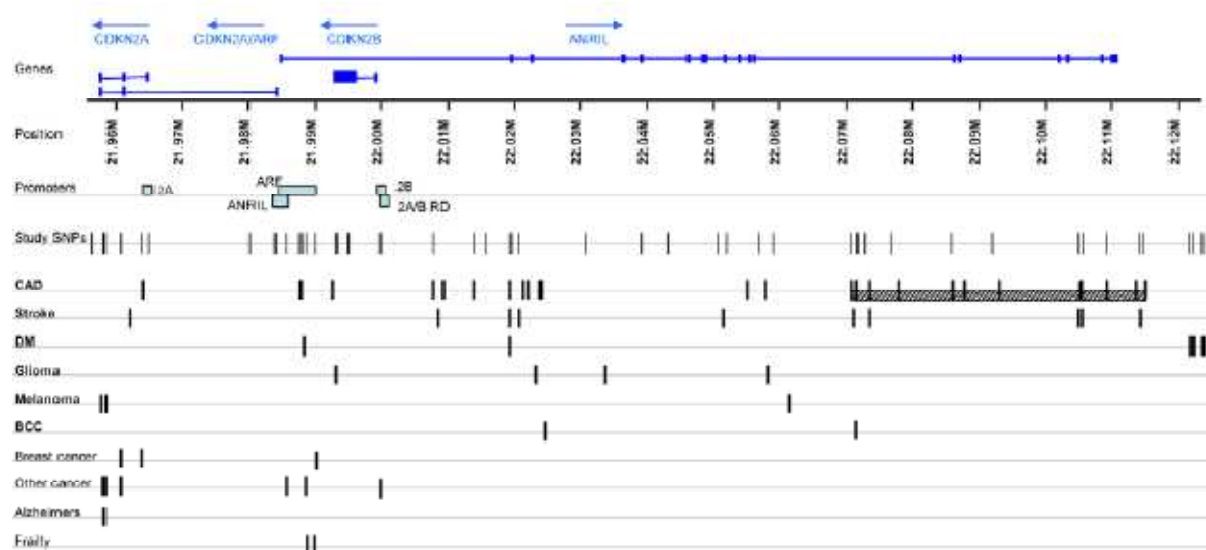


Fig. 1.15 SNPs associated with disease in the chromosome 9p21.3 region. Genes are illustrated in blue at the top, with arrows representing the direction of transcription. SNPs associated with various diseases are represented by black bars. Diseases in bold are those with association data from genomewide association studies. The hatched box represents the core risk haplotype for CAD defined by Broadbent et al⁶³. Promoter regions for each gene are shown as pale blue boxes. DM= diabetes mellitus type II; BCC = basal cell carcinoma. doi:10.1371/journal.pgen.1000899.g001⁴⁵.

Our laboratory (manuscript in press) performed a case-control association study by genotyping 23 SNPs spanning the *MTAP*, *CDKN2A/B* and *CDKN2BAS* loci, as well as relative intergenic regions, in a case-control cohort made up of 149 leukemia patients, including Ph+ acute lymphoblastic leukemia and AML samples, and 183 healthy controls. We found, among these genetic variations, a statistically significant association between a common *ANRIL* genetic variant, rs564398, mapping to the *CDKN2BAS* locus that encodes for *ANRIL*, and the ALL phenotype. This probably reflects a condition of high linkage disequilibrium between such polymorphism and a causative variant that is able to alter 3 *CDKN2A/B* expression profiles, thus leading to abnormal proliferative boosts and consequent increased ALL susceptibility.

1.7 PROGNOSTIC SIGNIFICANCE OF 9p21 INACTIVATION

The prognosis of B-lineage acute lymphoblastic leukemia (B-ALL) of children is significantly superior to that of adults^{98,99}. The difference in prognosis has been attributed to a differing incidence in genetic changes that determine the prognosis, such as the presence of the Philadelphia chromosome, ETV6/RUNX1 (formerly TEL/AML1) abnormality, MLL gene rearrangement, and ploidy changes. Nonetheless, the prognostic disparity between childhood and adult B-ALL is not fully explained by these genotypic differences, suggesting a role of other factors in the clinical behavior of B-ALL.

The silencing of the 9p21 gene cluster is thought to be one of the factors that cause a difference in the outcome^{69,98-100}. The band is identified like one of the major aberration hot spots in human cancers^{99,100}.

Many studies have been performed on the deletion or methylation patterns of *CDKN2A*, *ARF* and *CDKN2B* and their prognostic significance in ALL^{98,101,102}. Most studies, however, have been limited by a small study cohort, leading to uncertain statistical significance, a lack of concurrent deletion and methylation profiles, and a lack of comparison between adult and childhood B-ALL.

The interesting study on the pattern of deletion and methylation status of the *CDKN2A*, *ARF* and *CDKN2B* genes in the context of established prognostic cytogenetic changes in childhood and adult B-ALL, of Kim M. et al. (2009) suggest that (a) homozygous deletion occurs more frequently in adults than in children; (b) homozygous deletion affects OS only in adult B-ALL; (c) homozygous deletion, but not hemizygous deletion, has prognostic effect; and (d) methylation of p16, p14, and p15 does not affect the survival of B-ALL patients¹⁰³.

One thing that might explain the higher prevalence of homozygous deletion in adults than in children is cellular senescence, which increases with aging. Because the deletion of a gene results from faulty DNA replication, the homozygous deletion of tumor suppressor genes, which is a cumulative consequence of hemizygous deletion, could be associated with cell senescence.

Why homozygous deletion has little effect on survival in children is unclear. Other good prognostic factors or other oncogene alterations that were not investigated in that study might have prevented or weakened the negative effects of homozygous 9p21 deletion on disease progression.

The prognostic significance was limited to homozygous deletion of 9p21, which could be explained by loss of heterozygosity⁶⁵. Unlike homozygous deletion, hemizygous deletion might not be sufficient to turn off the function of these genes. Another explanation could be the high genomic instability in leukemia. Genomic instability, evidenced by the increased frequency of

cytogenetic, genetic, and epigenetic alterations, is a prominent hallmark of neoplastic evolution and tumor progression. Homozygous deletion of *CDKN2A*, *ARF* and *CDKN2B* might reflect the disease progression of B-ALL, for which the prognosis is worse than B-ALL with hemizygous deletion of *CDKN2A*, *ARF* and *CDKN2B* ¹⁰³.

As regards the prognostic relevance of *CDKN2A* deletions exclusively in childhood ALL, the literature is divided, with some studies have suggested that *CDKN2A* deletion is a poor prognostic factor ^{69,70,72,101,104,105}, whereas others show no correlation ^{74,76,100}. Beyond, Usvasalo et al. didn't observe any difference in the incidence of *CDKN2A* deletion between diagnosis and relapse ⁶⁴.

The prognostic significance of methylation of the *CDKN2A*, *ARF* and *CDKN2B* genes is also controversial and differs in several studies. The level of gene expression might be controlled by the extent of methylation, rather than by methylation itself, and thus further clarification requires the quantitation of methylation of *CDKN2A*, *ARF* and *CDKN2B* using pyrosequencing or methylation sequencing analysis ¹⁰³.

Although studied by several groups, the prognostic value of *CDKN2A* deletion in ALL remains uncertain, as summarized in the two tables below (Tab. 1.3 and 1.4).

Table 1.3 and 1.4 Prognostic relevance of *CDKN2A/ARF* (p16, p14) and *CDKN2B* (p15) alterations (summary of literature). Highlighted paper title refers to childhood (■) and adult (■) study.

	Author	Title	Journal	Year
Positive association	Kim M. et al. ¹⁰³	Homozygous deletion of <i>CDKN2A</i> (p16, p14) and <i>CDKN2B</i> (p15) genes is a poor prognostic factor in adult but not in childhood B-lineage acute lymphoblastic leukemia: a comparative deletion and hypermethylation study.(*)	Cancer Genet Cytogenet	2009
	Papadimitriou SI. et al. ¹⁰⁶	p16 inactivation associated with aggressive clinical course and fatal outcome in TEL/AML1-positive acute lymphoblastic leukemia .	J Pediatr Hematol Oncol.	2005
	Primo D. et al. ¹⁰²	Genetic heterogeneity of <i>BCR/ABL</i> ⁺ adult B-cell precursor acute lymphoblastic leukemia: impact on the clinical, biological and immunophenotypical disease characteristics.	Leukemia	2005
	Dalle JH. et al. ¹⁰⁷	p16(INK4a) immunocytochemical analysis is an independent prognostic factor in childhood acute lymphoblastic leukemia.	Blood	2002
	Calero Moreno TM. et al. ⁷⁰	Deletion of the <i>Ink4</i> -locus (the p16ink4a, p14ARF and p15ink4b genes) predicts relapse in children with ALL treated according to the Nordic protocols NOPHO-86 and NOPHO-92.	Leukemia	2002
	Hoshino K. et al. ¹⁰⁸	The absence of the p15INK4B gene alterations in adult patients with precursor B-cell acute lymphoblastic leukaemia is a favourable prognostic factor.	Br J Haematol	2002
	Carter TL. et al. ¹⁰¹	Hemizygous p16(INK4A) deletion in pediatric acute lymphoblastic leukemia predicts independent risk of relapse.	Blood	2001
	Ramakers-van Woerden NL. et al. ¹⁰⁹	<i>In vitro</i> drug resistance and prognostic impact of p16INK4A/P15INK4B deletions in childhood T-cell acute lymphoblastic leukaemia	Br J Haematol	2001
	Heerema NA. et al. ¹⁰⁵	Association of chromosome arm 9p abnormalities with adverse risk in childhood acute lymphoblastic leukemia: a report from the Children's Cancer Group.	Blood	1999
	Moreno TC et al. ¹¹⁰	Inverse correlation between <i>Ink4</i> -locus deletions and ICM-DNA hyperdiploidy in childhood acute lymphoblastic leukaemia, relation to clinical characteristics and outcome	Eur J Haematol.	2000
	Kees UR. et al. ⁶⁹	Homozygous deletion of the p16/MTS1 gene in pediatric acute lymphoblastic leukemia is associated with unfavorable clinical outcome.	Blood	1997
	Zhou M. et al. ¹¹¹	Incidence and clinical significance of <i>CDKN2/MTS1/P16ink4A</i> and <i>MTS2/P15ink4B</i> gene deletions in childhood acute lymphoblastic leukemia.	Pediatr Hematol Oncol	1997
	Heyman M. et al. ⁷²	Prognostic importance of p15INK4B and p16INK4 gene inactivation in childhood acute lymphocytic leukemia.	J Clin Oncol	1996
	Heyman M. et al. ¹¹²	Inactivation of the p15INK4B and p16INK4 genes in hematologic malignancies .	Leuk Lymphoma	1996
	Fizzotti M. et al. ¹⁰⁴	Detection of homozygous deletions of the cyclin-dependent kinase 4 inhibitor (p16) gene in acute lymphoblastic leukemia and association with adverse prognostic features.	Blood	1995

	Author	Title	Journal	Year
Negative association	Sulong S. et al. ⁶⁴	A comprehensive analysis of the CDKN2A gene in childhood acute lymphoblastic leukemia reveals genomic deletion, copy number neutral loss of heterozygosity, and association with specific cytogenetic subgroups.	Blood	2009
	Uvasalo A. et al. ¹	CDKN2A deletions in acute lymphoblastic leukemia of adolescents and young adults : an array CGH study.	Leuk Res	2008
	Mirebeau D. et al. ⁷⁴	The prognostic significance of CDKN2A, CDKN2B and MTAP inactivation in B-lineage acute lymphoblastic leukemia of childhood . Results of the EORTC studies 58881 and 58951.	Haematologica	2006
	L.J. van Zutven et al. ⁷⁶	CDKN2 deletions have no prognostic value in childhood precursor-B acute lymphoblastic leukaemia.	Leukemia	2005
	Cipollotti R. et al. ¹¹³	Inactivation of the p15 gene in children with acute lymphoblastic leukemia.	Sao Paulo Med J	2003
	Manero G.G. et al. ⁹⁹	Aberrant DNA methylation in pediatric patients with acute lymphocytic leukemia	Cancer	2003
	Manero G.G. et al. ⁹⁸	DNA methylation of multiple promoter-associated CpG islands in adult acute lymphocytic leukemia	Clin Cancer Res	2002
	Graf Einsiedel H. et al. ¹⁰⁰	Deletion analysis of p16INKa and p15INKb in relapsed childhood acute lymphoblastic leukemia.	Blood	2002
	Graf Einsiedel H. et al. ¹¹⁴	Prognostic value of p16(INK4a) gene deletions in pediatric acute lymphoblastic leukemia.	Blood	2001
	Chim CS. et al. ⁸⁴	Methylation of p15 and p16 genes in adult acute leukemia: lack of prognostic significance.	Cancer	2001
	Faderl S. et al. ¹¹⁵	The prognostic significance of p16INK4a/p14ARF and p15INK4b deletions in adult acute lymphoblastic leukemia.	Clin Cancer Res	1999
	Rubnitz JE. et al. ¹¹⁶	Genetic studies of childhood acute lymphoblastic leukemia with emphasis on p16, MLL, and ETV6 gene abnormalities: results of St Jude Total Therapy Study XII.	Leukemia	1997
	Dicianni MB et al. ¹¹⁷	Shortened survival after relapse in T-cell acute lymphoblastic leukemia patients with p16/p15 deletions.	Leuk Res	1997
	Batova A. et al. ¹¹⁸	Frequent deletion in the methylthioadenosine phosphorylase gene in T-cell acute lymphoblastic leukemia : strategies for enzyme-targeted therapy.	Blood	1996
	Ohnishi H. et al. ⁷⁸	Homozygous deletions of p16/MTS1 and p15/MTS2 genes are frequent in t(1;19)-negative, but not in t(1;19)-positive B precursor acute lymphoblastic leukemia in childhood .	Leukemia	1996
	Okuda T. et al. ¹¹⁹	Frequent deletion of p16INK4a/MTS1 and p15INK4b/MTS2 in pediatric acute lymphoblastic leukemia.	Blood	1995
	Stock W. et al.	High incidence of p16 deletion in adult acute lymphoblastic leukemia (ALL): correlation with clinical features and response to treatment: CALGB 8762.	Blood	1995
	Takeuchi S. et al. ⁸⁸	Analysis of a family of cyclin-dependent kinase inhibitors: p15/MTS2/INK4B, p16/MTS1/INK4A, and p18 genes in acute lymphoblastic leukemia of childhood .	Blood	1995

1.8 TREATMENT OF PH+ ACUTE LYMPHOBLASTIC LEUKEMIA

Until recently, Ph+ ALL carried a dismal prognosis in both children and adults. Patients with Ph+ ALL who received conventional chemotherapy reportedly had long-term survival rates of approximately 10%, and only allogeneic stem cell transplantation (alloSCT) extended long-term survival in 38% to 65% of patients. Outcomes for patients with Ph+ ALL improved substantially with the introduction of the tyrosine kinase inhibitor (TKI) imatinib mesylate. Although imatinib monotherapy in previously treated patients with Ph+ ALL produced only a modest, short-lived response, imatinib combined with chemotherapeutic regimens has induced complete remissions (CRs) in almost every patient (~95%) with newly diagnosed Ph+ ALL. However, imatinib resistance develops in a substantial proportion of imatinib-treated patients with Ph+ ALL. About 50–80% of the Ph+ ALL patients who achieved a CR with imatinib relapse within 1 year, mainly due to the emergence of Bcr-Abl kinase domain point mutations, which impair imatinib binding either by affecting critical contact residues or by inducing a Bcr-Abl conformation to which imatinib is unable to bind. Second-generation TKIs (eg, dasatinib and nilotinib) have demonstrated promising efficacy in the treatment of imatinib-resistant, Ph+ ALL^{2,34}.

1.8.1 Standard chemotherapy and allogeneic stem cell transplantation (alloSCT)

Although CRs may occur in 70% to 90% of patients with Ph+ ALL who receive intensive chemotherapy alone, most patients relapse and die within 6 to 11 months of treatment. AlloSCT substantially improves long-term survival rates. Several factors influence the outcome of patients who undergo alloSCT. Patients who underwent alloSCT during first CR had substantially better outcomes than patients who underwent alloSCT in second or later CR. Other favorable factors include younger age, total body irradiation conditioning, the use of a human leukocyte antigen-identical sibling donor, and the occurrence of acute graft-versus-host disease. The widespread use of alloSCT often is hindered by donor availability. This limitation has been overcome in part by the use of unrelated donors, nonmyeloablative conditioning regimens to facilitate the extension of eligibility for SCT, and harvesting stem cells from umbilical cord blood. Nevertheless, approximately 30% of patients who undergo SCT relapse, and treatment-related mortality (up to 40%) is a frequent cause of failure. The role of TKIs after alloSCT is discussed below. In summary, improved therapies for patients with Ph+ ALL are still needed².

1.8.2 Tyrosine kinase inhibitors

1.8.2.1 Imatinib mesylate. (*Gleevec, Glivec; STI571*)

The first BCR-ABL inhibitor to gain clinical approval was imatinib mesylate, which partially blocks the adenosine triphosphate (ATP) binding site of BCR-ABL, preventing a conformational switch of the oncogenic protein to the activated form. Early studies demonstrated that many patients with previously treated, Ph+ ALL initially responded to imatinib monotherapy with CR rates of 20% then but quickly relapsed after a median treatment duration of 58 days. Thus, although imatinib was well tolerated and produced a modest response in patients with previously treated, Ph+ ALL when it was used as single-agent therapy, responses were short-lived, and relapses were common.

Imatinib resistance has been attributed to BCR-ABL-dependent and BCR-ABL-independent mechanisms. BCR-ABL-dependent mechanisms include amplification of the BCR-ABL gene and mutations within ABL that reactivate BCR-ABL and disrupt binding to the drug target. Indeed, more than 90 separate resistance conferring point mutations at 57 residues in the Abl kinase have been documented, and these generally fall within four regions of the kinase domain: the ATP-binding pocket (P-loop), the contact site (eg, threonine at codon 315 [T315] and phenylalanine at codon 317 [F317]), the Src homology 2 (SH2) binding site (eg, methionine at codon 351 [M351]) and the activation loop (A-loop). A common mutation that occurs frequently after imatinib therapy in Ph+ ALL patients is the glutamic acid to lysine mutation at codon 255 (E255K). P-loop mutations are 70-fold to 200-fold less sensitive to imatinib compared with native BCR-ABL, and studies indicate that patients with these mutations have a worse prognosis. Gatekeeper mutations (eg, the threonine to isoleucine mutation at codon 315 [T315I] and the phenylalanine to leucine mutation at codon 317 [F317L]) impede contact between imatinib and BCR-ABL and, thus, contribute to imatinib resistance and resistance to other second-generation TKIs. Different mutants seem to have different degrees of resistance to imatinib: *in vitro* data indicate that while some mutations might be overcome by dose escalation, others confer a highly resistant phenotype, thereby suggesting withdrawal of imatinib in favour of alternative therapeutic strategies. Indeed, because resistance often coincides with reactivation of the kinase activity within the leukaemic clone, either Bcr-Abl itself or Bcr-Abl-triggered downstream signaling pathways remain good targets for molecular therapy. Soverini et al. reported a high rate of Bcr-Abl mutations in resistant Ph+ ALL patients. Although Bcr-Abl point mutations are primarily responsible for the development of secondary, or acquired, resistance in Ph+ ALL and CP CML, there are also Bcr-Abl independent mechanisms which are poorly

understood³⁴. BCR-ABL-independent mechanisms include chromosomal abnormalities in addition to the Ph chromosome abnormalities (clonal evolution), disruptions in drug uptake and efflux, and activation of alternative signaling pathways that cause proliferation or promote cell survival. Maintaining effective intracellular drug concentrations also is a major hurdle to imatinib efficacy. Imatinib is a substrate of the drug efflux permeability glycoprotein (Pgp), and increased Pgp expression can decrease intracellular concentrations of imatinib to confer drug resistance *in vitro*. Stromal support also has been proposed as a mechanism of resistance to TKIs in Ph+ ALL. One study reported that murine p190 BCR-ABL ALL cells with low BCR-ABL expression were able to grow in the presence of stroma. Another recently identified mechanism of TKI resistance involves the expression of spliced isoforms of IKAROS family zinc (Ikaros) (*IKZF1*), a critical regulator of normal lymphocyte development. Constitutive activation of downstream signaling molecules that results in pathway activation, regardless of BCR-ABL inhibition, represents another mechanism of imatinib resistance^{2,34}.

1.8.2.2 Second-generation tyrosine kinase inhibitors

Since point mutations are the major mechanism of resistance to first-line imatinib therapy in Ph+ leukemia, different drugs active on mutant BCR-ABL or on its signal transduction pathway have been developed and tested at clinical level.

Dasatinib (Sprycel)

Dasatinib (BMS-354825, Sprycel; Bristol Myers Squibb, New York, USA) has reached a peculiar and specific role. Dasatinib is a multi-target kinase inhibitor of Bcr-Abl, SFK, ephrin receptor kinases, *PDGFR* and Kit, has 325-fold greater potency than imatinib in cells transduced with unmutated BCR-ABL and is active against many of the BCR-ABL mutations, conferring imatinib resistance and is effective against the imatinib-resistant active conformation of the kinase domain. It is capable of inhibiting the proliferation and kinase activity of wild type and of 14 out of 15 Bcr-Abl mutant cell lines, except the T315I mutant. Furthermore, the cellular uptake of dasatinib is not dependent, as opposed to imatinib, on the organic cation transporter-1 (OCT-1) activity, although, like imatinib, it is a substrate for efflux proteins. Dasatinib is usually well tolerated, but grade 3–4 myelosuppression is common, especially in the advanced phases. Non-haematological side effects include diarrhea, nausea, headache, peripheral edema and pleural effusion. However, resistance to dasatinib is a crucial emerging problem. Not surprisingly, the pre-existence or selection of the T315I mutant is the most frequent mechanism of resistance. In addition, the emergence of a F317L mutant, which is sensitive to imatinib, has been commonly observed in dasatinib-resistant patients.

Dasatinib is approved in the United States for patients with Ph+ ALL who have failed to respond to imatinib, and clinical trials evaluating its efficacy in patients with newly diagnosed Ph+ ALL are ongoing^{2,34}.

Nilotinib (Tasignia, AMN107)

The N-methylpiperazine moiety was originally incorporated into imatinib to improve its solubility and oral bioavailability. Substitution of this amide moiety with alternative binding groups, while maintaining hydrogen-bond interactions to Glu286 and Asp381, led to the discovery of a more potent compound, nilotinib (Tasignia, AMN107, Novartis).

This highly specific BCR-ABL inhibitor is approximately 30-fold more potent than imatinib and is active *in vitro* against 32 of 33 BCR-ABL mutations, except the T315I mutant. It is a substrate for both OCT-1 and efflux proteins. It is superior to imatinib in reducing leukemic burden and prolonging the survival of mice transplanted with wild-type BCR-ABL, the M351T and E255V mutants. A phase I study of nilotinib in patients with imatinib-resistant CML and Ph+ ALL indicated that nilotinib had a relatively favorable safety profile, and responses were noted in a subset of adult patients with imatinib-resistant, Ph+ ALL. Specifically, 10% of patients who had hematologic relapses achieved a partial hematologic response, and 33% of patients with persistent molecular signs of ALL achieved complete molecular remission after nilotinib therapy. Myelosuppression was frequent, and common grade 3-4 nonhematologic toxicities included indirect hyperbilirubinemia, skin rashes and elevated serum lipase. A subsequent phase II study of nilotinib in relapsed or refractory Ph+ ALL reported that 24% patients attained a complete hematologic response (CHR). Data from studies in patients with CML indicate that BCR-ABL P-loop mutations (eg, tyrosine to phenylalanine or histidine mutation at codon 253 [Y253F/H] or glutamic acid to methionine or valine mutation at codon 255 [E255K/V]) are resistant to nilotinib. Nilotinib is approved only for imatinib-resistant or imatinib-intolerant chronic-phase and accelerated-phase CML^{2,120}.

Bosutinib (SKI-606; Wyeth)

Another Src kinase-active TKI is bosutinib (SKI-606; Wyeth). It has a potent anti-proliferative activity against imatinib-sensitive and -resistant Bcr-Abl-positive cell lines, including the Y253F, E255K and D276G mutants, but not the T315I form. It is able to bind to both inactive and intermediate conformations of Bcr-Abl. Unlike dasatinib, bosutinib does not significantly inhibit Kit or PDGFR and has a more favourable toxicity profile. The main adverse events are commonly gastrointestinal, including diarrhea, whereas myelosuppression usually occurs only in the advanced phases³⁴.

2. AIMS

The 9p21 chromosomal region is a frequent site of genetic loss in several human cancers, including solid tumors and hematologic malignancies. This region spans 40 kb of genomic DNA and has an unusual and complex genomic organization, encoding three important tumor suppressor genes (p16/*CDKN2A*, p14/*ARF* and p15/*CDKN2B*) involved in the regulation of cell cycle and/or apoptosis. Disruption of tumor suppressor genes and/or activation of oncogenic pathways by point-mutations, amplifications and phosphorylation result in constitutive mitogenic signalling and defective responses to anti-mitogenic stimuluses that contribute to unscheduled proliferation in tumor cells. Understanding and contrasting the causes of unlimited proliferation will allow us to fight the tumor cells.

In literature several groups studied how the 9p21 chromosome band is inactivated in acute lymphoblastic leukemia (ALL), but most of them referred to a small cohort of patients, mainly pediatrics, and using low resolution methodologies.

For example, traditional techniques, that have a limited number of probes, are not able to detect small deletions that often occur in this *locus*.

To exceed these restraints, in this study, we performed high resolution Affymetrix single nucleotide polymorphism (SNP) arrays in 112 Ph+ ALL adult patients (pts) to:

- Explore the frequency and size of deletions on 9p21 affecting the *CDKN2A/ARF/CDKN2B* gene in adult *BCR-ABL1*-positive ALL patients;
- Determine the main mechanism of inactivation of *CDKN2A/ARF/CDKN2B*;
- Investigate whether the *CDKN2A/ARF* deletions have any prognostic value;

We chose to investigate the frequency and role of 9p21 deletions in Ph+ ALL, since it represents the most frequent and the most unfavorable subtype of leukemia in adults. It has become clear that although BCR-ABL is responsible for transformation of a normal cell in a malignant cell, additional and cooperating events are required for leukemia progression. The identification of these genetic factors may lead to a more efficacious target therapies.

3. PATIENTS AND METHODS

PATIENTS

All patients gave informed consent to blood collection and biologic analyses, in agreement with the Declaration of Helsinki. The study was approved by the Department of Hematology and Oncological Sciences “Seràgnoli”. After obtaining informed consent, 112 adult *BCR-ABL1*-positive ALL patients, enrolled from 1996 to 2008 in different clinical trials of GIMEMA (Gruppo Italiano Malattie EMatologiche dell'Adulto) Acute Leukemia Working Party or in Institutional protocols, were analyzed.

101 (90%) were de novo ALL cases analyzed at the time of diagnosis, while 11 (10%) were relapse cases analyzed only at the time of treatment failure. In 19 cases out 101 (19%) both diagnosis and relapse samples were collected and thereafter analyzed (Tab. 3.1).

Tab. 3.1. Demographics and Clinical Characteristics of patients with *BCR-ABL1* positive ALL analyzed for the genomic status of *CDKN2A/ARF* and *CDKN2B*.

	Newly diagnosed <i>BCR-ABL1</i> ALL (n=101)	Unpaired Relapse <i>BCR-ABL1</i> ALL (n=11)	Paired Relapsed <i>BCR-ABL1</i> ALL (n=19)
Age (median, range)	51 yrs (18-81)	44 yrs (18-65)	54 yrs (23-74)
Gender (M/F)	56/45	6/5	10/9
Blast cell count (% , range)	90 (18-99)	90 (20-96)	90 (25-99)
BCR-ABL transcript			
p190	74 (73%)	5 (45%)	11 (58%)
p210	20 (20%)	5 (45%)	8 (42%)
p190-p210	7 (7%)	1 (10%)	-

SINGLE NUCLEOTIDE POLYMORPHISM (SNP) MICROARRAY ANALYSIS

Genomic DNA was extracted using the DNA Blood Mini Kit (Qiagen, Valencia, CA) from mononuclear cells isolated from peripheral blood or bone marrow aspirate samples by Ficoll gradient centrifugation. DNA was quantified using the Nanodrop Spectrophotometer and quality was assessed using the Nanodrop and by agarose gel electrophoresis.

83 samples (63 diagnosis, 20 relapse) were genotyped with GeneChip® Human Mapping 250K NspI and 48 samples (38 diagnosis, 10 relapse) with Genome-Wide Human SNP 6.0 array microarrays (Affymetrix Inc, Santa Clara, CA) following the manufacturer's instructions, as briefly described in the workflow in the Figure 3.2¹²¹.

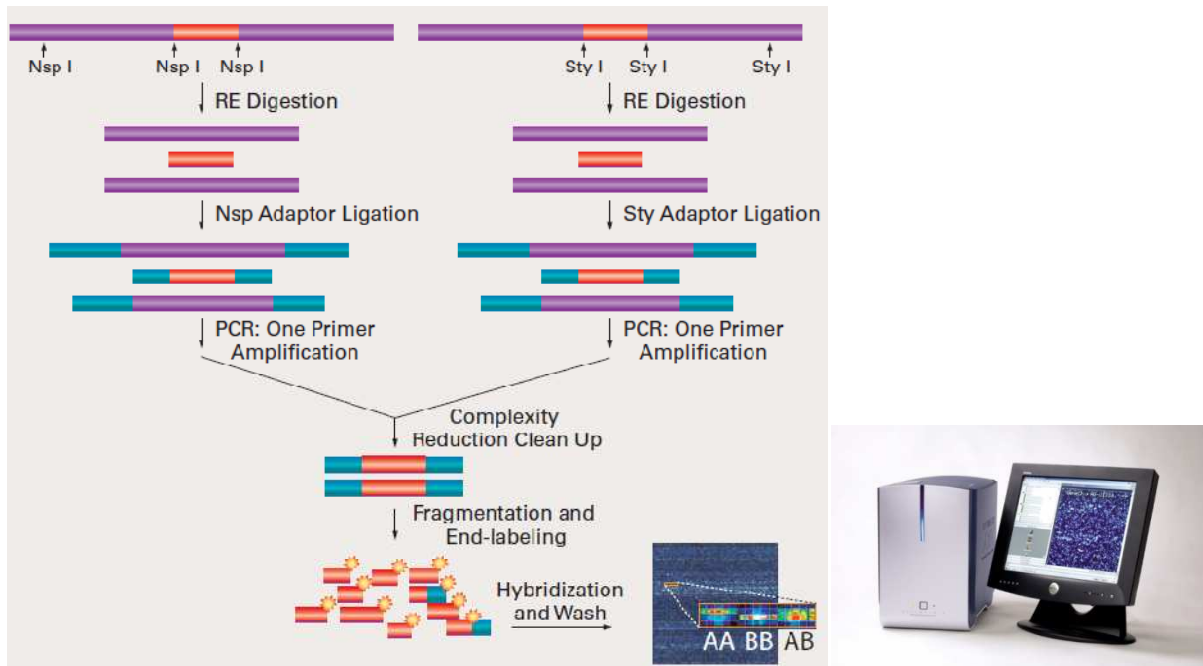


Fig. 3.2: Overview of the Genome-Wide Human SNP Assay 6.0. Briefly, total genomic DNA (500 ng) is digested with Nsp I and Sty I restriction enzymes and ligated to adaptors that recognize the cohesive 4 bp overhangs. All fragments resulting from restriction enzyme digestion, regardless of size, are substrates for adaptor ligation. A generic primer that recognizes the adaptor sequence is used to amplify adaptor-ligated DNA fragments. PCR conditions have been optimized to preferentially amplify fragments in the 200 to 1,100 bp size range. PCR amplification products for each restriction enzyme digest are combined and purified using polystyrene beads. The amplified DNA is then fragmented, labeled and hybridized to the array. <http://www.affymetrix.com/media/images/assayimage.gif>

The new Affymetrix Genome-Wide Human SNP Array 6.0 features 1.8 million genetic markers, including more than 906,600 single nucleotide polymorphisms (SNPs) and more than 946,000 probes for the detection of copy number variation. The high number of SNPs and non polymorphic probes (NNPs) enable to have a good coverage, spaced along the genome, with a median distance between markers of only 700 bp (Tab. 3.2).

Tab. 3.2 Genome-Wide Human SNP Assay 6.0 features.

Number of SNPs	906,600 + 946,000 *NPPs
DNA required	500ng
Fragment size amplified	200-1100bp
Median Distance between markers	<700bp
Average heterozygosity for each SNP	26.7-28.5% depending on population

Copy number aberrations were scored using the segmentation approach available within the Partek Genomics Suite™ software package (<http://www.partek.com/>) as well as by visual inspection and by a comparison with a set of 270 HapMap normal individuals and a set of samples obtained from 25 acute lymphoblastic leukaemia cases in remission in order to reduce the noise of raw copy number data. Affymetrix CEL files were also imported in and analyzed by dChip (www.dchip.org)¹²². Copy numbers per SNP marker were generated according to Mullighan et al.¹²³ and imported into UCSC Genome Browser website (<http://genome.ucsc.edu/>) for visualization. In the Figure 3.3 the probe density in *CDKN2A/ANRIL/CDKN2B* locus on Genome-Wide Human SNP 6.0 array is shown. Loss of heterozygosity (LOH) was analyzed using Genotyping Console v3.1 (Affymetrix Inc.).

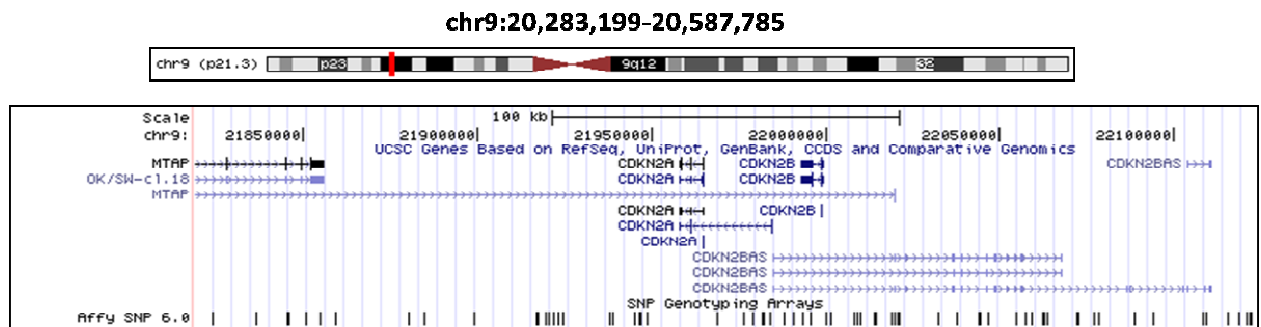


Fig. 3.3 UCSC genome browser screenshot of a region on chromosome 9p21 (20,283,199-20,587,785) containing the *CDKN2A* and *CDKN2B* genes and a newly annotated antisense noncoding RNA in the *INK4* locus (*ANRIL* or *CDKN2BAS*). Markers on Affymetrix SNP6.0 are shown as black lines on the bottom of the figure. *ANRIL* overlaps the two exons of *CDKN2B* and is transcribed in the orientation opposite to the *CDKN2B-CDKN2A-ARF* gene cluster. Exon 1 of *ANRIL* is present about 300 bp upstream of the transcription start site of exon 1 β of *CDKN2A*. Original image at http://genome.ucsc.edu/cgi-bin/hgTracks?insideX=118&revCmplDisp=0&hgSid=187245851&hgt_doJsCommand=&hgt.out1=1.5x&position=chr9%3A21869592-22072649&hgtgroup_map_close=0&hgtgroup_phenDis_close=1&hgtgroup_genes_close=0&hgtgroup_rna_close=0&hgtgroup_expression_close=0&hgtgroup_regulation_close=0&hgtgroup_compGeno_close=0&hgtgroup_neandertal_close=0&hgtgroup_denisova_close=0&hgtgroup_varRep_close=0&hgtgroup_encodeGenes_close=0&hgtgroup_encodeTxLevels_close=0&hgtgroup_encodeChip_close=0&hgtgroup_encodeChrom_close=0&hgtgroup_encodeCompAndVar_close=1.

FLUORESCENCE IN SITU HYBRIDIZATION (FISH) AND PROBES

FISH analysis was performed as previously described¹²⁴. Briefly, chromosome preparations from bone marrow cells were hybridized in situ with 1 µg of probe labeled by nick translation. Hybridization was performed at 37°C in 2X SSC, 50% (vol/vol) formamide, 10% (wt/vol) dextran sulfate, 5 µg COT1 DNA (Bethesda Research Laboratories, Gaithersburg, MD, USA), and 3 µg sonicated salmon sperm DNA in a volume of 10 µL. Post-hybridization washing was performed at 60°C in 0.1X SSC (three times). In cohybridization experiments, the probes were directly labeled with Fluorescein and Cy3. Chromosomes were identified by DAPI staining. Digital images were obtained using a Leica DMRXA epifluorescence microscope equipped with a cooled CCD camera (Princeton Instruments, Boston, MA). Cy3 (red; New England Nuclear, Boston, MA, USA), fluorescein (green; Fermentas Life Sciences, Milan, IT), and DAPI (blue) fluorescence signals, which were detected using specific filters, were recorded separately as gray-scale images. Pseudocoloring and merging of images were performed with Adobe Photoshop software.

Bacterial artificial chromosome (BAC) [RP11-70L8 (Accession Number AL359922)(chr9:21,732,609-21,901,258), RP11-149I2 (Accession Number AL449423)(chr9:21,899,259-22,000,413), and RP11-145E5 (Accession Number AL354709)(chr9:21,998,414-22,155,946)] and fosmid [G248P82557D2 (Accession Number WIBR2-1053H3) (chr9:21,975,653-22,011,179), and G248P82010F5 (Accession Number WIBR2-1034K10) (chr9:21,926,491-21,967,852)] probes, specific for the *MTAP-CDKN2A-CDKN2B* locus, as well as a BAC for *BCR* gene [RP11-164N13 (chr22:21,897,904-22,091,572)], were properly selected accordingly to the March 2006 release of the University Santa Cruz (UCSC) Human Genome Browser (<http://genome.ucsc.edu/cgi-bin/hgGateway?hgid=169374627&clade=mammal&org=Human&db=hg18>).

CDKN2A GENE EXPRESSION LEVELS

Total cellular RNA was extracted using the RNeasy total RNA isolation kit (Qiagen, Valencia, CA) and one microgram was reverse transcribed using the High Capacity cDNA Archive Kit (Applied Biosystems, Foster City, CA). Quantitative Polymerase chain reaction (PCR) analysis was performed using Hs00924091_m1 assay (Applied Biosystems) and the Fluidigm Dynamic Array 48 x 48 system, a real-time quantitative PCR assay which enables to automatically assemble 48 samples and 48 assays to create individual TaqMan reactions of a final volume of 6.75 nanolitres each (Fluidigm, San Francisco, CA, <http://www.fluidigm.com/>). The Fluidigm

BioMark system (Fig. 3.4-A) provides orders of magnitude higher throughput for real-time quantitative PCR compared to conventional platforms due to its dynamic arrays—nanofluidic chips that contain fluidic networks that automatically combine sets of samples with sets of assays.

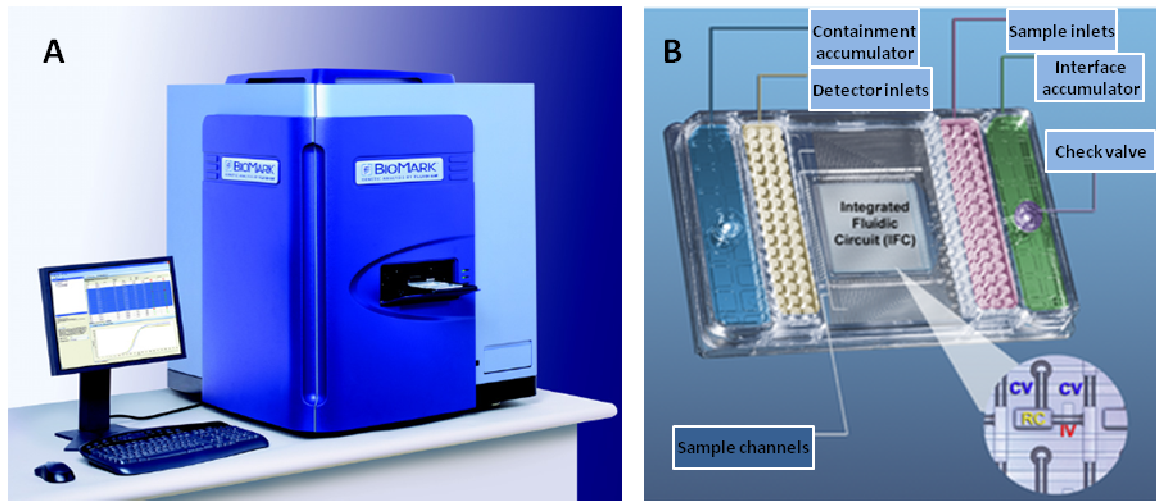


Fig 3.4 (A) The BioMark Real-Time PCR system. (B) Photograph of a 48x48 dynamic array chip showing the position of the sample inlets and the detector inlets in which the gene expression assay reagents are added. The check valves allow pressure to be applied and released. The accumulators provide reservoirs to hold the pressure and keep the valves closed during the reaction. The integrated Fluidic Circuit (IFC) is in the center of the chip. This is a network of fluid lines, NanoFlex™ valves and reaction chambers. The insert shows a blow-up of a portion of the IFC with one of the 2304 individual reaction chambers (RC) and the associated containment valves (CV) and interface valve (IV) There are two containment valves and one interface valve associated with each reaction chamber.

The BioMark cassette works using thousands of NanoFlex(TM) valves to fill thousands of individual reactions from a matrix of samples and primers. Particularly, the 48x48 Dynamic Array (Fig 3.4-B) systematically combine 48 samples and 48 assays in 2,304 real-time qPCR reactions, of final reaction volume of 6.75 nanolitres each. After setup, the dynamic array is placed on the BioMark Real Time PCR system for thermal cycling and real-time fluorescence detection. To examine, annotate, and archive the data (Fig. 3.5), the BioMark Real Time Analysis Software was used.

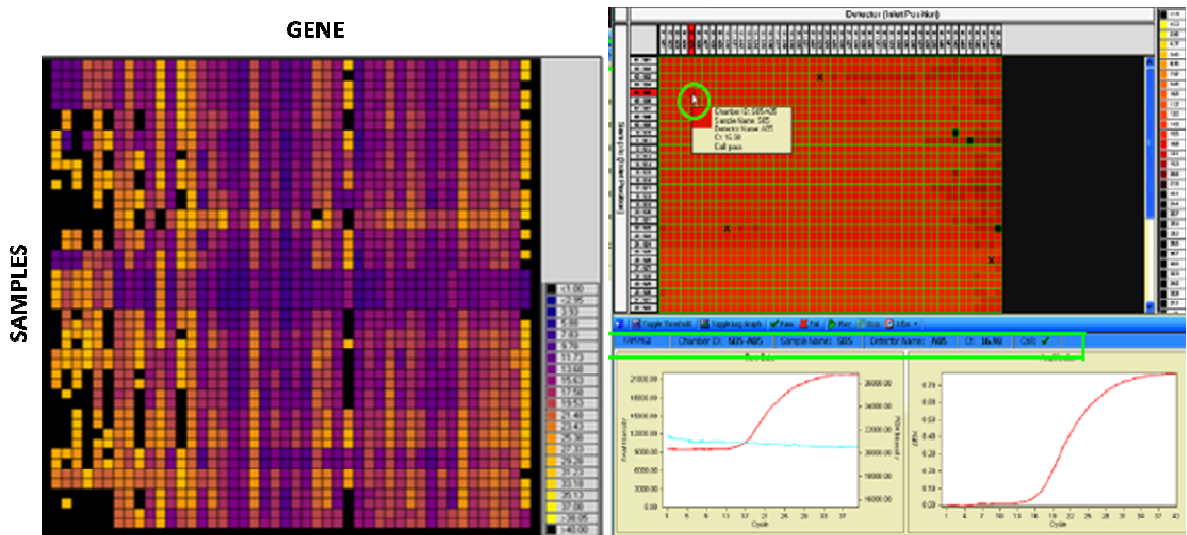


Fig 3.5 The BioMark Real Time Software generated image (left), **heat map**, of a 48x48 dynamic array chip obtained after thermal cycling of the chip. Each of the squares represents 1 reaction chamber from the chip. The color indicates the C_T value according to the legend shown on the right. Black chambers indicate a $C_T > 40$. Clicking on a cell, corresponding to a single reaction, its data and graph curves are activated (right).

RNA integrity was confirmed by PCR amplification of the *GAPDH* mRNA (Hs99999905_m1), which is expressed ubiquitously in human hematopoietic cells. Results were expressed as $2^{\exp(-\Delta\Delta Ct)}$. GraphPad Prism 5 software (GraphPad, Avenida de la Playa La Jolla, CA USA) was used to determine the statistical significance of *CDKN2A* expression levels in different groups of patients and to plot the data for the figure 4.4.

***CDKN2A/ARF* AND *CDKN2B* POINT MUTATION SCREENING**

Genomic re-sequencing of all coding exons of *CDKN2A/ARF* and *CDKN2B* was performed in search of mutations using primers listed in Table 1S. Two different Taq DNA polymerases were used in a final reaction of 25 μ l. For AmpliTaq Gold DNA Polymerase LD protocol (Applied Biosystems) each PCR reaction was performed using: 30-50 ng of genomic DNA; 25 pmoli of primers; 10X PCR Gold Buffer; 2.5 mM $MgCl_2$; 200 μ M dNTPs; DMSO 2.5%; 1U AmpliTaq Gold DNA Polymerase; water to final volume. For Fast Start Taq DNA Polymerase protocol (Roche, Mannheim, Germany), each PCR reaction was performed using: 30-50 ng of genomic DNA; 25 pmoli of primers; 10X PCR Buffer; 2.5 mM $MgCl_2$ Solution; 200 μ M dNTPs; 1U FastStart Taq DNA Polymerase; water to final volume (Tab. 3.3).

Gene	Exon	Sequence (5'→3')	T _m (C°)	Amplicon size (bp)	DNA polymerase	PCR protocol (*)
<i>CDKN2A</i>	1 α	AGTCCTCCTTCCTTGCCAAC	60.63	508	AmpliTaq Gold	95° x 30"
<i>CDKN2A</i>	1 α	CGCTGCAGACCCTCTACC	59.53			62° x 30"
<i>CDKN2A sequencing</i>	1 α	GCTGCAGACCCTCTACCC	58.32	-		72° x 50"
						40 cycles
<i>ARF</i>	1 β	TGCTCACCTCTGGTGCCAAAG	58.60	218	FastStart	95° x 30"
<i>ARF</i>	1 β	CTCAGTAGCATCAGCACGAGG	58.60			60° x 30"
						72° x 30"
						35 cycles
<i>CDKN2A/ARF</i>	2	CCTGGCTCTGACCATTCTGT	60.26	421	AmpliTaq Gold	95° x 30"
<i>CDKN2A/ARF</i>	2	GGCTGAACTTTCTGTGCTGG	60.98			63° x 30"
						72° x 1'
						40 cycles
<i>CDKN2A/ARF</i>	3	TACATGCACGTGAAGCCATT	60.14	685	FastStart	95° x 30"
<i>CDKN2A/ARF</i>	3	TCTTCCATGCGATGAAATTG	59.62			62° x 30"
						72° x 1'
						40 cycles
<i>CDKN2B</i>	1	TGAAAACGGAATTCTTTGCC	60.05	632	FastStart	95° x 30"
<i>CDKN2B</i>	1	ACATCGGCGATCTAGGTTC	61.38			62° x 30"
						72° x 1'
						35 cycles
<i>CDKN2B</i>	2	GGCTCTGACCACTCTGCTCT	59.74	463	FastStart	95° x 30"
<i>CDKN2B</i>	2	ATGGAAGGTTATCCCGGTC	60.02			62° x 30"
						72° x 1'
						35 cycles

Tab. 3.3 Primers used for amplification of *CDKN2A/ARF* and *CDKN2B* genes, and relative PCR protocol. (*) Protocols with AmpliTaq Gold polymerase involve an initial denaturation of 7' at 95°C, whereas protocols with FastStart polymerase involve an initial denaturation of 5' at 95°C. Both polymerase have an extension of 7' at 72°C.

PCR products were purified using QIAquick PCR purification kit (Qiagen) and then directly sequenced using an ABI PRISM 3730 automated DNA sequencer (Applied Biosystems, Foster City, CA) and a Big Dye Terminator DNA sequencing kit (Applied Biosystems, Foster City, CA). In some cases the PCR products were sub-cloned into the PCR@2.1-TOPO vector using the TOPO TA Cloning Kit (Invitrogen, San Diego, CA). The cloned PCR products were purified and sequenced as described above. All sequence variations were detected by comparison using the BLAST software tool (www.ncbi.nlm.nih.gov/BLAST/) to reference genome sequence data (GenBank accession number NM_000077.4, NM_058195.3 e NM_004936, for *CDKN2A*, *ARF*,

CDKN2B, respectively) obtained from the UCSC browser (<http://genome.ucsc.edu/cgi-bin/hgGateway?db=hg18>; March 2006 release).

MUTATION SCREENING IN SALIVA SAMPLES

Almost 2ml of saliva samples were collected from 5 patients and mixed with 2 ml DNA-preserving solution contained in the Oragene® DNA Self-Collection Kit Oragene (OG-500 Tube Format, DNA Genotek Inc., Kanata, Ontario, Canada - Fig. 3.6), according to the manufacturer's instructions (Fig. 3.7) and stored at room temperature or -20°C till DNA extraction.

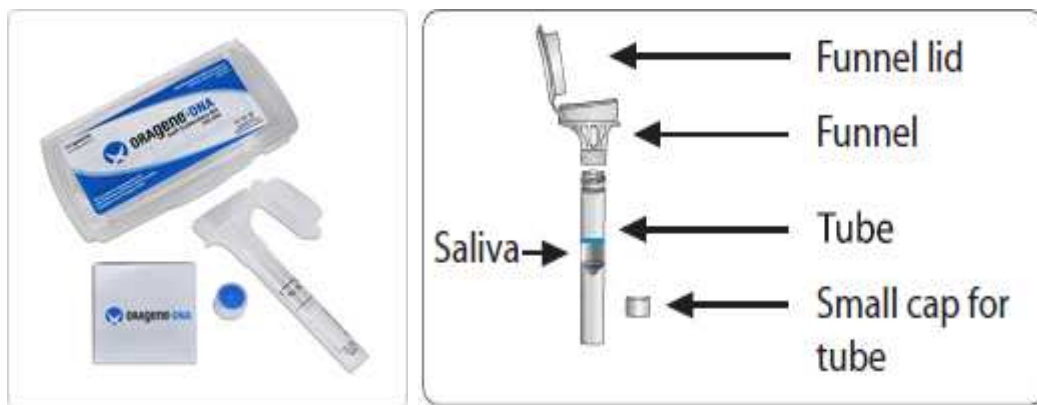


Fig. 3.6 Oragene® DNA Self-Collection Kit (OG-500 DNA Tube Format). The OG-500 DNA Collection Kit provides an all-in-one system for the collection, stabilization, transportation and purification of DNA from saliva. The kit contains a tube with 2 ml Oragene DNA solution in the funnel lid; a small cap to close the tube after removing the funnel; a multilanguage donor user instructions sheet.

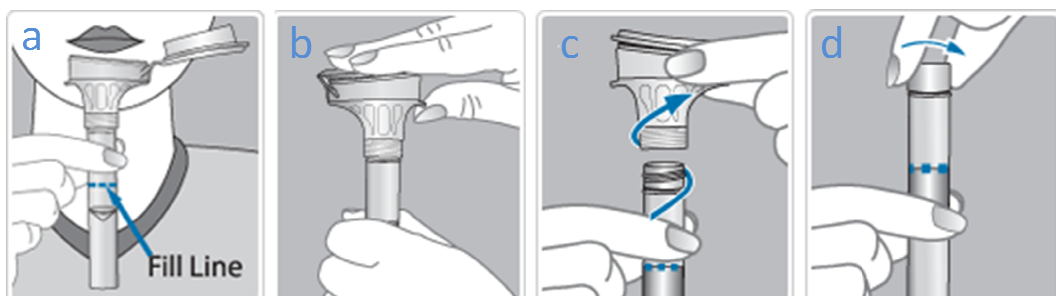


Fig. 3.7 Oragene® DNA Self-Collection Kit User Instructions. (a) Spit until the amount of saliva (not bubbles) reaches the fill line; (b) Close lid by pushing down hard on the funnel lid. The liquid in it will be released into the tube to mix with the saliva; (c) Unscrew the tube from the funnel; (d) Close tube tightly with small cap and mix.

Briefly, the vials were incubated for 1 hours and 30 minutes in a 50°C water incubator and then could be stored at room temperature or frozen (-15°C to -20°C), or it could be immediately processed. In this case, 500 µl of the mixed Oragene DNA/saliva sample were transferred to a 1.5 ml microcentrifuge tube, then 20 µl (1/25th volume) of Oragene DNA Purifier (OG-L2P, supplied) were added to it and were mixed by vortexing for a few seconds, before incubating on ice for 10 minutes. The samples were then centrifuged for 8 min at 13,000 rpm (15,000 × g) at room temperature and supernatants were transferred to new microcentrifuge tubes and discard the pellet containing impurities. 500 µl of room-temperature 95-100% ethanol were added to 500 µl of supernatant (an equal volume) and mixed gently by inversion 10 times. The samples were then centrifuged for 2 min at 13,000 rpm at room temperature, supernatants were discarded. 250 µl of 70% ethanol were added for 1 minute and carefully removed. DNA's pellets were dissolved in 30-50 µL AE buffer (Qiagen, Valencia, CA). The DNA samples were stored at -20°C until PCR analysis. DNA yield and purity were determined by measuring the absorbance at 260 nm (A260) and the ratio of absorbance at 260 nm and 280 nm (A260/A280) at the Nanodrop Spectrophotometer. The quality of DNA was confirmed by running 100 ng hydrated DNA on a 1% agarose gel.

STATISTICAL ANALYSIS

Differences in the distributions of prognostic factors in subgroups were analyzed by χ^2 or Fisher's exact test, and by Kruskal-Wallis test. Median follow-up time was estimated by reversing the codes for the censoring indicator in a Kaplan-Meier analysis¹²⁵. Overall Survival was defined as the time from diagnosis to date of death or date of the last follow-up. DFS and Cumulative Incidence of Relapse were calculated from the time of achieving CR to date of first relapse, death or date of last follow-up. The probabilities of OS and DFS were estimated using the Kaplan-Meier method¹²⁵ and the probability of Cumulative Incidence¹²⁶ of relapse was estimated using the appropriate non-parametric method, considering death in CR as competing risk. The log-rank test was used to compare treatment effect and risk factor categories for the Kaplan-Meier curves and the Gray test for the Incidence curves. Confidence intervals were estimated (95% CIs) using the Simon and Lee method¹²⁷.

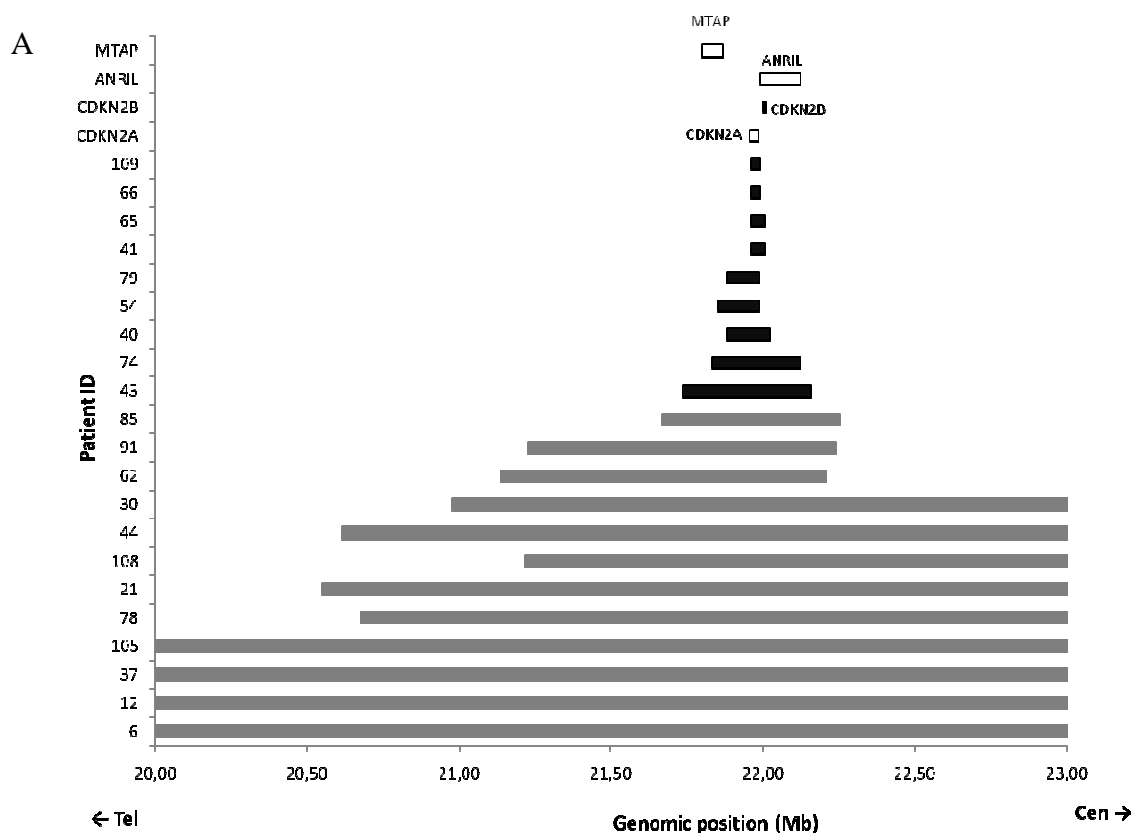
Cox proportional hazard regression model¹²⁸ was performed to examine and check for treatment results and the risk factors affecting Disease Free Survival.

All tests were 2-sided, accepting $p \leq 0.05$ as indicating a statistically significant difference. All analyses were performed using the SAS software (SAS Institute, Cary, NC).

4. RESULTS

SNP microarray analysis detects frequent and recurrent deletions in CDKN2A, ANRIL and CDKN2B genes at diagnosis and during leukemia progression

In order to detect the frequency and size of deletions occurring at 9p21 locus in *BCR-ABL1* positive ALL, data generated by high-resolution SNP arrays were analyzed in adult patients at diagnosis (n=82), relapse (n=11) or at both time points (n=19). At diagnosis, *CDKN2A* and *ANRIL* genomic alterations were identified in 29 (29%) patients. *ANRIL* has a first exon located about 300 bp upstream of the transcription start site of exon 1 β of *CDKN2A* and overlapping at its 5' end the two exons of *CDKN2B*. In 25 patients (25%) genomic deletions also included the two exons of *CDKN2B*. Deletions were monoallelic in the majority of cases (72%) with a median of 1,012 kb in size (range, 2.8-31,319 kb). In 9/29 (43%) patients with *CDKN2A/ANRIL/CDKN2B* losses, the minimal overlapping region of the lost area spanned only the two genes, but more often (12/29, 57%) the loss was considerable larger and extended sometimes (3/29, 10%) over the entire short chromosome arm eliminating a large number of genes (Fig. 4.1-A). In contrast, cases with bi-allelic inactivation were 8/29 (28%) with the majority of deletions (6/8, 75%) limited to *CDKN2A/ANRIL/CDKN2B* genes (Fig. 4.1-B).



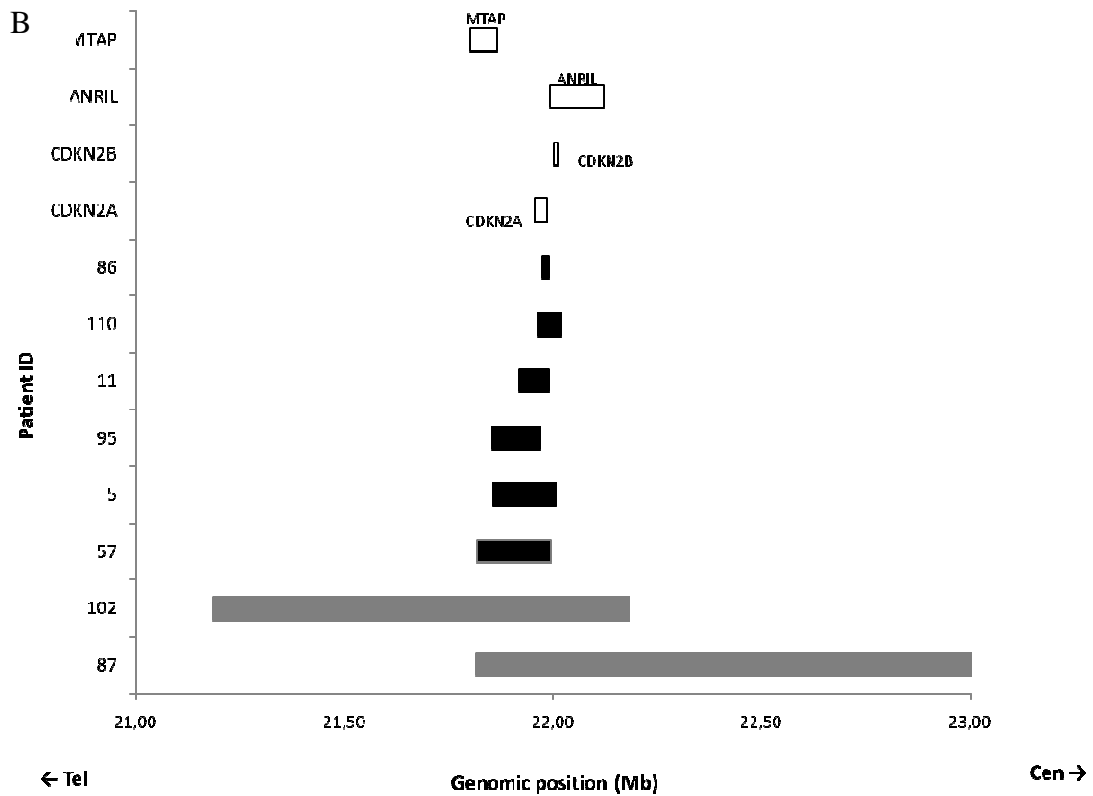


Fig. 4.1. Schematic representation of heterozygous (A) and homozygous (B) deletions occurring on 9p21 genomic locus in adult BCR-ABL1 positive ALL patients. Gray bars indicate large deletions extending over the *CDKN2A/ANRIL/ARF* genes; black bars indicate small deletions spanning only the *CDKN2A/ANRIL/ARF* genes. A schematic position and size of *MTAP*, *CDKN2A*, *ANRIL* and *CDKN2B* genes are also reported as white bars

Next, in order to investigate whether the deletions of *CDKN2A/ANRIL/CDKN2B* genes could be involved in disease progression, the genomic status of the 9p21 locus was assessed at the time of relapse in 30 patients (11 unpaired and 19 paired relapsed cases). In an unpaired analysis, an almost significant increase in the detection rate of *CDKN2A* loss (47%) compared to diagnosis (29%) ($p = 0.06$) was found by a non parametric *t*-test. When we analyzed the type of deletion, we found that both at diagnosis and relapse deletions were heterozygous in the majority of cases (72% vs 28%) (Tab. 4.1).

		Diagnosis (n = 101)	%	Relapse (n = 30)	%
CDKN2A Deletion	Heterozygous	21	20.8	10	33.3
	Homozygous	8	7.9	4	13.3
	Total	29	28.7	14	46.6
ANRIL Deletion	Heterozygous	23	22.8	10	33.3
	Homozygous	6	5.9	3	10.0
	Total	29	28.7	13	43.3
CDKN2B Deletion	Heterozygous	19	18.8	9	30.0
	Homozygous	6	5.9	3	10.0
	Total	25	24.8	12	40

Tab. 4.1. Deletion rates of *CDKN2A/ANRIL/CDKN2B* at diagnosis and relapse. 101 patients were analyzed at diagnosis, whereas 11 patients (including paired and unpaired cases) were analyzed at the time of relapse. The table shows the numbers and percentages of *BCR-ABL1*-positive ALL patients with heterozygous and homozygous deletions at diagnosis and at relapse.

FISH analysis confirmed large deletions

FISH experiments with BACs and fosmids encompassing the whole *MTAP-CDKN2A-CDKN2B* locus (Fig. 4.2-A) were performed in six *BCR-ABL1*-positive ALL patients, in order to confirm the deletion disclosed by SNP array analysis.

The deletion was detected (at FISH resolution) in two cases, as all the used *MTAP-CDKN2A-CDKN2B* probes were shown to be heterozygously deleted on chromosome der(9) in Ph+ metaphases [identified by the splitting signal of RP11-164N13, observed respectively on der(9) and Ph chromosomes] (Fig. 4. 2-B,C and data not shown).

The same probes failed to identify the deletion in the other four patients under study (data not shown), due to the limited size of the deletion spanning only the two genes and behind the limits of FISH resolution, as verified by SNP array.

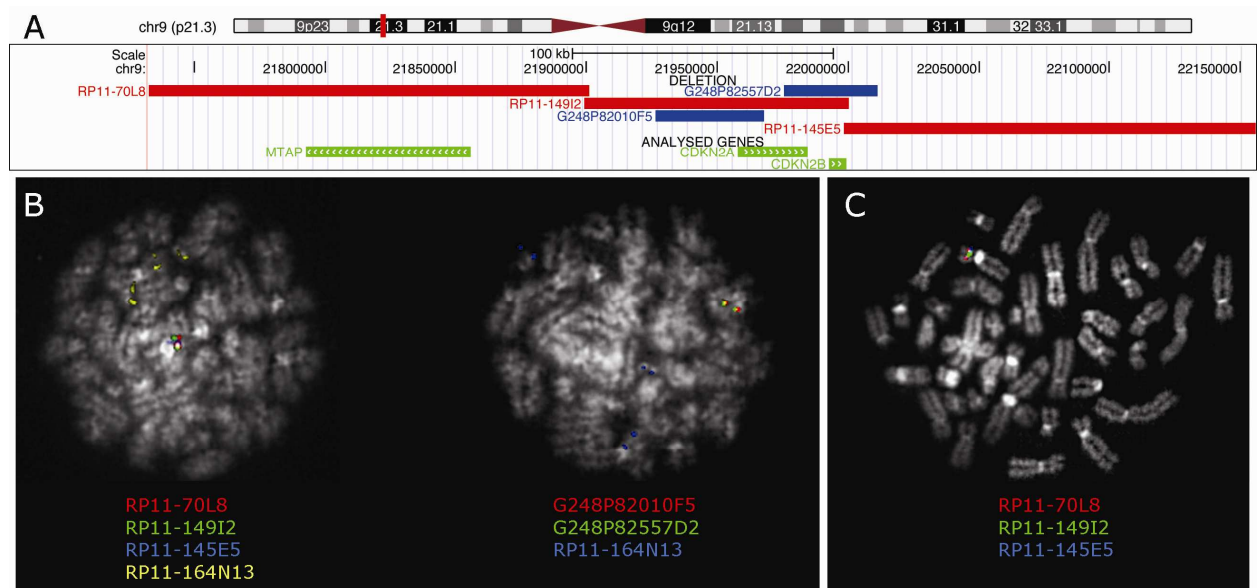


Fig. 4.2 (A) Map of the clones used in FISH experiments to detect *MTAP-CDKN2A-CDKN2B* deletions, showing BACs, fosmids, and genes respectively with red, blue, and green bars. (B) and (C) FISH results obtained in patients #1 and #2, respectively, showing a *MTAP-CDKN2A-CDKN2B* heterozygous deletion. (B) Only one fluorescent signal of both BACs (on the left) and fosmids (on the right) observed on normal chromosome 9 in Ph positive metaphases (as shown by the three signals of RP11-164N13); (C) Colocalization of all the *MTAP-CDKN2A-CDKN2B* BAC probes only on normal chromosome 9. No signal on der(9).

Deletions lead to a down-expression of CDKN2A levels

In order to investigate the functional consequences of genomic deletions affecting the 9p21 locus, the *CDKN2A* transcript levels were assessed by quantitative RT-PCR in three different groups of *BCR-ABL1* positive ALL patients: 1) *CDKN2A* wild-type cases (n = 18); 2) *CDKN2A* heterozygous deleted cases (n = 5); 3) *CDKN2A* homozygous deleted cases (n = 7). The Hs00924091_m1 assay (Applied Biosystems) amplifying the 1-2 exon boundary of *CDKN2A* (reference sequence NM_058195.3) was used. Results showed a significant decrease of the expression of *CDKN2A* in heterozygous deleted cases ($p = 0.04$) and in homozygous deleted cases ($p = 0.01$) compared to cases without deletion. The median *CDKN2A* expression level expressed as $2^{\exp(-\Delta\Delta\text{ct})}$ in diploid cases was 2.86 (range, 0.81-14.41) versus 0.19 (range, 0.10-0.53) and 0.004 (range, 0.0003-0.0653) of cases with mono-allelic and bi-allelic losses, respectively (Fig. 4.3).

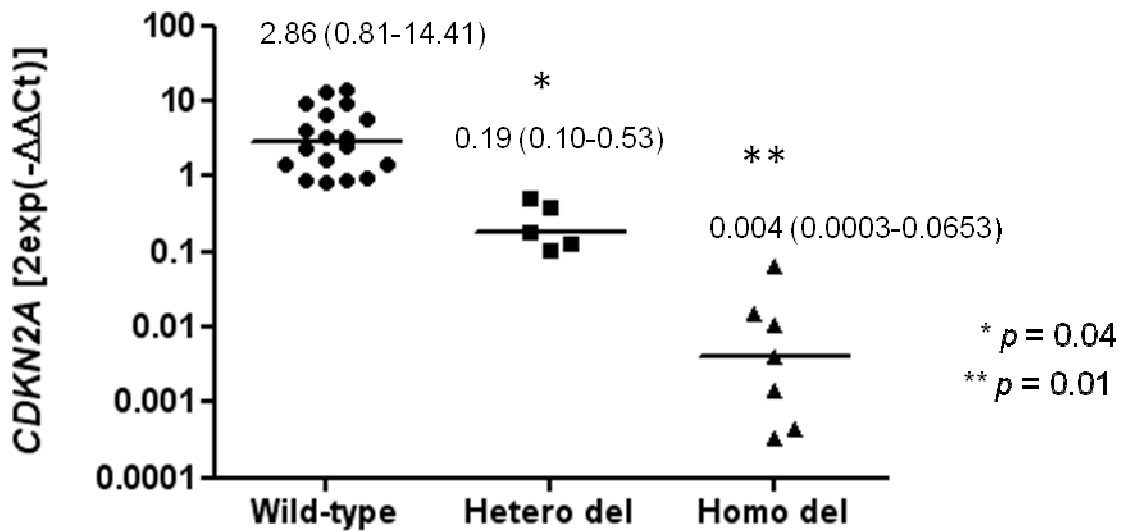


Fig. 4.3 Expression levels of *CDKN2A* in *BCR-ABL1* positive ALL patients with: 1) wild-type *CDKN2A*; 2) heterozygous *CDKN2A* deletion; 3) homozygous *CDKN2A* deletion. Results are expressed as $2^{\text{exp}(-\Delta\Delta\text{Ct})}$. Non-parametric t-test was used to compare group 1 vs group 2 ($p = 0.04$), group 1 vs group 3 ($p = 0.01$) and group 2 vs group 3 ($p = 0.004$).

A significant difference in the expression of *CDKN2A* was also observed among cases with heterozygous and homozygous deletions ($p = 0.004$). Overall, these results suggest that deletions lead to *CDKN2A* haploinsufficiency.

CDKN2A/ARF and *CDKN2B* mutation screening

9p21 locus can be inactivated in many tumors due to several mechanisms in addition to deletions, such as hypermethylation of promoter regions and inactivating mutations. Since hypermethylation is a rare event in acute lymphoblastic leukemia^{65,66,84,91}, here we aimed to investigate the frequency of point mutations occurring in *CDKN2A/ARF* and *CDKN2B* genes. To address this issue, a mutation screening of all coding exons of *CDKN2A/ARF* (exons 1 α , 1 β , 2 and 3) and *CDKN2B* (exons 1 and 2) genes was successfully performed on patients who were known to have retained by SNP array at least one *CDKN2A/CDKN2B* allele or who were wild-type (Tab. 4.2).

			N	%
CDKN2A Ex 1α	Diagnosis (n = 30)	WT	5	16.7
		5' UTR 21965017 A	11	36.6
		5' UTR 21965017 G/A	14	46.7
	All mutated pts		25	83.3
	Relapse (n = 10)	WT	1	10.0
		5' UTR 21965017 A	2	20.0
		5' UTR 21965017 G/A	6	60.0
5' UTR 21964851 C/T		1	10.0	
All mutated pts		9	90.0	
ARF Ex 1β			N	%
	Diagnosis (n = 35)	WT	35	100.0
	Relapse (n = 12)	WT	12	100.0
CDKN2A/ARF Ex 2			N	%
	Diagnosis (n = 32)	WT	24	75.0
		rs3731249 A A148T	1	3.0
		rs3731249 G/A A148T	5	16.0
		D146N ^{CDKN2A} /3'UTR ^{ARF} 21960922	1	3.0
		R128 ^{CDKN2A} /3' UTR ^{ARF} 21960974	1	3.0
	All mutated pts		2	6.3
Relapse (n = 12)	WT	12	100.0	
CDKN2A/ARF Ex 3			N	%
	Diagnosis (n = 36)	WT	2	6.0
		3' UTR rs11515 C	22	67.0
		3' UTR rs11515 C/G	11	34.0
		3' UTR rs11515 C	1	3.0
	Relapse (n = 11)	WT	0	0
		3' UTR rs11515 C	8	80.0
		3' UTR rs11515 C/G	2	20.0
3' UTR rs3088440 C/T		1	10.0	
CDKN2B Ex 1			N	%
	Diagnosis (n = 42)	WT	42	100.0
	Relapse (n = 14)	WT	14	100.0
CDKN2B Ex 2			N	%
	Diagnosis (n = 42)	WT	41	97,6
		P83	1	2,4
Relapse (n = 15)	WT	15	100,0	

Tab. 4.2. Amplification and sequencing of *CDKN2A/B* in *BCR-ABL1*-positive ALL patients (pts) at diagnosis and relapse; results including wild-type (WT) or mutated sequence are reported for each exon (Ex).

Samples tested were from diagnosis (n = 30 for exon 1 α of *CDKN2A*; n = 35 for exon 1 β of *CDKN2A*; n = 32 for exon 2 of *CDKN2A*; n = 36 for exon 3 of *CDKN2A*; n = 42 for exon 1 and 2 of *CDKN2B*) and relapse (n = 10 for exon 1 α of *CDKN2A*; n = 12 for exon 1 β of *CDKN2A* and exon 2 of *CDKN2A*; n = 11 for exon 3 of *CDKN2A*; n = 14 for exon 1 of *CDKN2B*; n = 14 for exon 2 of *CDKN2B*). Amplification and sequencing results showed that in the analyzed subset of patients non-synonymous point mutations in coding exons are rare with only one patient harboring a somatic non-synonymous mutation. This was detected in a diagnosed sample and involved a base substitution of G >A in exon 2 of *CDKN2A* at codon 146, that resulted in a substitution of aspartic acid in asparagine (D146N). A base substitution of G >A in the same exon at codon 128 was identified in another case but it resulted in a synonymous substitution of arginine (R128). Additional mutations have been identified in the 5' untranslated region (UTR) of *CDKN2A* exon 1 α at position 21965017, 191 bp before the start codon, (<http://genome.ucsc.edu/cgi-bin/hgGateway?db=hg18; March 2006 release>) with a heterozygous substitution of G > A in 46.7% of diagnosis patients and in 60.0% of relapse cases. This substitution was homozygous in 36.6 % of diagnosis cases and in 20.0% of relapse cases. In the same region but at position 21964851, 25 bp before the start codon, a heterozygous substitution of C >T was found in only one patient at relapse (10%). Frequent nucleotide variations were identified in exons 2 and 3 of *CDKN2A* but they resulted in known SNP after comparison with the database dbSNP (<http://www.ncbi.nlm.nih.gov/projects/SNP/>). These variations include the following known single nucleotide polymorphisms: rs3731249 G/A, rs11515 C/G and rs3088440 C/T. The rs3731249 G/A is located in the exon 2 of *CDKN2A* and it is responsible for a non-synonymous substitution of alanine with threonine at codon 148. The rs11515 C/G and rs3088440 C/T polymorphisms are located in the 3' UTR. The first and second exons of *CDKN2B* resulted wild-type, except for the silent mutation at codon 83 (P83) identified in one case at diagnosis (Tab. 4.2 and Fig. 4.4).

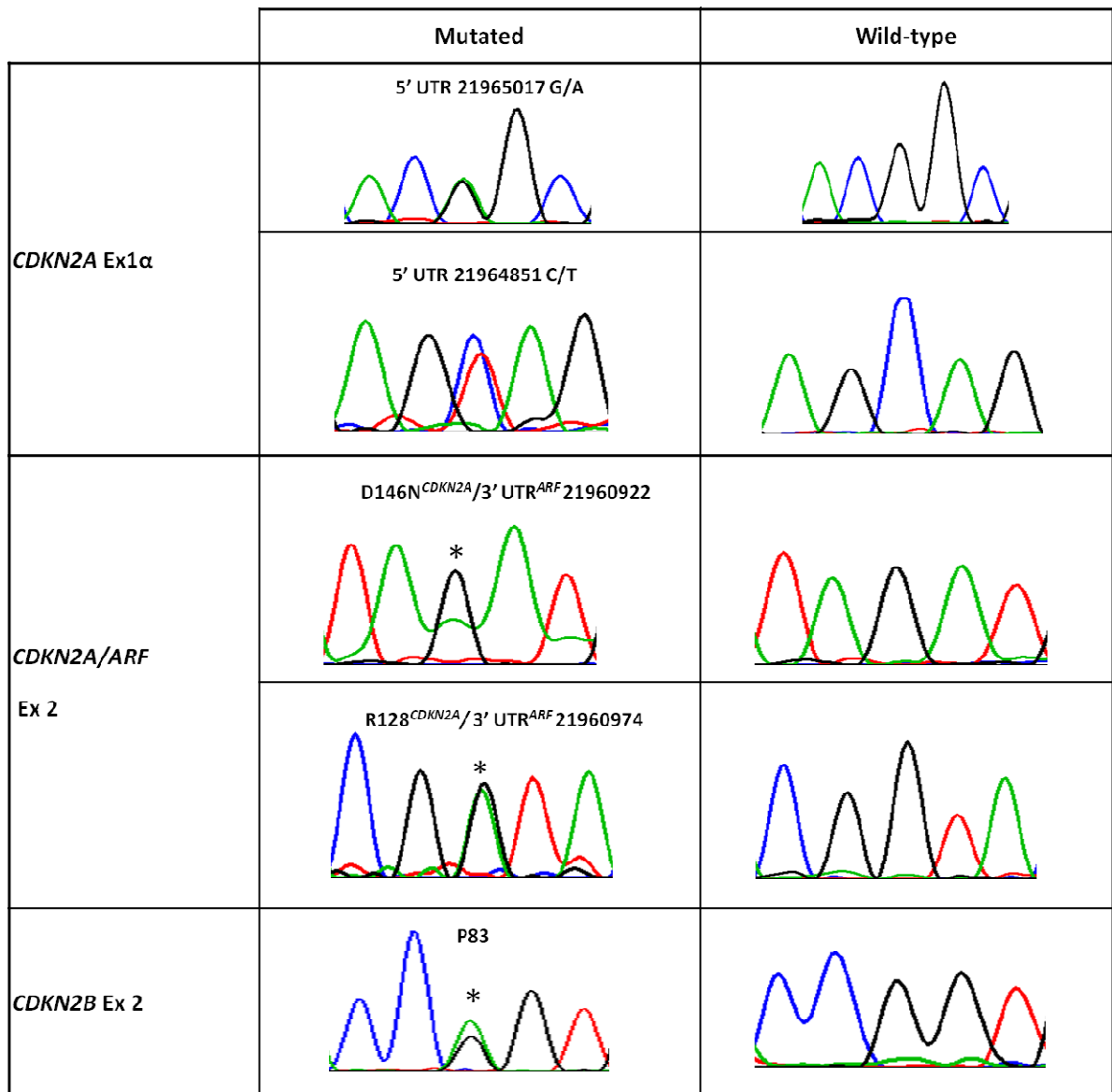


Fig. 4.4 Electropherograms of mutations identified by PCR and subsequent sequencing of *CDKN2A/ARF/CDKN2B* genes. For each mutation an electropherogram showing five nucleotides with the starred mutated base in the middle is showed in the first column. The wild-type alleles are reported in the second column. Overall we identified the following mutations: two nucleotide substitutions in the 5' untranslated region (UTR) of *CDKN2A*; one substitution at genomic position 21960922 corresponding to a non-synonymous mutation (D146N) in the exon 2 of *CDKN2A* and a variation in the 3'UTR of *ARF* gene; one substitution at genomic position 21960974 corresponding to a synonymous mutation of *CDKN2A* (R128) and a variation in the 3'UTR of *ARF* gene; a silent mutation in the exon 2 of *CDKN2B*.

Comparison between leukemia and germline DNA samples

In order to assess whether the nucleotide substitutions identified in *CDKN2A/B* genes were acquired at the time of leukemia (somatic mutations), we compared the leukemia DNA samples with those obtained from collection of saliva after written informed consent. For this analysis 5 cases were available. PCR was performed on the promoter region and exon 1 α of *CDKN2A* to assess the mutational status of the substitution at position 21965017 since the remaining exons resulted wild-type or containing single nucleotide polymorphisms. Results showed that the mutation was inherited for the cases #1, #2 and #3; it was acquired by the leukemia blast cells from the case #4 and interestingly the case #2 showed a weird pattern with the mutation in the germline/saliva sample and with the wild-type allele in the leukemia sample (Fig. 4.5).

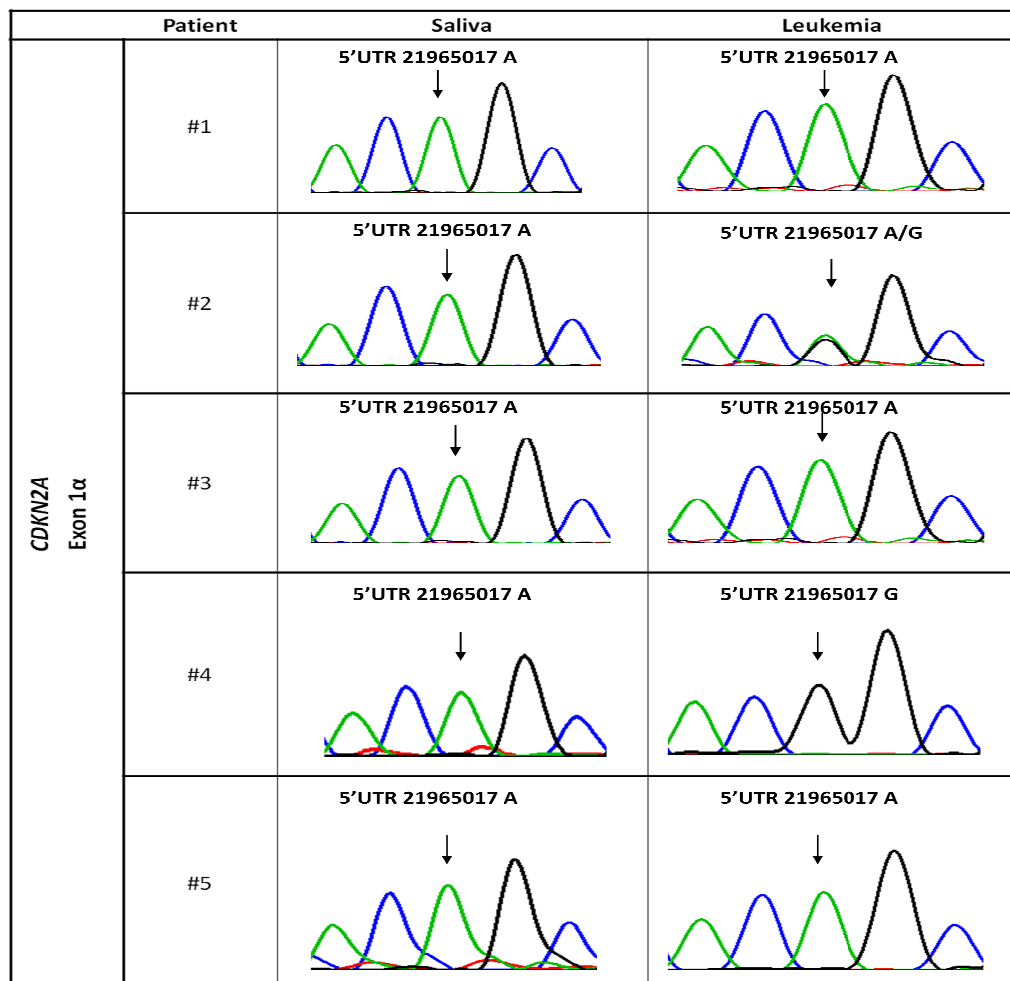


Fig. 4.5 Comparison between leukemia and saliva DNA samples. PCR was performed in 5 cases on on the promoter region and exon 1 α of *CDKN2A* to assess the mutational status of the substitution at position 21965017 since the remaining exons resulted wild-type or containing single nucleotide polymorphisms.

CDKN2A/B deletions and correlation with clinical outcome

Finally, after having demonstrated that deletions are the main mechanism of inactivation, we investigated their implications in leukemia. Therefore, in order to determine whether deletions in *CDKN2A/B* genes could impair response to treatment in *BCR-ABL1* positive ALL patients, clinical data were collected from 81 patients. The median follow-up was 25.2 months (range 2.1-148.1). Patient's characteristics are reported in Table 4.3.

<i>Variable</i>	<i>BCR-ABL1</i>-positive ALL patients (n=81)	%
Age (median, range)	53.71 yrs (18-76)	
Gender (M/F)	48/33	
White blood cell count (x10 ⁹ /L)	21.95 (0.40-302.00)	
<i>CDKN2A/B</i> Loss	29	35.80
<i>CDKN2A/B</i> Normal	52	64.20
Protocol*		
LAL2000	13	16.05
LAL1205	47	58.02
LAL0201-B	12	14.81
Institutional	9	11.11
Follow-up, months		
Median (range)	25.2 mesi (2.1-148.1)	

Tab. 4.3 Demographics and Clinical Characteristics of patients with *BCR-ABL1* positive ALL analyzed for the genomic status of *CDKN2A/ARF* and *CDKN2B* and for correlation with clinical outcome. *Protocol LAL0201-B enrolled elderly (>60 years) Ph+ ALL patients who received imatinib, 800 mg daily, associated to steroids as frontline treatment; LAL2000 enrolled adult (>18 years) ALL patients, including Ph+ cases, who received induction and consolidation chemotherapy followed by maintenance therapy with imatinib; LAL1205 enrolled adult Ph+ ALL patients who received Dasatinib 70mg/bid for 84 consecutive days, as induction therapy, initially associated to steroids without further chemotherapy as frontline treatment.

Briefly, the median age at diagnosis was 53.71 years (range, 18-76), the median white blood cell count was 21.95 (x10⁹/L) (range, 0.40-302.00) and *CDKN2A/B* was lost in 29 (35.80%) cases. 72 patients (89%) were enrolled in the GIMEMA clinical trials (12 patients in GIMEMA

LAL0201-B protocol, 13 in LAL2000 and 47 in the LAL1205 protocols), while 9 patients (11%) were enrolled into institutional protocols. Details of the treatment schemes have been previously reported¹²⁹. A univariate analysis of the *CDKN2A/B* genomic status and its association with outcome was performed. A shorter overall survival (OS) and disease-free survival (DFS) were found in patients with *CDKN2A/B* deletion compared with wild-type patients (OS: 27.7 v 38.2 months, respectively, $p = 0.0206$; DFS: 10.1 vs 56.1 months, respectively, $p = 0.0010$). Moreover, a higher cumulative incidence of relapse (CIR) for patients with *CDKN2A/B* deletion versus patients wild-type (73.3 vs 38.1; $p = 0.0014$) was also recognized (Fig. 4.6 and Tab. 4.4).

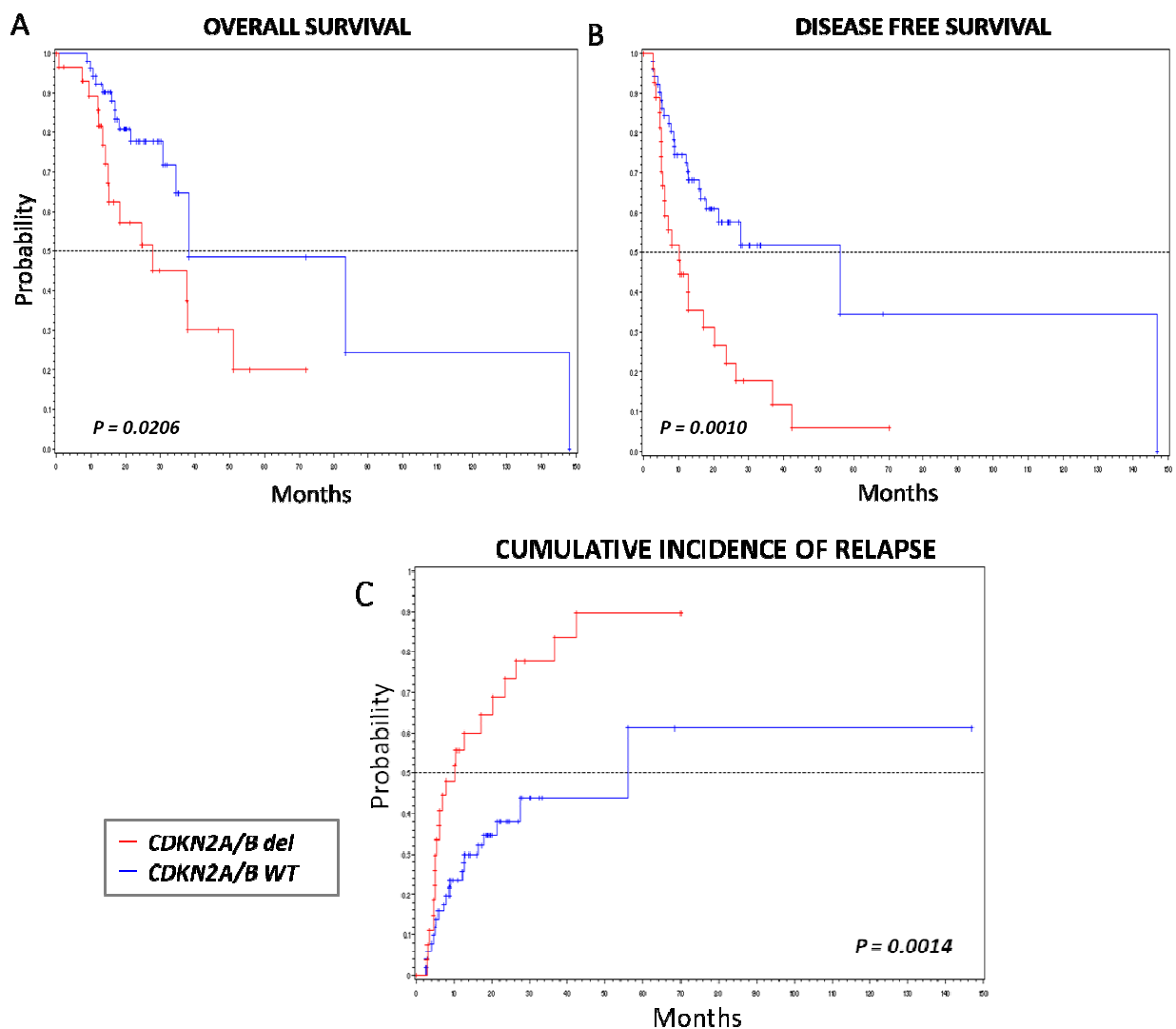


Fig. 4.6 Overall Survival (A), disease-free survival (B) and cumulative incidence of relapse (C) of de novo BCR-ABL1-ALL patients enrolled in different clinical trials of GIMEMA according to *CDKN2A/B* deletions.

		<i>CDKN2A/B</i> loss % (C.I. 95%)	<i>CDKN2A/B</i> wild- type % (C.I. 95%)	Pr > Chi- Square
Cumulative Incidence of Relapse (CIR)	Patients	27	51	0.0014
	at 24 mo	73.3% (71.6-75.1)	38.1% (37-39.2)	
	Median time	10.1 mo	56.1	
Disease free survival (DFS)	Patients	27	51	0.0010
	at 24 mo	22.2% (18.8-26.3)	57.6% (49.8-66.7)	
	Median time	10.1 mo	56.1 mo	
Overall survival (OS)	Patients	29	52	0.0206
	at 24 mo	57.2% (46.5-70.4)	77.8% (68.7-88.1)	
	Median time	27.7 mo	38.2 mo	

Tab. 4.4. Clinical outcome related to *CDKN2A/B* loss in univariate analysis. Abbreviations: mo (months), wt (wild-type); CIR: Cumulative Incidence of Relapse; DFS: Disease- Free Survival; OS: Overall Survival

Noteworthy, the multivariate analysis confirmed the negative prognostic impact of *CDKN2A/B* deletion on DFS ($p = 0.0051$; Tab. 4.5).

	Hazard ratio	95% CI	p-value
<i>CDKN2A/B</i> genomic status			
<i>CDKN2A/B</i> loss vs. <i>CDKN2A/B</i> wild-type	2.441	1.306-4.506	0.0051
Age	0.985	0.959-1.011	0.2405
Wbc at diagnosis	1.005	0.999-1.005	0.0734
Protocol treatment			
LAL1205 vs. LAL0201B	1.009	0.423-2.409	0.9839
LAL2000 vs. LAL0201B	1.641	0.536-5.024	0.3856
other protocols vs. LAL0201B	0.766	0.253-2.316	0.6366

Tab. 4.5. *CDKN2A/B* loss and other clinical relevant factors for predicting Disease Free Survival (multivariate analysis).

5. DISCUSSION

CDKN2A and *ARF* share common second and third exons, but different exon 1 (exon 1 α for *CDKN2A* and exon 1 β for *ARF*) and therefore they are translated in alternate reading frames, exhibiting no protein sequence similarity. Functionally, *CDKN2A* is a cyclin-dependent kinase inhibitor, whereas *ARF* (p19 Arf in mice) regulates p53 tumour suppressor function through its interaction with Mdm2¹³⁰. *CDKN2B* lies adjacent to *CDKN2A/ARF* and it encodes p15^{INK4B}, a cyclin-dependent kinase inhibitor, which forms a complex with CDK4 or CDK6, and prevents the activation of the CDK kinases, thus the encoded protein functions as a cell growth regulator that controls cell cycle G1 progression.

In literature several groups studied how the 9p21 chromosome band is inactivated in ALL, but most of them referred to a small cohort of patients, mainly pediatric and using low resolution methodologies. For example, traditional techniques, that have a limited number of probes, are not able to detect small deletions that often occurs in this locus and may underestimate the real occurrence.

Therefore, in this study, to exceed these restraints we performed high resolution Affymetrix SNP arrays in 112 Ph+ ALL adult patients with the aims to explore the frequency and size of deletions on 9p21 affecting the *CDKN2A/ARF/CDKN2B* genes in adult *BCR-ABL1*-positive ALL patients; to determine the main mechanism of inactivation and to correlate deletions with clinical outcome.

In ALL patient samples, the size and position of 9p21.3 deletions seem to vary substantially, but in most cases *CDKN2A* is co-deleted with *CDKN2B* and^{77,79,1} the frequency of genomic deletions is 21% in B-cell precursor ALL and 50% in T-ALL patients.

In this study, by high-resolution single nucleotide polymorphisms arrays we identified at diagnosis, *CDKN2A/ARF* and *ANRIL* genomic alterations in 29% of *BCR-ABL1* positive ALL patients. In 25% of cases genomic deletions also included the two exons of *CDKN2B*. Deletions were predominantly monoallelic and the minimal overlapping region of the lost area in more than half of leukemia cases (57%) was considerable large and extended sometimes (10%) over the entire short chromosome arm eliminating a large number of genes.

To investigate whether deletion of *CDKN2A/ARF* could be involved in disease progression, the genomic status of 9p21 locus was assessed at the time of relapse and an almost significant increase in the detection rate of *CDKN2A/ARF* loss (47%) compared to diagnosis ($p = 0.06$) was found, suggesting that loss of this genomic region is involved in disease progression. But are the deletions the only mechanism of 9p21 inactivation? It is well know that in addition to deletions, the *CDKN2A/B* locus can also be inactivated by epigenetic silencing through DNA methylation or by point mutations. Methylation of *CDKN2A* and *CDKN2B* seems to lack prognostic

significance in ALL⁸⁴, and the rate of point mutations has been extremely low in ALL^{1,78,85-89}. In line with these findings, by a gene candidate deep sequencing screening of *ARF*, *CDKN2A* and *CDKN2B*, in our *BCR-ABL1* positive ALL cohort point mutations were found at very low level with only a missense substitution in the exon 2 of *CDKN2A* (D146N). Additional mutations have been identified in the 5' UTR/promoter of *CDKN2A* exon 1 α at position 21965017, 191 bp before the start codon, with a heterozygous substitution of G > A and at position 21964851, 25 bp before the start codon, with a heterozygous substitution of C >T. There are only few studies, mainly conducted on melanoma, addressing the possible impact of 5'-UTR/promoter variants on the transcription or translation of the protein. In one of them, the variant at -25 C >T, not observed in the control population, exhibited an intermediate impact on functional defects, proposing that this variant should be considered as potential mutation¹³¹. Another study, on the other hand, indicates that the A-191G variant is probably a polymorphism and that is very unlikely to confer a high risk of melanoma, because it is present in the control population at approximately the same percentage as in melanoma cases^{132,133}.

Moreover, frequent nucleotide variations, known as SNP, were identified in exons 2 and 3 of *CDKN2A*: rs3731249 G/A, rs11515 C/G and rs3088440 C/T. 9p21 is an important susceptibility locus for several diseases. The SNPs identified and here showed have been already reported to be phenotypically associated with solid tumors like non-Hodgkin lymphoma¹³⁴, breast cancer¹³⁵, colorectal cancer^{136,137}, and they are also associated with disease such Alzheimer¹³⁸ and melanoma¹³⁹, but their role in leukemia has not yet been well established and a larger number of patients is required to demonstrate any potential association.

After having demonstrated that deletions are the main mechanism of inactivation, we investigated their implications in leukemia. Preliminary results have showed that in mice the combination of *BCR-ABL1* and *ARF* loss are sufficient to induce aggressive B-cell ALL, increased self-renewal capacity, inhibition of apoptosis and independence on cytokines, contributing to resistance to targeted therapy with TKIs^{140,141}. Moreover, recently Notta F. and colleagues¹⁴² showed that Ph+ ALL patient samples with a loss of *CDKN2A/B* had a tendency to poorer survival correlated with aggressive dissemination in xenografts and higher leukemia-initiating cell frequency compared to patients with normal *CDKN2A/B*, demonstrating that loss of *CDKN2A/B* contributes to clonal predominance at diagnosis and competitive xenograft growth.

How this may be translated *in vivo* in Ph+ ALL patients? In order to address this issue, we investigated the prognostic relevance of *CDKN2A/B* deletions in our study cohort. This matter is still controversial in literature with some studies suggesting that *CDKN2A/B* deletion is a poor

prognostic factor^{69,70,72,101,104,105}, whereas others showing no correlation^{74,76,100}. Beyond, Usvasalo et al. did not observe any difference in the incidence of deletion between diagnosis and relapse⁶⁴.

Our results showed that deletions of *CDKN2A/B* are significantly associated by univariate analysis with poor outcome in terms of overall survival ($p = 0.0206$), disease free survival ($p = 0.0010$) and cumulative incidence of relapse ($p = 0.0014$). The negative prognostic impact of *CDKN2A/B* deletion on DFS was thereafter confirmed by also a multivariate analysis ($p = 0.0051$). These results show that there are genetically distinct Ph+ ALL patients with a different risk of leukemia relapse and that testing for *CDKN2A/B* alterations at diagnosis may aid risk stratification. Furthermore, the awareness that genetically distinct patients experience different responses to treatment points to the need to develop more effective therapies able to eradicate all genetic leukemia cells and to prevent disease recurrence. Since the loss of *CDKN2A/B* eliminates the critical tumor surveillance mechanism and allows proliferation, cell growth and tumor formation by the action of Mdm2 and CDK4/6, attractive drugs could be represented by the inhibitors of Mdm2¹⁴³ and CDK4/CDK6¹⁴⁴.

In conclusions, our findings indicate that the inactivation of *CDKN2A/B* locus is a frequent event in Ph+ ALL. Deletions are frequently acquired at the leukemia progression and work as a poor prognostic marker, impairing overall survival, disease free-survival and cumulative incidence of relapse. Novel treatment strategies targeting the *ARF-Mdm2-p53* and the *CDKN2A/B-CDK4/6-Retinoblastoma* pathways may be effective in this subset of patients and *in vitro* studies are ongoing to confirm this hypothesis.

6. REFERENCES

1. Usvasalo A, Savola S, Raty R, et al. CDKN2A deletions in acute lymphoblastic leukemia of adolescents and young adults: an array CGH study. *Leuk Res.* 2008;32:1228-1235.
2. Lee HJ, Thompson JE, Wang ES, Wetzler M. Philadelphia chromosome-positive acute lymphoblastic leukemia: current treatment and future perspectives. *Cancer.* 2010.
3. Kurzrock R, Shtalrid M, Gutterman JU, et al. Molecular analysis of chromosome 22 breakpoints in adult Philadelphia-positive acute lymphoblastic leukaemia. *Br J Haematol.* 1987;67:55-59.
4. Bassan R, Gatta G, Tondini C, Willemze R. Adult acute lymphoblastic leukaemia. *Crit Rev Oncol Hematol.* 2004;50:223-261.
5. Reuther JY, Reuther GW, Cortez D, Pendergast AM, Baldwin AS, Jr. A requirement for NF-kappaB activation in Bcr-Abl-mediated transformation. *Genes Dev.* 1998;12:968-981.
6. He Y, Wertheim JA, Xu L, et al. The coiled-coil domain and Tyr177 of bcr are required to induce a murine chronic myelogenous leukemia-like disease by bcr/abl. *Blood.* 2002;99:2957-2968.
7. McWhirter JR, Wang JY. Effect of Bcr sequences on the cellular function of the Bcr-Abl oncoprotein. *Oncogene.* 1997;15:1625-1634.
8. Feller SM, Posern G, Voss J, et al. Physiological signals and oncogenesis mediated through Crk family adapter proteins. *J Cell Physiol.* 1998;177:535-552.
9. Sattler M, Salgia R, Okuda K, et al. The proto-oncogene product p120CBL and the adaptor proteins CRKL and c-CRK link c-ABL, p190BCR/ABL and p210BCR/ABL to the phosphatidylinositol-3' kinase pathway. *Oncogene.* 1996;12:839-846.
10. Van Etten RA. Mechanisms of transformation by the BCR-ABL oncogene: new perspectives in the post-imatinib era. *Leuk Res.* 2004;28 Suppl 1:S21-28.
11. Yuan Z, Mei HD. Inhibition of telomerase activity with hTERT antisense increases the effect of CDDP-induced apoptosis in myeloid leukemia. *Hematol J.* 2002;3:201-205.
12. Lewis ID, McDiarmid LA, Samels LM, To LB, Hughes TP. Establishment of a reproducible model of chronic-phase chronic myeloid leukemia in NOD/SCID mice using blood-derived mononuclear or CD34+ cells. *Blood.* 1998;91:630-640.
13. Ren R. Mechanisms of BCR-ABL in the pathogenesis of chronic myelogenous leukaemia. *Nat Rev Cancer.* 2005;5:172-183.
14. Melo JV. BCR-ABL gene variants. *Baillieres Clin Haematol.* 1997;10:203-222.
15. Pane F, Frigeri F, Camera A, et al. Complete phenotypic and genotypic lineage switch in a Philadelphia chromosome-positive acute lymphoblastic leukemia. *Leukemia.* 1996;10:741-745.
16. Konopka JB, Watanabe SM, Singer JW, Collins SJ, Witte ON. Cell lines and clinical isolates derived from Ph1-positive chronic myelogenous leukemia patients express c-abl proteins with a common structural alteration. *Proc Natl Acad Sci U S A.* 1985;82:1810-1814.
17. Louwagie A, Criel A, Verfaillie CM, et al. Philadelphia-positive T-acute lymphoblastic leukemia. *Cancer Genet Cytogenet.* 1985;16:297-300.
18. Gordon MY, Dowding CR, Riley GP, Goldman JM, Greaves MF. Altered adhesive interactions with marrow stroma of haematopoietic progenitor cells in chronic myeloid leukaemia. *Nature.* 1987;328:342-344.
19. Durig J, Schmucker U, Duhrsen U. Differential expression of chemokine receptors in B cell malignancies. *Leukemia.* 2001;15:752-756.
20. Deininger MW, Vieira S, Mendiola R, Schultheis B, Goldman JM, Melo JV. BCR-ABL tyrosine kinase activity regulates the expression of multiple genes implicated in the pathogenesis of chronic myeloid leukemia. *Cancer Res.* 2000;60:2049-2055.
21. Puil L, Liu J, Gish G, et al. Bcr-Abl oncoproteins bind directly to activators of the Ras signalling pathway. *Embo J.* 1994;13:764-773.
22. Oda T, Heaney C, Hagopian JR, Okuda K, Griffin JD, Druker BJ. Crkl is the major tyrosine-phosphorylated protein in neutrophils from patients with chronic myelogenous leukemia. *J Biol Chem.* 1994;269:22925-22928.

23. Sattler M, Mohi MG, Pride YB, et al. Critical role for Gab2 in transformation by BCR/ABL. *Cancer Cell*. 2002;1:479-492.
24. Ye D, Wolff N, Li L, Zhang S, Ilaria RL, Jr. STAT5 signaling is required for the efficient induction and maintenance of CML in mice. *Blood*. 2006;107:4917-4925.
25. Klejman A, Rushen L, Morrione A, Slupianek A, Skorski T. Phosphatidylinositol-3 kinase inhibitors enhance the anti-leukemia effect of STI571. *Oncogene*. 2002;21:5868-5876.
26. de Groot RP, Raaijmakers JA, Lammers JW, Koenderman L. STAT5-Dependent CyclinD1 and Bcl-xL expression in Bcr-Abl-transformed cells. *Mol Cell Biol Res Commun*. 2000;3:299-305.
27. Seki H, Seno A, Sakazume S, et al. [Clinical study of fluconazole-injectable and -granules in pediatric patients]. *Jpn J Antibiot*. 1994;47:289-295.
28. Gloc E, Warszawski M, Mlynarski W, et al. TEL/JAK2 tyrosine kinase inhibits DNA repair in the presence of amifostine. *Acta Biochim Pol*. 2002;49:121-128.
29. Afar DE, Witte ON. Characterization of breakpoint cluster region kinase and SH2-binding activities. *Methods Enzymol*. 1995;256:125-129.
30. Melo JV, Deininger MW. Biology of chronic myelogenous leukemia--signaling pathways of initiation and transformation. *Hematol Oncol Clin North Am*. 2004;18:545-568, vii-viii.
31. Vigneri P, Wang JY. Induction of apoptosis in chronic myelogenous leukemia cells through nuclear entrapment of BCR-ABL tyrosine kinase. *Nat Med*. 2001;7:228-234.
32. Lepelley P, Preudhomme C, Vanrumbeke M, Quesnel B, Cosson A, Fenaux P. Detection of p53 mutations in hematological malignancies: comparison between immunocytochemistry and DNA analysis. *Leukemia*. 1994;8:1342-1349.
33. Mullighan CG, Phillips LA, Su X, et al. Genomic analysis of the clonal origins of relapsed acute lymphoblastic leukemia. *Science*. 2008;322:1377-1380.
34. Martinelli G, Iacobucci I, Papayannidis C, Soverini S. New targets for Ph⁺ leukaemia therapy. *Best Pract Res Clin Haematol*. 2009;22:445-454.
35. Mullighan CG, Williams RT, Downing JR, Sherr CJ. Failure of CDKN2A/B (INK4A/B-ARF)-mediated tumor suppression and resistance to targeted therapy in acute lymphoblastic leukemia induced by BCR-ABL. *Genes Dev*. 2008;22:1411-1415.
36. Iacobucci I, Lonetti A, Messa F, et al. Expression of spliced oncogenic Ikaros isoforms in Philadelphia-positive acute lymphoblastic leukemia patients treated with tyrosine kinase inhibitors: implications for a new mechanism of resistance. *Blood*. 2008;112:3847-3855.
37. Nutt SL, Kee BL. The transcriptional regulation of B cell lineage commitment. *Immunity*. 2007;26:715-725.
38. Gallagher SJ, Kefford RF, Rizos H. The ARF tumour suppressor. *Int J Biochem Cell Biol*. 2006;38:1637-1641.
39. Aveyard JS, Knowles MA. Measurement of relative copy number of CDKN2A/ARF and CDKN2B in bladder cancer by real-time quantitative PCR and multiplex ligation-dependent probe amplification. *J Mol Diagn*. 2004;6:356-365.
40. Chin L, Pomerantz J, DePinho RA. The INK4a/ARF tumor suppressor: one gene--two products--two pathways. *Trends Biochem Sci*. 1998;23:291-296.
41. Riegert-Johnson DL. Cancer Syndromes. In: Douglas L Riegert-Johnson MLAB, MD,2 Timothy Hefferon, PhD,3 and Maegan Roberts, MS CGC ed; 2009.
42. Campisi J. Cancer and ageing: rival demons? *Nat Rev Cancer*. 2003;3:339-349.
43. Kim WY, Sharpless NE. The regulation of INK4/ARF in cancer and aging. *Cell*. 2006;127:265-275.
44. Healy J, Belanger H, Beaulieu P, Lariviere M, Labuda D, Sinnett D. Promoter SNPs in G1/S checkpoint regulators and their impact on the susceptibility to childhood leukemia. *Blood*. 2007;109:683-692.

45. Cunnington MS, Santibanez Koref M, Mayosi BM, Burn J, Keavney B. Chromosome 9p21 SNPs Associated with Multiple Disease Phenotypes Correlate with ANRIL Expression. *PLoS Genet.* 2010;6:e1000899.
46. Sharpless NE. INK4a/ARF: a multifunctional tumor suppressor locus. *Mutat Res.* 2005;576:22-38.
47. Stone S, Jiang P, Dayananth P, et al. Complex structure and regulation of the P16 (MTS1) locus. *Cancer Res.* 1995;55:2988-2994.
48. Mao L, Merlo A, Bedi G, et al. A novel p16INK4A transcript. *Cancer Res.* 1995;55:2995-2997.
49. Quelle DE, Zindy F, Ashmun RA, Sherr CJ. Alternative reading frames of the INK4a tumor suppressor gene encode two unrelated proteins capable of inducing cell cycle arrest. *Cell.* 1995;83:993-1000.
50. Ozenne P, Eymin B, Brambilla E, Gazzeri S. The ARF tumor suppressor: structure, functions and status in cancer. *Int J Cancer.* 2010;127:2239-2247.
51. Pollice A, Vivo M, La Mantia G. The promiscuity of ARF interactions with the proteasome. *FEBS Lett.* 2008;582:3257-3262.
52. Sharpless NE, Ramsey MR, Balasubramanian P, Castrillon DH, DePinho RA. The differential impact of p16(INK4a) or p19(ARF) deficiency on cell growth and tumorigenesis. *Oncogene.* 2004;23:379-385.
53. Rodway H, Llanos S, Rowe J, Peters G. Stability of nucleolar versus non-nucleolar forms of human p14(ARF). *Oncogene.* 2004;23:6186-6192.
54. Korgaonkar C, Hagen J, Tompkins V, et al. Nucleophosmin (B23) targets ARF to nucleoli and inhibits its function. *Mol Cell Biol.* 2005;25:1258-1271.
55. Greenblatt M.S. BJ, Gump JR, Godin KS, Trombley L, Koh J, Bond JP. Detailed computational study of p53 and p16: using evolutionary sequence analysis and disease-associated mutations to predict the functional consequences of allelic variants. *Oncogene* 2003;22, :1150-1163.
56. Ivanchuk SM, Mondal S, Dirks PB, Rutka JT. The INK4A/ARF locus: role in cell cycle control and apoptosis and implications for glioma growth. *J Neurooncol.* 2001;51:219-229.
57. Krimpenfort P IA, Song JY, van der Valk M, Nawijn M, Zevenhoven J, Berns A. p15Ink4b is a critical tumour suppressor in the absence of p16Ink4a. *Nature.* 2007;448(7156):943-946.
58. Herman JG JJ, Merlo A, Baylin SB. Hypermethylation-associated inactivation indicates a tumor suppressor role for p15INK4B. *Cancer Res.* 1996;56(4):722-727.
59. Tsellou E TC, Moschovi M, Athanasiadou-Piperopoulou F, Polychronopoulou S, Kosmidis H, Kalmanti M, Hatzakis A, Dessypris N, Kalofoutis A, Petridou E. Hypermethylation of CpG islands in the promoter region of the p15INK4B gene in childhood acute leukaemia. *Eur J Cancer.* 2005;41(4):584-589.
60. Pasmant E, Laurendeau I, Heron D, Vidaud M, Vidaud D, Bieche I. Characterization of a germ-line deletion, including the entire INK4/ARF locus, in a melanoma-neural system tumor family: identification of ANRIL, an antisense noncoding RNA whose expression coclusters with ARF. *Cancer Res.* 2007;67:3963-3969.
61. Jarinova O, Stewart AF, Roberts R, et al. Functional analysis of the chromosome 9p21.3 coronary artery disease risk locus. *Arterioscler Thromb Vasc Biol.* 2009;29:1671-1677.
62. Yu W, Gius D, Onyango P, et al. Epigenetic silencing of tumour suppressor gene p15 by its antisense RNA. *Nature.* 2008;451:202-206.
63. Broadbent HM, Peden JF, Lorkowski S, et al. Susceptibility to coronary artery disease and diabetes is encoded by distinct, tightly linked SNPs in the ANRIL locus on chromosome 9p. *Hum Mol Genet.* 2008;17:806-814.
64. Sulong S, Moorman AV, Irving JA, et al. A comprehensive analysis of the CDKN2A gene in childhood acute lymphoblastic leukemia reveals genomic deletion, copy number neutral

- loss of heterozygosity, and association with specific cytogenetic subgroups. *Blood*. 2009;113:100-107.
65. Drexler HG. Review of alterations of the cyclin-dependent kinase inhibitor INK4 family genes p15, p16, p18 and p19 in human leukemia-lymphoma cells. *Leukemia*. 1998;12:845-859.
66. Krug U, Ganser A, Koeffler HP. Tumor suppressor genes in normal and malignant hematopoiesis. *Oncogene*. 2002;21:3475-3495.
67. Sherborne AL, Hosking FJ, Prasad RB, et al. Variation in CDKN2A at 9p21.3 influences childhood acute lymphoblastic leukemia risk. *Nat Genet*. 2010;42:492-494.
68. Liggett WH, Jr., Sidransky D. Role of the p16 tumor suppressor gene in cancer. *J Clin Oncol*. 1998;16:1197-1206.
69. Kees UR, Burton PR, Lu C, Baker DL. Homozygous deletion of the p16/MTS1 gene in pediatric acute lymphoblastic leukemia is associated with unfavorable clinical outcome. *Blood*. 1997;89:4161-4166.
70. Calero Moreno TM, Gustafsson G, Garwicz S, et al. Deletion of the Ink4-locus (the p16ink4a, p14ARF and p15ink4b genes) predicts relapse in children with ALL treated according to the Nordic protocols NOPHO-86 and NOPHO-92. *Leukemia*. 2002;16:2037-2045.
71. Lee DS, Lee JH, Min HC, et al. Application of high throughput cell array technology to FISH: investigation of the role of deletion of p16 gene in leukemias. *J Biotechnol*. 2007;127:355-360.
72. Heyman M, Rasool O, Borgonovo Brandter L, et al. Prognostic importance of p15INK4B and p16INK4 gene inactivation in childhood acute lymphocytic leukemia. *J Clin Oncol*. 1996;14:1512-1520.
73. Kuiper RP, Schoenmakers EF, van Reijmersdal SV, et al. High-resolution genomic profiling of childhood ALL reveals novel recurrent genetic lesions affecting pathways involved in lymphocyte differentiation and cell cycle progression. *Leukemia*. 2007;21:1258-1266.
74. Mirebeau D, Acquaviva C, Suci S, et al. The prognostic significance of CDKN2A, CDKN2B and MTAP inactivation in B-lineage acute lymphoblastic leukemia of childhood. Results of the EORTC studies 58881 and 58951. *Haematologica*. 2006;91:881-885.
75. Irving JA, Minto L, Bailey S, Hall AG. Loss of heterozygosity and somatic mutations of the glucocorticoid receptor gene are rarely found at relapse in pediatric acute lymphoblastic leukemia but may occur in a subpopulation early in the disease course. *Cancer Res*. 2005;65:9712-9718.
76. van Zutven LJ, van Drunen E, de Bont JM, et al. CDKN2 deletions have no prognostic value in childhood precursor-B acute lymphoblastic leukaemia. *Leukemia*. 2005;19:1281-1284.
77. Bertin R, Acquaviva C, Mirebeau D, Guidal-Giroux C, Vilmer E, Cave H. CDKN2A, CDKN2B, and MTAP gene dosage permits precise characterization of mono- and bi-allelic 9p21 deletions in childhood acute lymphoblastic leukemia. *Genes Chromosomes Cancer*. 2003;37:44-57.
78. Ohnishi H, Hanada R, Horibe K, et al. Homozygous deletions of p16/MTS1 and p15/MTS2 genes are frequent in t(1;19)-negative but not in t(1;19)-positive B precursor acute lymphoblastic leukemia in childhood. *Leukemia*. 1996;10:1104-1110.
79. Strefford JC, Worley H, Barber K, et al. Genome complexity in acute lymphoblastic leukemia is revealed by array-based comparative genomic hybridization. *Oncogene*. 2007;26:4306-4318.
80. Sasaki S, Kitagawa Y, Sekido Y, et al. Molecular processes of chromosome 9p21 deletions in human cancers. *Oncogene*. 2003;22:3792-3798.
81. Mullighan CG GS, Radtke I, Miller CB, Coustan-Smith E, Dalton JD, Girtman K, Mathew S, Ma J, Pounds SB, Su X, Pui CH, Relling MV, Evans WE, Shurtleff SA, Downing JR. Genome-wide analysis of genetic alterations in acute lymphoblastic leukaemia. *Nature*. 2007;446(7137):758-764.

82. Kawamata N, Ogawa S, Zimmermann M, et al. Molecular allelokaryotyping of pediatric acute lymphoblastic leukemias by high-resolution single nucleotide polymorphism oligonucleotide genomic microarray. *Blood*. 2008;111:776-784.
83. Paulsson K CJ, Macdougall F, Stevens J, Stasevich I, Vrcelj N, Chaplin T, Lillington DM, Lister TA, Young BD. Microdeletions are a general feature of adult and adolescent acute lymphoblastic leukemia: Unexpected similarities with pediatric disease. *Proc Natl Acad Sci U S A*. 2008;105(18):6708-6713.
84. Chim CS, Tam CY, Liang R, Kwong YL. Methylation of p15 and p16 genes in adult acute leukemia: lack of prognostic significance. *Cancer*. 2001;91:2222-2229.
85. Guidal-Giroux C, Gerard B, Cave H, et al. Deletion mapping indicates that MTS1 is the target of frequent deletions at chromosome 9p21 in paediatric acute lymphoblastic leukaemias. *Br J Haematol*. 1996;92:410-419.
86. Lemos JA, Defavery R, Scrideli CA, Tone LG. Analysis of p16 gene mutations and deletions in childhood acute lymphoblastic leukemias. *Sao Paulo Med J*. 2003;121:58-62.
87. Kawamura M, Ohnishi H, Guo SX, et al. Alterations of the p53, p21, p16, p15 and RAS genes in childhood T-cell acute lymphoblastic leukemia. *Leuk Res*. 1999;23:115-126.
88. Takeuchi S, Bartram CR, Seriu T, et al. Analysis of a family of cyclin-dependent kinase inhibitors: p15/MTS2/INK4B, p16/MTS1/INK4A, and p18 genes in acute lymphoblastic leukemia of childhood. *Blood*. 1995;86:755-760.
89. Rasool O, Heyman M, Brandter LB, et al. p15ink4B and p16ink4 gene inactivation in acute lymphocytic leukemia. *Blood*. 1995;85:3431-3436.
90. Irvani M, Dhat R, Price CM. Methylation of the multi tumor suppressor gene-2 (MTS2, CDKN1, p15INK4B) in childhood acute lymphoblastic leukemia. *Oncogene*. 1997;15:2609-2614.
91. Wong IH, Ng MH, Huang DP, Lee JC. Aberrant p15 promoter methylation in adult and childhood acute leukemias of nearly all morphologic subtypes: potential prognostic implications. *Blood*. 2000;95:1942-1949.
92. Gutierrez MI, Siraj AK, Bhargava M, et al. Concurrent methylation of multiple genes in childhood ALL: Correlation with phenotype and molecular subgroup. *Leukemia*. 2003;17:1845-1850.
93. Chim CS, Wong AS, Kwong YL. Epigenetic inactivation of INK4/CDK/RB cell cycle pathway in acute leukemias. *Ann Hematol*. 2003;82:738-742.
94. Matsushita C, Yang Y, Takeuchi S, et al. Aberrant methylation in promoter-associated CpG islands of multiple genes in relapsed childhood acute lymphoblastic leukemia. *Oncol Rep*. 2004;12:97-99.
95. Kral BG, Mathias RA, Suktitipat B, et al. A common variant in the CDKN2B gene on chromosome 9p21 protects against coronary artery disease in Americans of African ancestry. *J Hum Genet*. 2011.
96. Hribal ML PI, Procopio T, Marini MA, Stančáková A, Kuusisto J, Andreozzi F, Hammarstedt A, Jansson PA, Grarup N, Hansen T, Walker M, Stefan N, Fritsche A, Häring HU, Pedersen O, Smith U, Laakso M, Sesti G; on behalf of the EUGENE2 Consortium. Glucose tolerance, insulin sensitivity and insulin release in European non-diabetic carriers of a polymorphism upstream of CDKN2A and CDKN2B. *Diabetologia*. 2011.
97. Liu Y, Sanoff HK, Cho H, et al. INK4/ARF transcript expression is associated with chromosome 9p21 variants linked to atherosclerosis. *PLoS One*. 2009;4:e5027.
98. Garcia-Manero G, Daniel J, Smith TL, et al. DNA methylation of multiple promoter-associated CpG islands in adult acute lymphocytic leukemia. *Clin Cancer Res*. 2002;8:2217-2224.
99. Garcia-Manero G, Jeha S, Daniel J, et al. Aberrant DNA methylation in pediatric patients with acute lymphocytic leukemia. *Cancer*. 2003;97:695-702.

100. Graf Einsiedel H, Taube T, Hartmann R, et al. Deletion analysis of p16(INKa) and p15(INKb) in relapsed childhood acute lymphoblastic leukemia. *Blood*. 2002;99:4629-4631.
101. Carter TL, Watt PM, Kumar R, et al. Hemizygous p16(INK4A) deletion in pediatric acute lymphoblastic leukemia predicts independent risk of relapse. *Blood*. 2001;97:572-574.
102. Primo D, Tabernero MD, Perez JJ, et al. Genetic heterogeneity of BCR/ABL+ adult B-cell precursor acute lymphoblastic leukemia: impact on the clinical, biological and immunophenotypical disease characteristics. *Leukemia*. 2005;19:713-720.
103. Kim M, Yim SH, Cho NS, et al. Homozygous deletion of CDKN2A (p16, p14) and CDKN2B (p15) genes is a poor prognostic factor in adult but not in childhood B-lineage acute lymphoblastic leukemia: a comparative deletion and hypermethylation study. *Cancer Genet Cytogenet*. 2009;195:59-65.
104. Fizzotti M, Cimino G, Pisegna S, et al. Detection of homozygous deletions of the cyclin-dependent kinase 4 inhibitor (p16) gene in acute lymphoblastic leukemia and association with adverse prognostic features. *Blood*. 1995;85:2685-2690.
105. Heerema NA, Sather HN, Sensel MG, et al. Association of chromosome arm 9p abnormalities with adverse risk in childhood acute lymphoblastic leukemia: A report from the Children's Cancer Group. *Blood*. 1999;94:1537-1544.
106. Papadhimitriou SI, Polychronopoulou S, Tsakiridou AA, Androutsos G, Paterakis GS, Athanassiadou F. p16 inactivation associated with aggressive clinical course and fatal outcome in TEL/AML1-positive acute lymphoblastic leukemia. *J Pediatr Hematol Oncol*. 2005;27:675-677.
107. Dalle JH, Fournier M, Nelken B, et al. p16(INK4a) immunocytochemical analysis is an independent prognostic factor in childhood acute lymphoblastic leukemia. *Blood*. 2002;99:2620-2623.
108. Hoshino K, Asou N, Okubo T, et al. The absence of the p15INK4B gene alterations in adult patients with precursor B-cell acute lymphoblastic leukaemia is a favourable prognostic factor. *Br J Haematol*. 2002;117:531-540.
109. Ramakers-van Woerden NL, Pieters R, Slater RM, et al. In vitro drug resistance and prognostic impact of p16INK4A/P15INK4B deletions in childhood T-cell acute lymphoblastic leukaemia. *Br J Haematol*. 2001;112:680-690.
110. Moreno TC, Widell S, Czader M, et al. Inverse correlation between Ink4-locus deletions and ICM-DNA hyperdiploidy in childhood acute lymphoblastic leukaemia, relation to clinical characteristics and outcome. *Eur J Haematol*. 2000;65:390-398.
111. Zhou M, Gu L, Yeager AM, Findley HW. Incidence and clinical significance of CDKN2/MTS1/P16ink4A and MTS2/P15ink4B gene deletions in childhood acute lymphoblastic leukemia. *Pediatr Hematol Oncol*. 1997;14:141-150.
112. Heyman M, Einhorn S. Inactivation of the p15INK4B and p16INK4 genes in hematologic malignancies. *Leuk Lymphoma*. 1996;23:235-245.
113. Cipolotti R, Lemos JA, Defavery R, Scrideli CA, Dal Fabbro AL, Tone LG. Inactivation of the p15 gene in children with acute lymphoblastic leukemia. *Sao Paulo Med J*. 2003;121:203-206.
114. Graf Einsiedel H, Taube T, Hartmann R, et al. Prognostic value of p16(INK4a) gene deletions in pediatric acute lymphoblastic leukemia. *Blood*. 2001;97:4002-4004.
115. Faderl S, Kantarjian HM, Manshour T, et al. The prognostic significance of p16INK4a/p14ARF and p15INK4b deletions in adult acute lymphoblastic leukemia. *Clin Cancer Res*. 1999;5:1855-1861.
116. Rubnitz JE, Behm FG, Pui CH, et al. Genetic studies of childhood acute lymphoblastic leukemia with emphasis on p16, MLL, and ETV6 gene abnormalities: results of St Jude Total Therapy Study XII. *Leukemia*. 1997;11:1201-1206.
117. Diccianni MB, Batova A, Yu J, et al. Shortened survival after relapse in T-cell acute lymphoblastic leukemia patients with p16/p15 deletions. *Leuk Res*. 1997;21:549-558.

118. Batova A, Diccianni MB, Nobori T, et al. Frequent deletion in the methylthioadenosine phosphorylase gene in T-cell acute lymphoblastic leukemia: strategies for enzyme-targeted therapy. *Blood*. 1996;88:3083-3090.
119. Okuda T, Shurtleff SA, Valentine MB, et al. Frequent deletion of p16INK4a/MTS1 and p15INK4b/MTS2 in pediatric acute lymphoblastic leukemia. *Blood*. 1995;85:2321-2330.
120. Martinelli G, Iacobucci I, Soverini S, Piccaluga PP, Cilloni D, Pane F. New mechanisms of resistance in Philadelphia chromosome acute lymphoblastic leukemia. *Expert Rev Hematol*. 2009;2:297-303.
121. Iacobucci I, Storlazzi CT, Cilloni D, et al. Identification and molecular characterization of recurrent genomic deletions on 7p12 in the IKZF1 gene in a large cohort of BCR-ABL1-positive acute lymphoblastic leukemia patients: on behalf of Gruppo Italiano Malattie Ematologiche dell'Adulto Acute Leukemia Working Party (GIMEMA AL WP). *Blood*. 2009;114:2159-2167.
122. Li C, Hung Wong W. Model-based analysis of oligonucleotide arrays: model validation, design issues and standard error application. *Genome Biol*. 2001;2:RESEARCH0032.
123. Mullighan CG, Goorha S, Radtke I, et al. Genome-wide analysis of genetic alterations in acute lymphoblastic leukaemia. *Nature*. 2007;446:758-764.
124. Storlazzi CT, Albano F, Dencic-Fekete M, Djordjevic V, Rocchi M. Late-appearing pseudocentric fission event during chronic myeloid leukemia progression. *Cancer Genet Cytogenet*. 2007;174:61-67.
125. Kaplan E, Meier P. Non parametric estimation from incomplete observation. *J Am Stat Assoc* 1958;53:457-481.
126. Gooley TA, Leisenring W, Crowley J, Storer B. Estimation of failure probabilities in the presence of competing risks: new representations of old estimators. *Statistics in Medicine*. 1999;18:695-706.
127. Simon R, Lee Y. Nonparametric confidence limits survival probabilities and median survival time. *Cancer Treat Res*. 1982;66:37-42.
128. Cox D. Regression models and life-tables. *J R Stat Soc*. 1972;34:187-220.
129. Martinelli G, Iacobucci I, Storlazzi CT, et al. IKZF1 (Ikaros) deletions in BCR-ABL1-positive acute lymphoblastic leukemia are associated with short disease-free survival and high rate of cumulative incidence of relapse: a GIMEMA AL WP report. *J Clin Oncol*. 2009;27:5202-5207.
130. Sherr CJ. The INK4a/ARF network in tumour suppression. *Nat Rev Mol Cell Biol*. 2001;2:731-737.
131. Bisio A, Nasti S, Jordan JJ, et al. Functional analysis of CDKN2A/p16INK4a 5'-UTR variants predisposing to melanoma. *Hum Mol Genet*. 2010;19:1479-1491.
132. Harland M, Holland EA, Ghiorzo P, et al. Mutation screening of the CDKN2A promoter in melanoma families. *Genes Chromosomes Cancer*. 2000;28:45-57.
133. Pollock PM, Stark MS, Palmer JM, et al. Mutation analysis of the CDKN2A promoter in Australian melanoma families. *Genes Chromosomes Cancer*. 2001;32:89-94.
134. Wang SS, Cozen W, Severson RK, et al. Cyclin D1 splice variant and risk for non-Hodgkin lymphoma. *Hum Genet*. 2006;120:297-300.
135. Debniak T, Cybulski C, Gorski B, et al. CDKN2A-positive breast cancers in young women from Poland. *Breast Cancer Res Treat*. 2007;103:355-359.
136. McCloud JM, Sivakumar R, Greenhough A, et al. p16INK4a polymorphism: associations with tumour progression in patients with sporadic colorectal cancer. *Int J Oncol*. 2004;25:1447-1452.
137. Polakova V, Pardini B, Naccarati A, et al. Genotype and haplotype analysis of cell cycle genes in sporadic colorectal cancer in the Czech Republic. *Hum Mutat*. 2009;30:661-668.
138. Zuchner S, Gilbert JR, Martin ER, et al. Linkage and association study of late-onset Alzheimer disease families linked to 9p21.3. *Ann Hum Genet*. 2008;72:725-731.

139. Kumar R, Smeds J, Berggren P, et al. A single nucleotide polymorphism in the 3'untranslated region of the CDKN2A gene is common in sporadic primary melanomas but mutations in the CDKN2B, CDKN2C, CDK4 and p53 genes are rare. *Int J Cancer*. 2001;95:388-393.
140. Williams RT, den Besten W, Sherr CJ. Cytokine-dependent imatinib resistance in mouse BCR-ABL+, Arf-null lymphoblastic leukemia. *Genes Dev*. 2007;21:2283-2287.
141. Williams RT, Roussel MF, Sherr CJ. Arf gene loss enhances oncogenicity and limits imatinib response in mouse models of Bcr-Abl-induced acute lymphoblastic leukemia. *Proc Natl Acad Sci U S A*. 2006;103:6688-6693.
142. Notta F, Mullighan CG, Wang JC, et al. Evolution of human BCR-ABL1 lymphoblastic leukaemia-initiating cells. *Nature*. 2011;469:362-367.
143. Voltan R, Celeghini C, Melloni E, Secchiero P, Zauli G. Perifosine plus nutlin-3 combination shows a synergistic anti-leukaemic activity. *Br J Haematol*. 2010;148:957-961.
144. Dickson MA, Schwartz GK. Development of cell-cycle inhibitors for cancer therapy. *Curr Oncol*. 2009;16:36-43.

APPENDIX A

CDKN2A/ARF/CDKN2B ISOFORMS and ANRIL

CDKN2A/ARF



1. NCBI Reference Sequences (RefSeq)

Cyclin-dependent kinase inhibitor 2A isoform 4

<http://www.ncbi.nlm.nih.gov/gene/1029>

NM_058195.3: mRNA-cyclin-dependent kinase inhibitor 2A (melanoma, p16, inhibits CDK4), transcript variant 4

Total range: NC_000009.11 (21,967,751-21,994,490)

Total length: 26,740

mRNA product length: 1,164

Related Ensembl: [ENSP00000355153](#), [ENST00000361570](#)

Transcript Variant: This variant (4), also known as β , encodes isoform 4, which is also called **p14^{ARF}**. This variant may use an alternative upstream start codon, which would produce an isoform that is 41 aa longer at the N-terminus, or an alternative downstream start codon, which would produce an isoform (smARF, described in PMID:16713577) that is 47 aa shorter at the N-terminus; it is unclear if the isoforms derived from the alternative start codons are present in vivo. The p14^{ARF} isoform is known to be nucleoplasmic but may also be recruited to mitochondria, as described in PMID:20107316.

ENSEMBL card

Cyclin-dependent kinase inhibitor 2A isoform 4

http://www.ensembl.org/Homo_sapiens/Transcript/Summary?db=core;g=ENSG00000147889;t=9:21967752-21995300;t=ENST00000361570

HGNC Symbol: CDKN2A-201

Transcript [ENST00000361570](#)

Gene [ENSG00000147889](#)

Protein product [ENSP00000355153](#)

Location [Chromosome 9: 21,967,997-21,994,490](#)

Total length: 26,493

Gene type Known protein coding
Transcript type Known nonsense mediated decay
Strand Reverse
Base pairs 905
Amino acids 173

ENSEMBL card

http://www.ensembl.org/Homo_sapiens/Transcript/Summary?db=core;g=ENSG00000147889;r=9:21967752-21995300;t=ENST00000530628

HGNC Symbol: CDKN2A-004
Transcript [ENST00000530628](#)
Gene [ENSG00000147889](#)
Protein product [ENSP00000432664](#)
Location [Chromosome 9: 21,967,997-21,994,490](#)
Total length: 26,493
Gene type Known protein coding
Transcript type Known protein coding
Strand: Reverse
Base pairs:905
Amino acids :132

2. NCBI Reference Sequences (RefSeq)

Cyclin-dependent kinase inhibitor 2A isoform 1
http://www.ncbi.nlm.nih.gov/nuccore/NM_000077.4

NM_000077.4: mRNA-cyclin-dependent kinase inhibitor 2A (melanoma, p16, inhibits CDK4), transcript variant 1
total range: NC_000009.11 (21,967,751-21,975,132)
total length: 7,382
mRNA product length: 1,267
Related Ensembl: [ENSP00000307101](#), [ENST00000304494](#)

Transcript Variant: This variant (1), also known as alpha, contains an alternate open reading frame (ARF), when compared to variant 4. The ARF results from an alternative splicing between a downstream first exon, which contains the translation start codon, and the common second exon. Thus, the protein encoded by this variant (isoform 1) lacks sequence similarity to the protein product of variant 4. Isoform 1 is also called **p16INK4a**.

ENSEMBL card

HGNC Symbol: CDKN2A-001
Transcript [ENST00000304494](#)
Gene [ENSG00000147889](#)

Protein product [ENSP00000307101](#)
Location [Chromosome 9: 21,967,752-21,975,097](#)
Total length: 7,345
Gene type Known protein coding
Transcript type Known protein coding
Strand Reverse
Base pairs 1,218
Amino acids 156

3. NCBI Reference Sequences (RefSeq)

Cyclin-dependent kinase inhibitor 2A p12,variant 3
http://www.ncbi.nlm.nih.gov/nuccore/NM_058197.4

NM_058197.4: mRNA-cyclin-dependent kinase inhibitor 2A (melanoma, p16, inhibits CDK4), transcript variant 3
total range: NC_000009.11 (21,967,751-21,974,826)
total length: 7,076
mRNA product length: 1,235
Related Ensembl: [ENSP00000369496](#), [ENST00000380151](#)

Transcript Variant: This variant (3) contains an alternate open reading frame (ARF), when compared to variant 4. The ARF results from an alternative splicing between a downstream first exon, which contains the translation start codon, and the common second exon. Thus, the protein encoded by this variant (p12 or isoform 3) lacks sequence similarity to the protein product of variant 4. This variant is specifically expressed in [pancreas](#), and has been described in PMID:10445844. It is a candidate for nonsense-mediated mRNA decay (NMD), but it is not known if the endogenous protein is expressed in vivo.

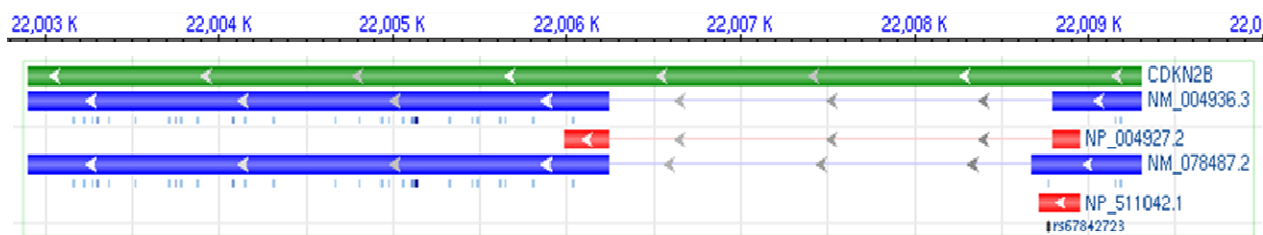
ENSEMBL card

Cyclin-dependent kinase inhibitor 2A p12,variant 3
http://www.ensembl.org/Homo_sapiens/Transcript/Summary?db=core;g=ENSG00000147889;r=9:21967752-21995300;t=ENST00000380151

HGNC Symbol: CDKN2A-003
Transcript [ENST00000380151](#)
Gene [ENSG00000147889](#)
Protein product [ENSP00000369496](#)
Location [Chromosome 9: 21,968,179-21,974,826](#)
Total length: 6,647
Gene type Known protein coding
Transcript type Known nonsense mediated decay
Strand Reverse
Base pairs 794
Amino acids 116

CDKN2B

Synonyms *CDK4I*, *INK4B*, *MTS2*, *P15*, *p15INK4b*, *TP15*



1. NCBI Reference Sequences (RefSeq)

Cyclin-dependent kinase 4 inhibitor B isoform 1

http://www.ncbi.nlm.nih.gov/nuccore/NM_004936.3

NM_004936.3: mRNA-cyclin-dependent kinase inhibitor 2B (p15, inhibits CDK4), transcript variant 1

total range: NC_000009.11 (22,002,902-22,009,312)

total length: 6,411

mRNA product length: 3,878

Amino acids 138

Related Ensembl [ENSP00000276925](#), [ENST00000276925](#)

Transcript Variant: This variant (1) encodes the longer isoform (1).

ENSEMBL card

Cyclin-dependent kinase 4 inhibitor B isoform 1

HGNC Symbol: CDKN2B-001

Transcript [ENST00000276925](#)

Gene [ENSG00000147883](#)

Protein product [ENSP00000276925](#)

Location [Chromosome 9: 22,002,902-22,009,280](#)

Total length 6378

Gene type Known protein coding

Transcript type Known protein coding

Strand Reverse

Base pairs 3,829

Amino acids 138

2. NCBI Reference Sequences (RefSeq)

Cyclin-dependent kinase 4 inhibitor B isoform 2

http://www.ncbi.nlm.nih.gov/nuccore/NM_078487.2

M_078487.2: mRNA-cyclin-dependent kinase inhibitor 2B (p15, inhibits CDK4), transcript variant 2

total range: NC_000009.11 (22,002,902-22,009,312)

total length: 6,411

mRNA product length: 4,001

Amino acids 78

Related Ensembl [ENSP00000369487](#), [ENST00000380142](#)

Transcript Variant: This variant (2) uses a different splice site, which leads to a translation frame shift, when compared to variant 1. The resulting protein (isoform 2) is shorter and has a distinct C-terminus when compared to isoform 1.

ENSEMBL card

HGNC Symbol: CDKN2B-002

Transcript [ENST00000380142](#)

Gene [ENSG00000147883](#)

Protein product [ENSP00000369487](#)

Location [Chromosome 9: 22,005,986-22,009,271](#)

Total length: 3,285

Gene type Known protein coding

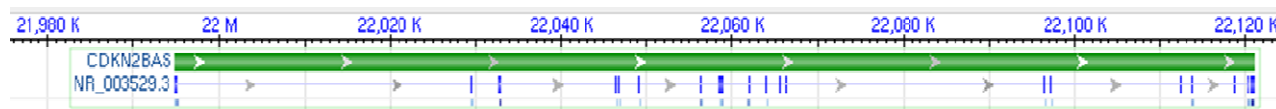
Transcript type Known protein coding

Strand Reverse

Base pairs 859

Amino acids 78

CDKN2BAS-ANRIL



NCBI Reference Sequences (RefSeq)

CDKN2B antisense RNA 1 (non-protein coding)

<http://www.ncbi.nlm.nih.gov/gene/100048912>

NR_003529.3: CDKN2B antisense RNA (non-protein coding)

total range: NC_000009.11 (21,994,790-22,121,096)

total length: 126,307

processed length: 3,837

product length: 3,85

Source sequence(s) [AL354709,BC038540,CB109081,DQ485453](#)

ENSEMBL card

HGNC Symbol: CDKN2B-AS-004

Transcript [ENST00000428597](#)

Gene [ENSG00000240498](#)

Location [Chromosome 9: 21,994,790-22,121,094](#)

Gene type Known processed transcript

Transcript type Known antisense

Strand Forward

Base pairs 3,835